


2018

## Seepage and Stability Analysis of the Earth Dams under Drawdown Conditions by using the Finite Element Method

Salama Al-Labban  
*University of Central Florida*

 Part of the [Civil Engineering Commons](#), and the [Hydraulic Engineering Commons](#)  
Find similar works at: <https://stars.library.ucf.edu/etd>  
University of Central Florida Libraries <http://library.ucf.edu>

This Doctoral Dissertation (Open Access) is brought to you for free and open access by STARS. It has been accepted for inclusion in Electronic Theses and Dissertations by an authorized administrator of STARS. For more information, please contact [STARS@ucf.edu](mailto:STARS@ucf.edu).

---

### STARS Citation

Al-Labban, Salama, "Seepage and Stability Analysis of the Earth Dams under Drawdown Conditions by using the Finite Element Method" (2018). *Electronic Theses and Dissertations*. 6157.  
<https://stars.library.ucf.edu/etd/6157>

# SEEPAGE AND STABILITY ANALYSIS OF THE EARTH DAMS UNDER DRAWDOWN CONDITIONS BY USING THE FINITE ELEMENT METHOD

by

SALAMA N. AL-LABBAN  
B.S. University of Kufa, 2003  
M.S. University of Kufa, 2007

A dissertation submitted in partial fulfillment of the requirements  
for the degree of Doctor of Philosophy  
in the Department of Civil, Environmental and Construction Engineering  
in the College of Engineering and Computer Science  
at the University of Central Florida  
Orlando, Florida

Fall Term  
2018

Major Professor: Manoj B. Chopra

## ABSTRACT

One of the major concerns in the behavior of an earth dam is the change in the exit gradient and the impact on the slope stability under drawdown conditions. Drawdown can cause increased seepage forces on the upstream slope which may result in the movement of soil particles in the flow direction and cause erosion problems. In this research, a numerical approach, based on the finite element method (FEM) is used to analyze the seepage through the dam and its foundation to study exit gradients and slope stability under both steady-state and transient conditions. The results show that a central core is important in reducing the flux through the dam. Constructing a cutoff under the core further increases the efficiency of the core and lowers the phreatic line. However, it is seen that the submerged weight increases when the earth dam with a core or with a complete cutoff which causes higher water flux to flow out of the dam under the drawdown condition. The exit gradient at the upstream slope may reach critical levels and cause failure of the dam due to erosion. Adding an upstream filter is studied as a possible solution to this problem. Two configurations of the filters are modeled and the slope filter configuration performed best in reducing the exit gradient at the upstream face. A low permeability core with a cutoff increases deformation of the soil because of increased saturated areas in the upstream region. The factor of safety of the slope is also reduced because of the increased buoyancy of the soil at the upstream side of the dam. The soil properties of the *upstream* filter have a significant influence on the slope stability against sliding. An upstream slope filter increases the stability of the slope while a central filter decreases it.

**Keywords:** Earth dam; finite element; drawdown; seepage; exit gradient; filter; slope stability

*This dissertation is dedicated:*

*To my mother, **Rafeqa**, and my father **Nasim**,*

*To my beloved wife **Zumurrud**, and my wonderful daughters **Zahraa** and **Sarah**,*

*To my sisters **Evian** and **Mariam**, and my brother **Osama**,*

*for*

*their love, patience, support, encouragement and help.*



## ACKNOWLEDGMENTS

Many thanks and praise are due first of all and above all to my Creator, almighty **ALLAH**, most beneficent, most gracious and most merciful, who gave me the ability and the desire to complete this research work despite of all the hurdles and constraints in the way of its completion.

Special thanks are presented for my country, IRAQ, with deepest wishes for the greatest land and greatest people to stay in peace forever. I am grateful to Ministry of Higher Education and Scientific Research, Iraqi Cultural Office, and University of Kufa. The work would not have been possible without their support.

I wish to express his cordial thanks and deepest gratitude towards my supervisor, Dr. Manoj B. Chopra, for his appreciated guidance, encouragement, valuable advice, inspiration, patience, and constant help. This was done despite the huge responsibilities burdened on his shoulders.

Sincere thanks are expressed to all my Dissertation Committee, Dr. Ahmed Elshennawy, Dr. Kevin Mackie, and Dr. Dingbao Wang. Each of the members has provided me extensive personal and professional guidance and taught me a great deal about both scientific research and life in general.

Sincere thanks are presented to my family for their patience and support. Finally, a special acknowledgment is expressed to my colleagues in postgraduate studies, to all my friends who helped, encouraged and supported me and to all those who had participated in any way or another in accomplishing this work.

## TABLE OF CONTENTS

LIST OF FIGURES .....	ix
LIST OF TABLES .....	xviii
CHAPTER ONE: INTRODUCTION .....	1
1.1 Background .....	1
1.2 History of Failures of Earth Dams due to Drawdown .....	2
1.2.1 Pilarcitos Dam .....	2
1.2.2 Walter Bouldin Dam .....	2
1.2.3 Teton Dam .....	3
1.2.4 San Luis Dam .....	3
1.3 Objectives of this Dissertation .....	4
1.4 Organization of the Dissertation .....	5
CHAPTER TWO: LITERATURE REVIEW .....	8
2.1 Seepage Analysis .....	8
2.2 Slope Stability Analysis .....	10
CHAPTER THREE: NUMERICAL MODELS FOR THE SEEPAGE AND STABILITY ANALYSIS USING THE FINITE ELEMENT METHOD (FEM) .....	17
3.1 Introduction .....	17
3.2 Seepage Analysis .....	17

3.2.1 The Governing Equation .....	17
3.2.2 The Finite Element Equations .....	19
3.3 Stress-Deformation Analysis.....	21
3.4 Slope Stability Analysis .....	23
3.5 Validation Problems.....	26
3.5.1 Steady-State Problem Case.....	26
3.5.2 Transient Case .....	29
CHAPTER FOUR: EFFECT OF THE CORE ON INCREASING THE INTERNAL EROSION POTENTIAL UNDER DRAWDOWN CONDITIONS.....	33
4.1 Introduction .....	33
4.2 Seepage Force and the Exit Gradient .....	34
4.3 Current Study .....	38
4.4 Description of the Earth Dam.....	38
4.5 Results and Discussion.....	42
4.5.1 Homogenous Earth Dam (Case 1) .....	42
4.5.2 Earth Dam with a Core (Case 2).....	47
4.5.3 Earth Dam has a Core and a Complete Cutoff (Case 3).....	50
4.6 Comparison of the Three Cases .....	54
4.7 Influence of Foundation Impermeability.....	57

CHAPTER FIVE: EFFECT OF THE UPSTREAM FILTER IN INCREASING THE STABILITY OF THE DAM .....	65
5.1 Introduction .....	65
5.2 Effect of the Filter Location .....	67
5.3 Effect of the Filter Permeability .....	72
5.4 Effect of the Transition Zone .....	77
CHAPTER SIX: ANALYSIS OF THE EARTH DAMS UNDER DRAWDOWN CONDITIONS FOR SLOPE AND DEFORMATION STABILITY .....	82
6.1 Introduction .....	82
6.2 Numerical Models .....	82
6.3 Deformation Analysis of the Earth Dams .....	85
6.3.1 With a Permeable Foundation .....	86
6.3.2 With an Impermeable Rigid Foundation .....	88
6.4 Slope Stability Analysis of the Earth Dams .....	90
6.4.1 Factor of Safety Against Sliding .....	92
6.4.2 Driving Forces in the Finite Slope.....	92
6.5 Analysis of the Slope Stability .....	96
6.5.1 Effect of the Core .....	96
6.5.2 Influence of the Foundation Material .....	105

6.5.3 Effect of the Upstream Filter .....	108
CHAPTER SEVEN: SEEPAGE AND SLOPE STABILITY OF A REAL DAM UNDER DRAWDOWN CONDITIONS .....	112
7.1 Introduction .....	112
7.2 Al-Adhaim Dam .....	113
7.3 Numerical Models of the Dam .....	114
7.4 Seepage Analysis of Al-Adhaim Dam .....	116
7.5 Effect of the Upstream Filter.....	121
7.6 Deformation of Al-Adhaim Dam under Drawdown Conditions.....	124
7.7 Factor of Safety Against the Sliding under the Drawdown Conditions.....	128
7.7.1 Slope Stability Analysis of Al-Adhaim Dam .....	128
7.7.2 Influence of the Upstream Filter.....	131
CHAPTER EIGHT: CONCLUSIONS AND RECOMMENDATIONS FOR FUTURE WORK ..	135
8.1 Conclusions .....	135
8.2 Recommendations .....	138
REFERENCES .....	139

## LIST OF FIGURES

Figure 3.1: The diagram of forces acting on an earth slope for a circular and noncircular slip surface (SLOPE/W, 2012). .....	24
Figure 3.2: Boundary conditions and the finite element mesh for the dam model. ....	27
Figure 3.3: Comparison of the results of the seepage analysis between the flow net method and the finite element method (FEM). ....	28
Figure 3.4: Profile section of the experiment and the boundary conditions of the model. ....	30
Figure 3.5: Finite element mesh and phreatic surfaces for the steady-state and transient conditions. ....	30
Figure 3.6: Comparisons of the total head in (in.) for the pore pressure cells. ....	31
Figure 4.1: Flow of the water flux independent of soil direction (Cedergren, 1977). ....	35
Figure 4.2: Seepage force acting on the dam slope and its foundation (Cedergren, 1977; Reddi, 2003). ....	36
Figure 4.3: Profile Sections of the three dam cases; (a) without core; (b) with core; (c) with core and a complete cutoff. ....	40
Figure 4.4: Boundary conditions for the dam model used for the seepage analysis. ....	41
Figure 4.5: Finite element mesh for the three dam cases. ....	41
Figure 4.6: Total head contours (in m) and flow directions of the water flux for Case 1; (a) before the drawdown event, (b) after the reservoir is dropped to half in one day. ....	43

Figure 4.7: The behavior of the water flux flowing out of the upstream face after the drawdown conditions; (a) drawdown 25% of the reservoir, (b) drawdown 50% of the reservoir. .....	44
Figure 4.8: Maximum exit gradient on various locations of the upstream face due to the drawdown conditions; (a) drawdown a 25% of the reservoir, (b) drawdown a 50% of the reservoir. ....	46
Figure 4.9: Total head contours (in m) and flow directions of the water flux for Case 2; (a) before the drawdown event, (b) after the reservoir is dropped to half in one day. ....	47
Figure 4.10: The behavior of the water flux flowing out of the upstream face after the drawdown conditions; (a) drawdown 25% of the reservoir, (b) drawdown 50% of the reservoir. .....	48
Figure 4.11: Maximum exit gradient on various locations of the upstream face due to the drawdown conditions; (a) drawdown 25% of the reservoir, (b) drawdown 50% of the reservoir. .....	50
Figure 4.12: Total head contours (in m) and flow directions of the water flux for Case 3; (a) before the drawdown event, (b) after the reservoir is dropped to half in one day. ....	52
Figure 4.13: The behavior of the water flux flowing out of the upstream face after the drawdown conditions; (a) drawdown 25% of the reservoir, (b) drawdown 50% of the reservoir. .....	53

Figure 4.14: Maximum exit gradient on various locations of the upstream face due to the drawdown conditions; (a) drawdown a 25% of the reservoir, (b) drawdown a 50% of the reservoir. ....	54
Figure 4.15: Comparison of the water flux and the reduced percent for all dam cases in the steady-state analysis. ....	56
Figure 4.16: Comparison of the water flux that flows out of the dam body through the upstream face for the dam cases under different drawdown conditions; (a) drawdown 25% of the reservoir, (b) drawdown 50% of the reservoir. ....	56
Figure 4.17: Comparison of the maximum values of the exit gradient for the dam cases under different drawdown conditions; (a) drawdown 25% of the reservoir, (b) drawdown 50% of the reservoir. ....	58
Figure 4.18: Profile section of the dam models applied on impermeable foundation. ....	59
Figure 4.19: The results of the seepage analysis for Case 4 and Case 5.....	59
Figure 4.20: The results of the seepage analysis for Case 4 and Case 5 after the drawdown event. ....	60
Figure 4.21: The behavior of the water flux flowing out of the upstream face after drawdown 25% of the reservoir at various rates; (a) without core case, (b) with core case.....	61
Figure 4.22: The behavior of the water flux flowing out of the upstream face after drawdown 50% of the reservoir at various rates; (a) without core case, (b) with core case.....	61
Figure 4.23: Maximum exit gradient on various locations of the upstream face due to draw down 25% of the reservoir; (a) without core case, (b) with core case.....	63



Figure 4.24: Maximum exit gradient on various locations of the upstream face due to draw down 50% of the reservoir; (a) without core case, (b) with core case.....	63
Figure 5.1: Profile section of the base soil and the filter soil (Das & Sobhan, 2014). ....	66
Figure 5.2: Location of the upstream filter; (a) central filter, (b) slope filter. ....	68
Figure 5.3: Comparison of the effect of the upstream filter on the phreatic surface in the 1 <sup>st</sup> , 4 <sup>th</sup> , 8 <sup>th</sup> , and 12 <sup>th</sup> days when the drawdown of the reservoir occurs in one day.....	68
Figure 5.4: Comparison of the water flux behavior that flows out of the dam for different filter location under the drawdown condition at a rate of 4 m/day; (a) through the slope face, (b) through the foundation surface. ....	69
Figure 5.5: Comparison of the effect of the location of the upstream filter on the exit gradient when the reservoir level is dropped to 14 m at a rate of 4 m/day. ....	71
Figure 5.6: Comparison of the effect of the location of the upstream filter on the exit gradient when the reservoir level is dropped to 14 m at a rate of 1 m/day. ....	72
Figure 5.7: Comparison of the effect of the permeability of the central filter on the exit gradient when the drawdown of the reservoir occurs in one day. ....	75
Figure 5.8: Comparison of the effect of the permeability of the slope filter on the exit gradient when the drawdown of the reservoir occurs in one day. ....	75
Figure 5.9: Comparison of the effect of the permeability of the central filter on the exit gradient when the drawdown of the reservoir occurs in four days.....	76

Figure 5.10: Comparison of the effect of the permeability of the slope filter on the exit gradient when the drawdown of the reservoir occurs in four days. ....	76
Figure 5.11: Location of the transition layer for the central filter and the slope filter. ....	78
Figure 5.12: Comparison of the effect of the upstream filter on the phreatic surface in the 1 <sup>st</sup> , 2 <sup>nd</sup> , 3 <sup>rd</sup> , and 4 <sup>th</sup> days of the drawdown of the reservoir at a rate of 4 m/day.....	78
Figure 5.13: Comparison of the effect of both the upstream filter and the transition layer on the exit gradient for different hydraulic conductivities when the drawdown of the reservoir occurs in one day. ....	80
Figure 5.14: Comparison of the effect of both the upstream filter and the transition layer on the exit gradient for different hydraulic conductivities when the drawdown of the reservoir occurs in four days.....	81
Figure 6.1: Profile sections of the three dam models.....	83
Figure 6.2: Vectors and shapes of the soil deformation for the dam cases under sudden drawdown condition (at a scale of 50x).....	87
Figure 6.3: Contour lines of the maximum soil displacement (in m) for the dam cases under sudden drawdown condition.....	88
Figure 6.4: Vectors and shapes of the soil deformation for the dam cases under sudden drawdown condition (at a scale of 50x).....	89
Figure 6.5: Contour lines of the maximum soil displacement (in m) for the dam cases under sudden drawdown condition.....	90

Figure 6.6: Circular and non-circular slip surface in an earth slope and the force diagram in an element (Budhu, 2011).....	91
Figure 6.7: The dry case of the slope (Reddi, 2003; Taylor, 1948). .....	93
Figure 6.8: The submerged case (Taylor, 1948). .....	94
Figure 6.9: Friction circle method for the drawdown case (Taylor, 1948). .....	95
Figure 6.10: Analysis of the steady seepage case (Reddi, 2003; Taylor, 1948). .....	96
Figure 6.11: Critical slip surface for Case 1 under sudden drawdown of 4 m/day.....	97
Figure 6.12: Influence of the upstream slope stability for Case 1 under different drawdown rates; (a) drawdown 25% of the reservoir, (b) drawdown 50% of the reservoir. ....	98
Figure 6.13: Critical slip surface for Case 2 under sudden drawdown of 4 m/day.....	99
Figure 6.14: Influence of the upstream slope stability for Case 2 under different drawdown rates; (a) drawdown 25% of the reservoir, (b) drawdown 50% of the reservoir. ....	100
Figure 6.15: Critical slip surface for Case 3 under sudden drawdown of 4 m/day.....	101
Figure 6.16: Influence of the upstream slope stability for Case 3 under different drawdown rates; (a) drawdown 25% of the reservoir, (b) drawdown 50% of the reservoir. ....	102
Figure 6.17: Comparison of the factor of safety for the dam cases under different drawdown conditions; (a) drawdown 25% of the reservoir, (b) drawdown 50% of the reservoir. .....	105
Figure 6.18: Critical slip surface for the dam cases after drawdown 50% of the reservoir at a rate of 4 m/day. ....	106

Figure 6.19: Influence of the dam foundation on the upstream slope stability under different drawdown conditions. ....	107
Figure 6.20: Critical slip surface of the upstream slope before and after the sudden drawdown condition. ....	109
Figure 6.21: Influence of the filter permeability on the upstream slope stability under sudden drawdown condition.....	110
Figure 7.1: Profile section of Al-Adhaim dam ( <i>Al-Adhaim Earth Dam</i> , 1994). ....	114
Figure 7.2: Boundary conditions for the seepage analysis and the finite element mesh. ....	115
Figure 7.3: Total head contours (in m) and flow directions for Al-Adhaim dam; (a) the steady-state condition, (b) the drawdown condition. ....	117
Figure 7.4: The behavior of the water flux flowing out of the upstream face under various drawdown conditions.; (a) drawdown 25% of the reservoir, (b) drawdown 50% of the reservoir. ....	118
Figure 7.5: Maximum exit gradient on various locations of the upstream face under different drawdown rates; (a) drawdown 25% of the reservoir, (b) drawdown 50% of the reservoir. ....	120
Figure 7.6: The maximum values of the exit gradient on the upstream face after dropping the water level to level 116 m, 50% of the reservoir, in one day. ....	122
Figure 7.7: The maximum values of the exit gradient on the upstream face after dropping the water level to level 116 m, 50% of the reservoir, in one day. ....	123

Figure 7.8: The maximum values of the exit gradient on the upstream face after dropping the water level to level 116 m, 50% of the reservoir, in one day.....	124
Figure 7.9: Vectors and deformation shape of the dam (at a scale of 50x) after sudden drawdown condition.....	126
Figure 7.10: Contour lines of the maximum soil displacement (in m) in the $x$ - and $y$ - directions under drawdown conditions.....	126
Figure 7.11: Contour lines of the maximum soil displacement (in m) in the $x$ -direction under drawdown conditions.....	127
Figure 7.12: Contour lines of the maximum soil displacement (in m) in the $y$ -direction under drawdown conditions.....	128
Figure 7.13: Slip surfaces that may cause cracking or sinkhole on the slope surface after the drawdown event.....	129
Figure 7.14: Slip surfaces of the upstream slope for the dam cases before and after the sudden drawdown event.....	130
Figure 7.15: Factor of safety with time for the different dam cases under drawdown conditions; (a) drawdown 25% of the reservoir, (b) drawdown 50% of the reservoir.....	131
Figure 7.16: Slip surfaces of the upstream slope for the dam cases before and after the drawdown 50% of the reservoir.....	132
Figure 7.17: Factor of safety with time for the different dam cases under sudden drawdown condition; (a) $k_f/k_s = 25$ . (b) $k_f/k_s = 50$ . ....	133

Figure 7.18: Factor of safety with time for the different dam cases under sudden drawdown condition; (a)  $k_f/k_s = 25$ . (b)  $k_f/k_s = 50$ . ..... 134

## LIST OF TABLES

Table 3.1: Comparison of the seepage quantity under the steady-state condition.....	28
Table 4.1: Material properties of the earth dam used for stresses and slope analysis. ....	40
Table 4.2: Summary of the total flux (in $\text{m}^3/\text{m}$ ) that flows out of the earth dam for a period of 30 days under the drawdown conditions.....	45
Table 4.3: Summary of the total flux (in $\text{m}^3/\text{m}$ ) that flows out of the earth dam for a period of 30 days under the drawdown conditions.....	49
Table 4.4: Summary of the total flux (in $\text{m}^3/\text{m}$ ) that flows out of the earth dam for a period of 30 days under the drawdown conditions.....	53
Table 4.5: Summary of the total flux (in $\text{m}^3/\text{m}$ ) that flows out of the earth dam for a period of 30 days under the drawdown conditions.....	62
Table 5.1: Summary of the total flux (in $\text{m}^3/\text{m}$ ) that flows out of the earth dam for a period of 30 days under the drawdown conditions.....	70
Table 5.2: Summary of the total flux (in $\text{m}^3/\text{m}$ ) that flows out of the earth dam for a period of 30 days under the drawdown conditions.....	73
Table 5.3: Summary of the total flux (in $\text{m}^3/\text{m}$ ) that flows out of the earth dam for a period of 30 days under the drawdown conditions.....	79
Table 6.1: Material properties of the earth dam used for seepage, stresses and slope analysis....	84
Table 6.2. Factor of safety in the steady-state analysis for all dam cases at different reservoir levels .....	103

Table 6.3: Factor of safety in the steady-state analysis for all dam cases at different reservoir levels	106
Table 6.4: Factor of safety in the steady-state analysis for all dam cases at different reservoir levels.	109
Table 7.1: The surface area and the water volume for Al-Adhaim reservoir. (Al-Majid, 2008)	113
Table 7.2: Material properties of the earth dam used for seepage, stress, and slope stability analyses ( <i>Al-Adhaim Earth Dam</i> , 1994).	114
Table 7.3: Summary of the total flux (in m <sup>3</sup> /m) that flows out of the earth dam for a period of 60 days under the drawdown conditions.	119



# **CHAPTER ONE: INTRODUCTION**

## **1.1 Background**

The erosion of the soil within earth dams due to seepage is one of the major concerns for geotechnical engineers. Drawdown of the reservoir water levels at a sudden rate results in a high gradient between the dam shell and the reservoir, which in turn causes an increase of the seepage rate flowing out the dam, both on the slope face and the foundation surface at the upstream region. The hydraulic gradient can reach the critical level when the average seepage pressure becomes the same as the submerged weight of the sand, and the effective stress at that depth becomes equal to zero (Terzaghi et al., 1996). The erosive potential of the soil is increased gradually until it reaches a high value where the seepage is concentrated at an exit point. The seepage developing on the upstream face after the drawdown event has an effect on the slope stability. The seepage reduces the effective stress by producing higher pore water pressures and also increases the driving forces in the soil mass due to the additional seepage forces (Reddi, 2003). This, in turn, can reduce the stability of the slope greatly (Abramson et al., 2002).

One of the common methods to control the seepage is using filters. Filters are commonly used on the earth dams to prevent the finer soil particle than transfer through the coarse particles and to control the direction of the water flowing. The particle size of the filter should be large enough to prevent increase excess pore pressure (Reddi, 2003). The particle shape of the filter and the base materials is not to be similar (Sherard, Dunnigan, & Talbot, 1984). The permeability criteria of the filter are specified to be 25 to 100 times higher than the permeability of the base soil (Reddi, 2003).

## 1.2 History of Failures of Earth Dams due to Drawdown

### 1.2.1 Pilarcitos Dam

Pilarcitos dam is a 95 ft height of the earth dam with a clay puddle core. The construction of the dam began in 1864 and completed in 1866. The reservoir was raised in 1867 and 1874 (*San Francisco Public Utilities Commission Peninsula Watershed*, n.d.). The upstream material is classified as a sandy clay (CL) with a slope of 3H:1V above elevation 123 ft and 2.5H:1V below elevation 123 ft. the unit weight of the soil is 135 pcf with a percentage of 60-70 of the passing No. 200. The permeability of the soil was  $4 \times 10^{-8}$  cm/sec with the liquid limit of 45% and the plastic limit of 23%. (Duncan et al., 1990)

The dam failed by sliding of the upstream because of a drawdown event where the upstream water level was suddenly lowered from elevation 692 ft to elevation 657 ft at a rate of 1.7 ft/day between the period of October 7 – November 19, 1969.

### 1.2.2 Walter Bouldin Dam

Walter Boulding Dam is an earth dam constructed in 1967 by Alabama Power Company. The dam is located near the mouth of the Coosa River and the town of Wetumpka, Alabama (*Walter Bouldin Dam failure and reconstruction*, 1978). On February 10, 1975, the sliding failure of the upstream slope occurred during a sudden the drawdown of 32 ft of the reservoir in 5.5 hours (Duncan et al., 1990). In the beginning, a piping failure occurred at another portion of the dam. The sliding extended to length about 10 ft below the slope surface near the edge of the slide. The height of the slope at the failed location was approximately 60 ft, supported by an 80 ft layer of clayey sand and

gravel. The slope of the dam was 2H:1V above elevation 245 ft and 2.5H:1 below elevation 245 ft. (Duncan et al., 1990)

### 1.2.3 Teton Dam

Teton dam is a zoned dam constructed on the Teton River, three miles northeast of Newdale, Idaho, United State and opened in November 1975 (Independent Panel, 1976). The shell material of the upstream and downstream mainly consist of sand, gravel, and cobbles. On June 5, 1976, the dam failed at a water level 9 m below the dam crest and 1 m below the spillway crest. Initially, seepage was observed 460 m downstream of the dam and then the seepage appeared on the downstream face. On the morning of June 5, the seepage rate increased on the downstream side near the abutment about 40 m below the top end of the dam. About 10:30 am, the seepage rate increased to a value of  $0.4 \text{ m}^3/\text{sec}$  and continued increasing, which caused erosion of the soil particles and formed a tunnel inside the dam on the downstream end with a diameter of 1.8 m. A vortex was developed at the upstream (on the reservoir) by 11:00 am. The seepage rate increased rapidly on the downstream caused a breach of the dam crest at about 11:55 am. The dam failure led to the loss of 14 lives and resulted in damage estimated at about \$400 million. (Bosela et al., 2012)

### 1.2.4 San Luis Dam

San Luis Dam is the largest reservoir in the United States. The dam is located approximately 170 km southeast of San Francisco, California. The dam was constructed in 1969 (Duncan et al., 2014) with a capacity of 252 million  $\text{m}^3$  (Stark et al., 2017).

A massive slide of the upstream slope occurred in the San Luis Dam in California in 1981. The slide happened on September 4 after a drawdown of 55 m of the reservoir occurred in 120 days (Stark & Duncan, 1991; Stark et al., 2017). The historical record over the period of 12 years showed a significant fluctuation of the water level in the reservoir between the wet season and the dry season. (Duncan et al., 2014).

### 1.3 Objectives of this Dissertation

The main objective of the dissertation is to study the seepage problems that develop on the slope face of an earth dam due to sudden drawdown that may cause the erosion of the soil particles. This, in turn, may lead to the failure of the earth dam. The dissertation includes the influence of the dam components on reducing the likelihood of reduced slope stability under these drawdown conditions and the effect of using the upstream filter on the reduction of the hydraulic gradients at the upstream face. The objectives of are summarized as:

- To study the effect of the earth dam core, with and without a cutoff, on the seepage flow before and after the drawdown conditions.
- To study mechanisms to control and reduce the influence of the seepage flow on the stability of the earth dams by using the upstream filter.
- To study the influence of the water leaving the dam from different parts of the dam (upstream, foundation, filters) on the deformation field and volume change of the earth dams.
- To study the *upstream* slope stability for all cases before and after the drawdown conditions.

Numerical models are prepared and analyzed to determine the water flux, the upstream exit gradients, the deformation of the dam (i.e. volume change of the soil) and slope stability factors of safety against sliding. The directions of the water flow, the total head contours, the vectors and the contour lines of the soil deformation, and the critical slip surface of the *upstream* slope are also plotted before and after the drawdown condition.

#### 1.4 Organization of the Dissertation

This dissertation is divided into eight chapters. Chapter one presents the background of the seepage problems which cause erosion of the dam soils leading to reduced slope stability during and after the drawdown events. In addition, some of the earth dam failures due to drawdown events are discussed. The objectives of the dissertation are also presented in this chapter.

Chapter two presents a literature review of research that includes the effect of changes in the water level on the dam stability. The chapter is divided into two sections: a section dealing with the seepage analysis of the earth dams and another section which deals with the stability analysis of the earth dams.

Chapter three describes the numerical models used for seepage and stability analyses using the finite element method (FEM). This chapter presents the background theory and equations used for the seepage analysis through the dam as well as the equations of the stability analysis of the dam. It also describes the method used to estimate the factor of safety against sliding. The last part of this chapter presents a verification of the software used for the analysis. The purpose of this exercise is to confirm that the program's functions are working correctly when compared to known analytical or measured solutions from literature.

Chapter four presents the seepage analysis of three typical design of earth dams. This chapter includes the study of the effect of the core on the seepage behavior before and after the drawdown condition. The study consists of an estimate of the water flux in the study-state condition and magnitude of the water flux that flows out of the dam through the *upstream* slope face as well as the foundation surface after dropping the water reservoir to two different levels under various drawdown rates. The effect of these upstream flux conditions is compared against those causing critical erosion conditions.

Chapter five proposes a suitable method to control the development of the excess pore water pressure after the drawdown events. This method recommends installing vertical filters on the upstream region and a horizontal filter on the foundation surface, at locations where the exit gradient can reach critical levels. The study uses the results of chapter four to develop critical design configurations. In particular, it includes investigating a suitable location of the upstream filter that provides effective results in reducing the exit gradient on the upstream face. The influence of the filter permeability on the seepage behavior is also studied.

Chapter seven presents the stability analysis of the dam under the influence of the drawdown event in the reservoir. The analysis is divided into two parts: the deformation field of the dam soil and the factor of safety against sliding failure. The first part includes estimating the deformed shape of the dam, and the magnitude and direction of movement of the soil particles under the sudden drawdown condition. The second part includes estimating the upstream factor of safety against sliding before and after the various drawdown conditions.

The numerical analysis conducted in chapter seven is next applied to a real-world earth dam to study the effect of drawdown conditions, in chapter eight. The study is performed on the Al-Adhaim Dam in Iraq. The seepage analysis includes estimation of the water flux, the exit gradient, and the influence of the upstream filter on protecting the upstream slope against the erosion. Lastly, a stability analysis is also conducted including a deformation analysis and the calculation of upstream factor of safety against sliding.

Chapter eight is the final chapter of the dissertation and includes the conclusions and recommendations for further research on this topic. The references are presented at the end of the dissertation.

## **CHAPTER TWO: LITERATURE REVIEW**

This chapter presents a review of the previous research on the earth dams to study the influence of some factors on the stability of earth dams. It is also focused on the factors that lead to some earth dam failures. This topic is understandably broad and the literature review focuses primarily on the influence of filters and the impact of the sudden drawdown of reservoir levels. The chapter is divided into two parts: the first deals with the seepage analysis, while the second part deals with the stability analysis. Additionally, references to relevant literature are included in individual chapters also to prepare them independently as publications.

### 2.1 Seepage Analysis

Li and Desai (1983) developed a procedure for seepage and stress analysis of earth dams based on FEM. Linear elastic, non-linear or piecewise linear elastic (hyperbolic) and plasticity (Drucker-Prager) models are used to model the soil constitutive behavior. They solved applications involving steady and transient free surface seepage and coupled stress and seepage analysis. The results were found to be comparable to field observations.

Lane and Griffiths (2000) produced operating charts for structure safety using FEM to provide a direct method to assess slope stability of the partial and complete submerged soil under the different rates of reservoir drawdown.

Flores-Berrones et al. (2011) describe the causes of the failure of the El Batán dam, located in El Pueblito River in central Mexico, twelve days before the complete filling of the reservoir in December of 1990. They found that there was a large variation of the water content within the



impervious core. Some elevations measured showed that the water content fell below the optimum water content on the dry side, which caused an increase in the horizontal permeability. This induced hydraulic fracturing of the core material and resulted in the internal erosion of the soil.

López-Acosta et al. (2014) utilized the SEEP/W program, based on FEM, to study the influence of filter in the reduction of the soil erosion problems under drawdown condition. Three filter types were analyzed at a drawdown rate of 1 m/day. The results showed a better efficiency in reducing the pore water pressure when using two horizontal filters at the toes of the upstream and downstream slope.

Moharrami et al. (2014) modeled an earth dam based on the finite element method by using the SEEP/W program for the seepage analysis and the SLOPE/W program for the stability analysis. The study focused on investigating the use of a number of horizontal filters, with various lengths and locations, on reducing the excess pore water pressure developed due to rapid drawdown of the upstream level. The results showed a very slight change of the seepage flow when increasing the number of the horizontal filter. However, the factor of safety of the slope increased with the increase in the number of horizontal drains. The stability of the upstream slope is further increased when drains are installed at the lower region of the upstream shell in comparison to a higher level.

Alonso and Pinyol (2016) calculated the distributions of the pore water pressure within the slope under rapid drawdown condition using different approaches. They analyzed two real cases to study the effect of rapid drawdown. The first case study involved the Glen Shira Dam in Scotland. The dam was mainly made of well graded and non-plastic moraines. The upstream slope was covered by a rockfill filter for increasing the stability of the slope. A thin wall of reinforced concrete was

also used in the dam center. Another case modeled was the slope failure of the Canelles Reservoir in Spain after a reservoir drawdown event. The rainfall effect was also simulated into the model. The results showed that coupled flow-deformation analysis is necessary for saturated and unsaturated soils to measure the distribution of the pore water pressure within the slope.

Tiwari et al. (2018) made several physical models of soil to study the influence of soil density of the slope on the soil deformation and the stability of the slope. The soil used in the experiments was obtained from a housing development project in Fullerton, California. The study included nine different densities of the soil with the relative compactions ranging from 60% to 80%. The slope inclinations modeled varied between 40 and 45 degrees. The slopes were subjected to a uniform intensity of rainfall at a rate of 3 cm/hr until it reached saturated conditions. Then, the seepage velocities were measured at various locations on the slope. The results showed the lowest level of the seepage velocity occurred at the slope toe, while the velocity increases gradually toward the top of the slope until reach to the maximum magnitude of the seepage velocity at the crest. The settlement in the soil is influenced by its compaction density in the slope. The experiment results for relative densities close to 60%, the slope showed low settlement values. For samples with relative compaction larger than 65%, the velocity of the seepage increased when the relative compaction is decreased.

## 2.2 Slope Stability Analysis

Tang and Zheng (2008) adopted the PLAXIS program, based on the finite element method, to analyze the slope stability under drawdown condition. They simulated an ideal elastic-plastic soil model and used the yield criterion from the Mohr-Columb theory. The dam is analyzed under both

drained and undrained conditions, and the results were compared. The results showed a reduction in the factor of safety when the water level was drawn down under the drained condition. The drawdown process develops unfavorable excess pore water pressure inside the slope which reduces its stability. However, the stability factor under the undrained condition was higher when the water level was lowered by more than 20 m because of the vertical action of the excess pore water pressure under undrained condition.

Fredlund et al. (2011) combined the analysis of seepage and slope stability for levee design under rapid drawdown conditions. The SVSLOPE and SVFLUX software were utilized for analysis of the 3-stage Duncan total stress approach and the effective stress analysis. The analysis showed a difference in the results between the total stress and the effective stress analysis. The reason is consideration of transient pore water pressure in the slope stability analysis and influence of the geometry on the flow system in an earth dam or levee.

Jiang et al. (2011) utilized a numerical model to investigate the effect of dropping the level of a river on the stability of the slope that resulted in the famous Qiautou Landslide in the Three Gorges Dam. The field investigation showed that the soil in the area of the landslide mainly consisted of thick, loose silt and clay mixed with fragments of rock, while the bedrock was made up of silty sandstone. Field and laboratory tests showed a high permeability of the landslide mass. The landslide mass was modeled by using FLAC<sup>3D</sup> and the drawdown of the reservoir is simulated from level 175 to 145 m at a drawdown rate of 25 cm/day. The results indicate a large amount of deformation of the landslide mass at this drawdown rate. The deformation in the initial stage mainly takes place because of the seepage force, but then changes to the effect of consolidation.

The maximum deformation appears on the top of the landslide at a displacement of 24.5 cm, where the surface of the bedrock is steeper and the loose deposits are not as thick.

Khanna et al. (2014) identify the influence of the vertical core thickness on the slope stability of earth and rock fills dams. An analytical study was applied to a 180 m high earth and rock fill dam placed on a strong layer. The study showed that the slope stability may or may not be influenced if the core thickness is between 50%-150% of the dam height. The factor of safety of the slope begins to reduce when the core thickness is more than 150% of the dam height. These ratios can be influenced by the relative strength of core to shell. It is showed that a much weaker core in comparison to the shell begins to cause a reduction of the slope stability at a core thickness of 100% of the dam height. For the upstream slope stability under rapid drawdown condition, the results showed that the influence of drawdown depth and dam height have no influence on the slope stability and the core thickness is the main influence.

López-Acosta et al. (2014) used the SLOPE/W software to analyze the slope stability of levees on both the upstream and the downstream sides. The Morgenstern-Price limit equilibrium method is utilized for this analysis. The results showed that the factor of safety (FoS) depends on the water level at the upstream and decreases with the decrease of the upstream water level. The FoS of both upstream and downstream slopes can reach maximum values if using two horizontal filters on the upstream and downstream toes.

Vandenberge (2014) analyzed the upstream slope stability of the Pilarcitos Dam under rapid drawdown condition. The upstream slope of the dam failed in 1969 after the water level in the reservoir was rapidly lowered by 10.7 m in 43 days. The slip surface is observed to lie in the

middle of the slope with the perpendicular depth of 5 m. Vandenberg (2014) used a new total stress rapid drawdown method for the analysis based on the finite element method. Prior to the drawdown event, linear elastic finite element analysis is used to determine the effective consolidation stresses in the upstream slope. The results showed a close match with the results of limit equilibrium and the observed failure surface when using the average strength envelopes. The failure mechanism predicted for Pilarcitos Dam response is sensitive to the relationship between undrained strength and consolidation stress.

Fattah et al. (2015) utilized the finite element method to estimate the flux amount through the earth dam and test behavior of earth dams during the rapid drawdown of water in the reservoir. The software SEEP/W and SLOPE/W, subprograms of Geostudio 2007, are used for this purpose. The Dau Tieng reservoir, located in Tay Ninh province in South Vietnam, is used as a case study. It was concluded that the flux amount through the earth dam decreases with time after the rapid drawdown of water in the reservoir begins. The stability of the slope is also decreased at the beginning of drawdown and then start increasing after a period. The reason is that the excess pore water pressure dissipates with time. The slope stability factors become unsafe as soon as the water level in reservoir drawdown becomes lower than  $1/3$  of the dam height.

Alonso and Pinyol (2016) studied the effect of the rapid drawdown on two real cases. The first study was applied to the Glen Shira Dam. The dam is 16 m high and mainly made of well graded and non-plastic moraines. The upstream slope is covered by a rockfill filter for increasing the strength and slope stability. A thin wall of the reinforced concrete is used in the dam center as a core. The second case modeled was the failure of the slope of the Canelles Reservoir in Spain after

a drawdown event. The rainfall effect is also simulated within the model. The increase in the pore water pressure was found to be the reason for the slope failure.

Luo and Zhang (2016) performed experiments to study the deformation of the upstream slope that occurs as a result of dropping the water level in a reservoir. The experimental device consists of the slope model and the drawdown simulation which consists of the water tank, two valves, segments of piping, the digital control module, and pore pressure sensors. The results showed an increase of the slope deformation with an increase of the slope gradients. The slip surface under the drawdown event becomes deeper with an increase in the slope gradient. The deformation starts at the top of the slope and extends downward following the drawdown.

VandenBerge and Wright (2016) improved the linear interpolation method to calculate undrained strength interpolation for the entire slip surface under rapid drawdown condition. This method can be applied for cases with the drained cohesion intercept equals to zero. The improved method can also be used for the nonlinear envelopes in a piecewise linear fashion. For seismic analysis, the new method can be used to determine the undrained shear strength or for cases at low effective consolidation stresses.

Stark et al. (2017) studied the upstream slide of the San Luis Dam which occurred in 1981 because of the reservoir drawdown. SEEP/W and SLIDE 6 software are used to model the dam for both saturated and unsaturated soil. The model is used to predict the phreatic surface and to evaluate the pore water pressure at the failure time. As a consequence, it is possible to analyze a slope stability without requiring undrained shear strength.

Sui and Zheng (2017) also prepared an experiment to investigate the failure of the soil slope during drawdown conditions. They used transparent soils for the experiment and developed a control system to simulate the drawdown at various speeds. In addition, they used the charge-coupled camera to record the failure process. The results showed that the process of the slope failure is divided into two stages. The first stage is surface sliding, while the second stage is the overall bulk sliding caused by partial instability which develops gradually. The results also showed an influence of the drawdown on the slope angle.

Zhang and Luo (2017) developed a simplified method to analyze the stability of a strain-softening slope for determining the subsidiary shear deformation under drawdown events. This method is based on a new algorithm and was verified to be effective in the stability evolution analysis of the strain-softening slopes caused by the dropping of the water level. The results showed that the behavior of the strain-softening and the initial level of water have a significant effect on the critical slip surface and the slope stability under the drawdown event. The behavior of the progressive failure is important to prevent the overestimation of the slope factor of safety.

Stark and Jafari (2018) recently utilized the finite element method to investigate the reasons that caused the upstream slope failure of the San Luis Dam under a drawdown event. 2D SEEP/W program is used for the seepage analysis to predict changes in the phreatic line under various water level and investigate the effect of the unsaturated properties on dissipation of the pore water pressure under the drawdown event. SLOPE/W program is performed for the effective stress drawdown stability analyses to estimate the factor of safety by using the Spencer method. Stress-dependent drained shear strengths were used in effective stress analyses for the fine-grained core

and slopewash materials. The pore water pressures induced by the seepage were estimated in the slopewash and fine-grained core through a correction of the saturated and unsaturated parameters from piezometers installed inside the dam after the slope failure. The results showed the ability to use the steady-state seepage analysis to estimate the initial suction conditions for the unsaturated and transient analysis of the seepage. The pore water pressure induced by changes in the hydraulic conditions can be obtained from an unsaturated transient analysis of seepage. The stability analysis methodology incorporates stress-dependent drained shear strength envelopes and shear-induced pore-water pressures to determine the factor of safety. The shear strengths and the factor of safety, estimated at different water levels, are used to provide recommendations for calibrating unsaturated soil properties, integrating seepage-induced, and shear-induced pore-water pressures in analyses of the stability, and validating the use of commercial software for analyses of the stability under drawdown conditions. This approach is used in the present study.



## **CHAPTER THREE: NUMERICAL MODELS FOR THE SEEPAGE AND STABILITY ANALYSIS USING THE FINITE ELEMENT METHOD (FEM)**

### 3.1 Introduction

A numerical model is a powerful tool that can be used to simulate a real physical process mathematically. In groundwater applications, numerical models are useful in studying various seepage cases and simulating the flow of water through an earthen structure. The soil behavior is simulated mathematically instead of using scaled or full-size physical models of the dam in the lab. Researchers can set up the model very quickly, supply a wide range of the boundary conditions, and provide results at any location of the model (SEEP/W, 2012). Numerical model can also take into account gravitational forces in the analysis, which are difficult to account for when using a scaled model in the laboratory, unless one uses a centrifuge (SEEP/W, 2012; SIGMA/W, 2012). However, numerical models also have some limitations. For instance, it is not possible to associate temperature changes, volume changes and chemical changes coupled with seepage flow concurrently in the current model (SEEP/W, 2012; SIGMA/W, 2012).

### 3.2 Seepage Analysis

#### 3.2.1 The Governing Equation

The long-term study state and the transient analysis of the seepage are conducted by using numerical models. SEEP/W is a numerical model is used which is a tool using the finite element method to simulate the water flowing through porous media (SEEP/W, 2012). SEEP/W is used to simulate the groundwater movement in both the steady or transient states. The program is

formulated based on the flow of water through both saturated and unsaturated soils following Darcy's Law, which may be expressed as:

$$q = k \cdot i \quad (3.1)$$

with  $q$  being the specific discharge,  $k$  being the hydraulic conductivity, and  $i$  being the gradient of the total hydraulic head. The hydraulic conductivity in Equation (3.1) is maintained as a constant value for the full saturated soil, while it is modeled as various values for the unsaturated soil changing with the water content of the soil.

The general governing differential equation for two-dimensional seepage can be expressed mathematically as (SEEP/W, 2012):

$$\frac{\partial}{\partial x} \left( k_x \frac{\partial H}{\partial x} \right) + \frac{\partial}{\partial y} \left( k_y \frac{\partial H}{\partial y} \right) + Q = \frac{\partial \theta}{\partial t} \quad (3.2)$$

with  $H$  the total head,  $k_x$  the hydraulic conductivity in the x-direction,  $k_y$  the hydraulic conductivity in the y-direction,  $Q$  the applied boundary flux,  $\theta$  the volumetric water content, and  $t$  time.

Mainly, this equation equates the water flux flowing through a two-dimensional elemental volume in  $x$ - and  $y$ -directions plus the applied boundary flux to the volumetric water content with consideration to the time (SEEP/W, 2012). The change in the volumetric water content is related to the changes in the stress state variables:  $(\sigma - u_a)$  and  $(u_a - u_w)$ , where  $\sigma$  is the total stress,  $u_a$  is the pore-air pressure, and  $u_w$  is the pore water pressure. SEEP/W (2012) considers the total stress in the soil is constant, which means there is no change in the variable of  $(\sigma - u_a)$ . Also, the program assumes no change in the pore air pressure ( $u_a$ ). Therefore, the change in the volumetric

water content of a soil depends only on the change in the pore water pressure ( $u_w$ ). The volumetric water content is calculated by using the following equation:

$$\partial\theta = m_w\gamma_w\partial(H - y) \quad (3.3)$$

With  $m_w$  the storage curve slope,  $\gamma_w$  the unite weight of water,  $H$  the total hydraulic head, and  $y$  the elevation. By substituting Equation (3.3) into Equation (3.2), the general governing differential equation may be stated as (SEEP/W, 2012):

$$\frac{\partial}{\partial x}\left(k_x \frac{\partial H}{\partial x}\right) + \frac{\partial}{\partial y}\left(k_y \frac{\partial H}{\partial y}\right) + Q = m_w\gamma_w \frac{\partial(H - y)}{\partial t} \quad (3.4)$$

### 3.2.2 The Finite Element Equations

The Galerkin method is applied to the governing differential equation (Equation 3.2) to drive the finite element equation used for the two-dimension seepage is express as (SEEP/W, 2012):

$$\tau \int_A ([B]^T[C][B])dA \{H\} + \tau \int_A (\lambda < N >^T < N >)dA \{H\}, t = q\tau \int (< N >^T)dL \quad (3.5)$$

with  $[B]$  the gradient matrix,  $[C]$  the hydraulic conductivity matrix of the element,  $\{H\}$  the vector of nodal heads,  $\lambda$  the storage term in the transient condition of the seepage which is equal to  $m_w\gamma_w$ ,  $< N >$  the interpolating function vector,  $q$  the magnitude of the unit flux across the element edge,  $\tau$  the element thickness,  $t$  the time,  $A$  and  $L$  are the designation for summation over the area and the edge of an element, respectively. Equation (3.5) can be reduced by using the element characteristic matrix term  $[K]$ , the mass matrix term  $[M]$ , and the element applied flux vector  $[Q]$ , to the following expression (SEEP/W, 2012):

$$[K]\{H\} + [M]\{H\}, t = \{Q\} \quad (3.6)$$

Under steady-state conditions, the term  $\{H\}, t$  is equal to zero and Equation (3.6) is simplified to:

$$[K]\{H\} = \{Q\} \quad (3.7)$$

The hydraulic conductivity matrix is (SEEP/W, 2012):

$$[C] = \begin{bmatrix} C_{11} & C_{12} \\ C_{21} & C_{22} \end{bmatrix} \quad (3.8)$$

where:  $C_{11} = k_x \cos^2 \alpha + k_y \sin^2 \alpha$

$$C_{22} = k_x \sin^2 \alpha + k_y \cos^2 \alpha$$

$$C_{11} = k_x \cos^2 \alpha + k_y \sin^2 \alpha$$

$$C_{21} = C_{12}$$

with  $k_x$  the hydraulic conductivity in the  $x$ -direction,  $k_y$  the hydraulic conductivity, and  $\alpha$  the direction angle (in degrees) of the hydraulic conductivity. Equation (3.8) reduces to a simplified form when the direction angle of the hydraulic conductivity is zero and the hydraulic conductivity matrix becomes:

$$[C] = \begin{bmatrix} k_x & 0 \\ 0 & k_y \end{bmatrix} \quad (3.9)$$

The hydraulic conductivity ( $k_y$ ) is computed by using the equation for the ratio as:

$$k_y = k_x \times k_{Ratio} \quad (3.10)$$

### 3.3 Stress-Deformation Analysis

The second step of the modeling process is to analysis the stress-deformation response of the dam. Stress and deformation analyses can be performed for earth structures by using SIGMA/W program. SIGMA/W is also a finite element approach and is a comprehensive formulation that makes it possible to analyze both simple and highly complex problems. The program is formulated in the strain plane for two-dimension or axisymmetric problems by using the small strain theory. The finite element equation for this formulation can be stated as (SIGMA/W, 2012):

$$\int_v [B]^T [C] [B] dv \{a\} = b \int_v \langle N \rangle^T dv + p \int_A \langle N \rangle^T dA + \{F_n\} \quad (3.11)$$

with  $[B]$  strain-displacement matrix,  $[C]$  constitutive matrix,  $\{a\}$  column vector of nodal incremental x- and y-displacements,  $\langle N \rangle$  row vector of interpolating functions,  $A$  area along the boundary of an element,  $v$  volume of an element,  $b$  unit body force intensity,  $p$  incremental surface pressure, and  $\{F_n\}$  concentrated nodal incremental loads. SIGMA/W (2012) consider the thickness of all elements ( $t$ ) as constants for the two-dimension analysis. Thus, Equation (3.11) can be expressed as:

$$t \int_A [B]^T [C] [B] dA \{a\} = bt \int_A \langle N \rangle^T dA + pt \int_L \langle N \rangle^T dL \quad (3.12)$$

The equation can be abbreviated further by using the element characteristic matrix term  $[K]$  instead of the left side of the equation,  $t \int_A [B]^T [C] [B] dA$ , and using the incremental force  $\{F\}$  applied on the nodes instead of the term in the right side. Equation (3.12) becomes:

$$[K]\{a\} = \{F\} \quad (3.13)$$

where  $\{F\}$  consist of incremental body forces, incremental pressures applied on the surface boundary, and concentrated nodal incremental forces.

SIGMA/W (2012) solves this finite element equation for each time step to obtain incremental displacements and calculates the resultant incremental stresses and strains. It then sums all these increments cumulatively from the first-time step and reports the summed values in the output files.

The program also defines the strain vector in the three directions by using the engineering shear strain as follows:

$$\{\varepsilon\} = \begin{Bmatrix} \varepsilon_x \\ \varepsilon_y \\ \varepsilon_z \\ \gamma_{xy} \end{Bmatrix} \quad (3.14)$$

For two direction, the strain vector in the  $z$ -direction ( $\varepsilon_z$ ) is assumed to be zero. The displacement in the field takes place because of the changes in the stress and is correlated with the strain vector.

The strain matrix for two directions is express as (SIGMA/W, 2012):

$$\{\varepsilon\} = [B] \begin{Bmatrix} u \\ v \end{Bmatrix} = \begin{bmatrix} \frac{\partial N_1}{\partial x} & 0 & \dots & \frac{\partial N_8}{\partial x} & 0 \\ 0 & \frac{\partial N_1}{\partial y} & \dots & 0 & \frac{\partial N_8}{\partial y} \\ 0 & 0 & \dots & 0 & 0 \\ \frac{\partial N_1}{\partial x} & \frac{\partial N_1}{\partial y} & \dots & \frac{\partial N_8}{\partial x} & \frac{\partial N_8}{\partial y} \end{bmatrix} \begin{Bmatrix} u \\ v \end{Bmatrix} \quad (3.15)$$

with  $[B]$  the strain matrix,  $u$  the nodal displacement in  $x$ - direction, and  $v$  the nodal displacement in  $y$ - direction. The stresses in the soil are correlated to the strains under the elasticity theory assumption and the stress-strain equation becomes (SIGMA/W, 2012):

$$\{\sigma\} = [C]\{\varepsilon\} = \frac{E}{(1 + \nu)(1 - 2\nu)} \begin{bmatrix} 1 - \nu & \nu & \nu & 0 \\ \nu & 1 - \nu & \nu & 0 \\ \nu & \nu & 1 - \nu & 0 \\ 0 & 0 & 0 & \frac{1 - 2\nu}{2} \end{bmatrix} \{\varepsilon\} \quad (3.16)$$

where  $[C]$  is the property matrix of elements,  $E$  is the Young's modulus, and  $\nu$  is the Poisson's ratio. The matrix  $[C]$  in the strain plane is the same for the two-dimension cases.

### 3.4 Slope Stability Analysis

The section discusses the underlying theory used in the analysis of the stability of slopes in this research. The critical surface of failure may lie between the top soil and a cylindrical surface in a finite slope. The shear strength on the critical surface consists of two components, soil cohesion, and frictional resistance. The driving shear forces consist of self-weight of the soil mass in the downward direction of the slope. The failures occur generally when the driving shear forces are greater than the shear strength. (Duncan et al., 2014) The General Limit Equilibrium (GLE) theory is presented below and used as the context for relating the factors of safety for all commonly used methods of slices.

A factor of safety is defined as that factor by which the shear strength of the soil must be reduced to bring the mass of soil into a state of limiting equilibrium along a selected slip surface (SLOPE/W, 2012). **Figures 3.1** shows the acting forces on a slope slice through a sliding mass, where  $A$  is the resultant external water force,  $E$  is the horizontal interslice normal force,  $N$  is the total normal force acting on the slice base,  $S_m$  is the shear force acting on each slice base,  $X$  is the vertical interslice shear force,  $kW$  is the horizontal seismic load applied on each slice center, and  $W$  is the total weight of a slice. SLOPE/W (2012) uses the theory of limit equilibrium of forces

and moments to compute the factor of safety against failure. The program uses two independent equations to estimate the factor of safety. The factor of safety can be related to the moment equilibrium when only the moment equilibrium is satisfied as follow (SLOPE/W, 2012):

$$F_m = \frac{\sum(\dot{c}\beta R + (N - u\beta)R \tan \phi)}{\sum Wx - \sum Nf + \sum kW e \pm \sum Dd \pm \sum Aa} \quad (3.17)$$

For the horizontal force equilibrium, the factor of safety equation is written as (SLOPE/W, 2012):

$$F_f = \frac{\sum(\dot{c}\beta \cos \alpha + (N - u\beta) \tan \phi \cos \alpha)}{\sum N \sin \alpha + \sum kW - \sum D \cos \omega \pm \sum A} \quad (3.18)$$

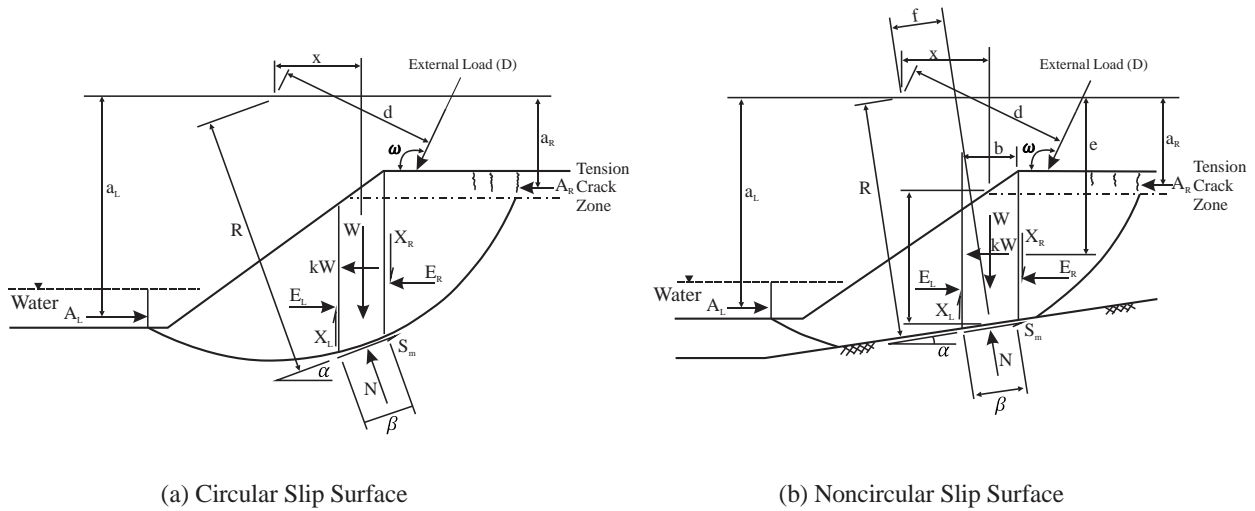


Figure 3.1: The diagram of forces acting on an earth slope for a circular and noncircular slip surface (SLOPE/W, 2012).

In general, the slope of the dam is divided into unsaturated and saturated soil zones separated by the phreatic line. Negative pore water pressure develops above the phreatic line relative to air



pressure. The shear strength of the soil in the unsaturated state of the soil is stated through modified Mohr-Coulomb form. The equation of the soil shear strength ( $s$ ) is written as (SLOPE/W, 2012):

$$s = c' + (\sigma_n - u_a) \tan \phi' + (u_a - u_w) \tan \phi^b \quad (3.19)$$

with  $u_a$  the pore-air pressure,  $u_w$  the pore water pressure, and  $\phi^b$  the increase in shear strength for an increase in suction. As presented in Equation (3.19), the shear strength of a slope requires the knowledge of the cohesive strength ( $c'$ ), the frictional strength ( $\phi'$ ), and the suction strength ( $\phi^b$ ). Under the unsaturated condition of the soil, the factor of safety related to the moment equilibrium is modified and expressed as (SLOPE/W, 2012):

$$F_m = \frac{\sum \left( \dot{c}\beta R + \left[ N - u_w\beta \frac{\tan \phi^b}{\tan \phi'} - u_a\beta \left( 1 - \frac{\tan \phi^b}{\tan \phi'} \right) R \tan \phi' \right] \right)}{\sum Wx - \sum Nf + \sum kW_e \pm \sum Dd \pm \sum Aa} \quad (3.20)$$

$$F_f = \frac{\sum \left( \dot{c}\beta \cos \alpha + \left[ N - u_w\beta \frac{\tan \phi^b}{\tan \phi'} - u_a\beta \left( 1 - \frac{\tan \phi^b}{\tan \phi'} \right) \tan \phi' \cos \alpha \right] \right)}{\sum N \sin \alpha + \sum kW - \sum D \cos \omega \pm \sum A} \quad (3.21)$$

where  $N$  is the normal force acting on the slice base and calculated by using the equation:

$$N = \frac{W + (X_R - X_L) - \frac{[c'\beta \sin \alpha + u_a\beta \sin \alpha (\tan \phi' - \tan \phi^b) + u_w\beta \sin \alpha \tan \phi^b]}{F} + D \sin \omega}{\cos \alpha + \frac{\sin \alpha \tan \phi'}{F}} \quad (3.22)$$

In fact, equation (3.22) can be used in both soil conditions, unsaturated and saturated soil. SLOPE/W (2012) uses  $\phi^b$  for the saturated soil where the pore water pressure is negative, and  $\phi'$  for the saturated soil where the pore water pressure is positive.

In this dissertation, the method used to calculate the factor of safety is Spencer's Method. Spencer's Method assumes that all side forces are inclined at the same angle. Unlike the Modified Swedish Method, the side force is calculated as part of the equilibrium solution and not assumed. Spencer's Method also assumes that the normal forces on the bottom of the slice act at the center of the base. Spencer's Method fully satisfies the requirements for both force and moment equilibrium (Spencer, 1967). In contrast, the Simplified Bishop method satisfied only vertical force and overall moment equilibrium, while the Simplified Janbu method satisfies only vertical and horizontal force equilibrium (SIGMA/W, 2012; U.S. Army Corps of Engineers, 2003). Spencer's Method requires the use of a computer program to perform the calculations because of the complexity of the method and the lengthy calculations involved (U.S. Army Corps of Engineers, 2003). The method is used where a statically complete solution is desired. It is also used as a check on final designs where simpler methods performed the slope stability computations.

### 3.5 Validation Problems

This section presents the results of the seepage analysis for two different cases. The purpose is to verify that the GeoStudio software is providing results that are reasonable when compared to analytical and observed results. The first case is using simple flow net method for seepage analysis under the steady-state condition and the second is a comparison with results from laboratory tests under transient condition.

#### 3.5.1 Steady-State Problem Case

This section presents a comparison results between the flow net method using flow nets for seepage analysis and GeoStudio software using the FEM. The model includes a dam of height 50 m and

length 100 m. The water level at the upstream side is 35 m and is zero at the downstream side.

**Figure 3.2** shows the boundary conditions and the finite element mesh used for this purpose. Three dam cases are used to plot the flow net and calculate the seepage quantity through the dam. The profile section of the dam cases and the soil properties are presented in **Figure 3.3a**. The dam cases, presented in **Figure 3.3a**, are: (Smith, 2014)

- Homogenous isotropic soil (Case A).
- Homogenous isotropic with a downstream filter (Case B).
- Homogenous anisotropic soil with a downstream filter (Case C).

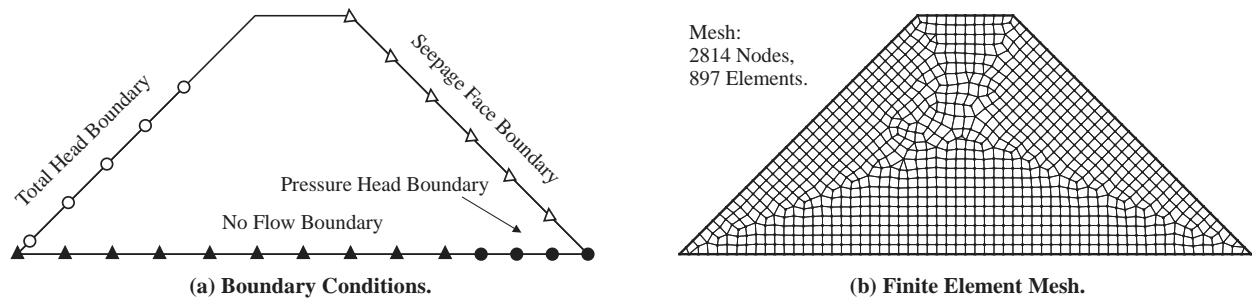


Figure 3.2: Boundary conditions and the finite element mesh for the dam model.

**Table 3.1** shows the saturated hydraulic conductivity for the dam cases and the results of the seepage quantity, flowing through the dam, calculated by the flow net method and FEM. The contours lines of the total head and the flow net calculated by the finite element method are presented in **Figure 3.3b**.

Table 3.1: Comparison of the seepage quantity under the steady-state condition.

Dam Cases	Hydraulic Conductivity (m/s)		Seepage Quantity (m <sup>3</sup> /day/m)	
	$k_x$	$k_y$	Flow Net	FEM
A	$5.8 \times 10^{-7}$	$5.8 \times 10^{-7}$	0.39	0.3447
B	$5.8 \times 10^{-7}$	$5.8 \times 10^{-7}$	0.5	0.466
C	$5.8 \times 10^{-7}$	$2.3 \times 10^{-7}$	0.3933	0.433

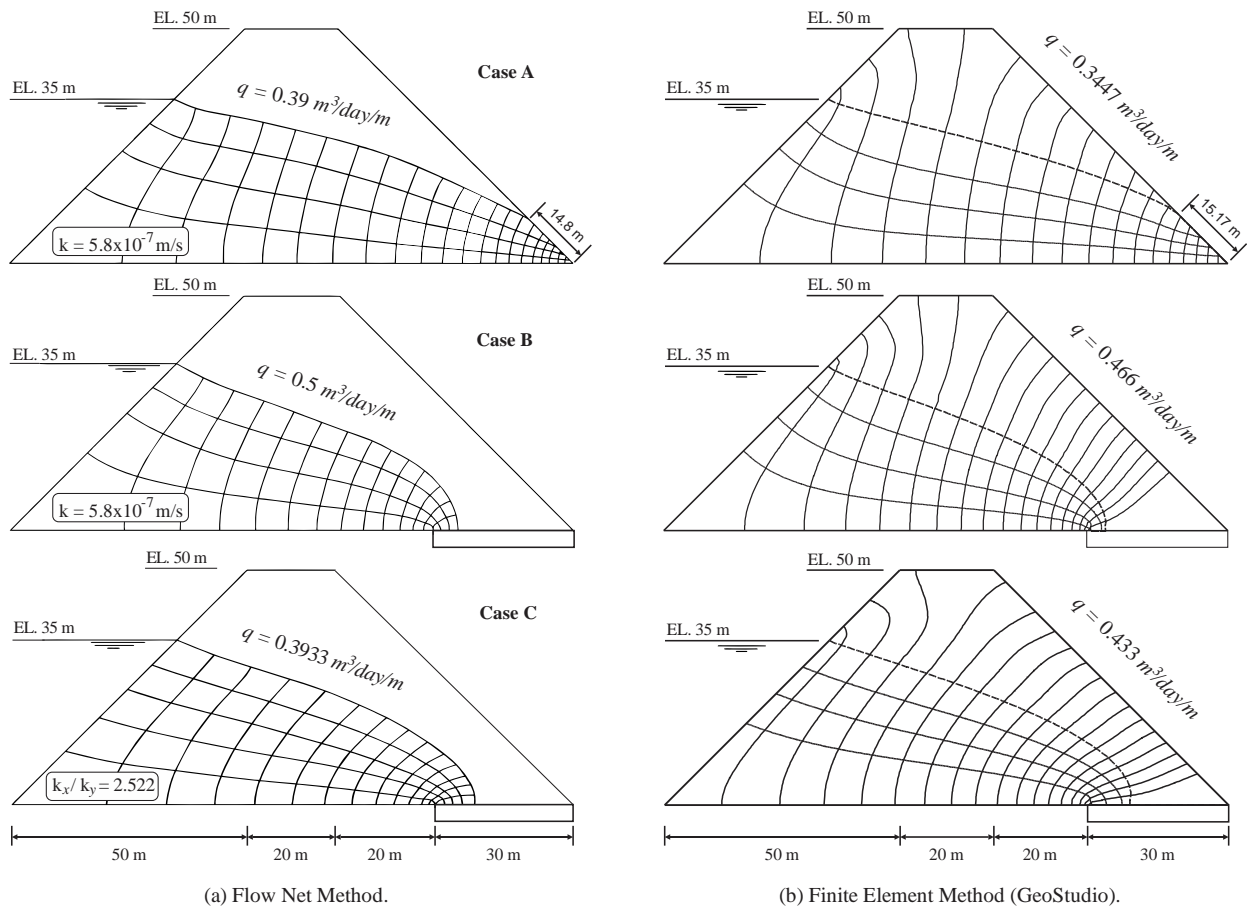


Figure 3.3: Comparison of the results of the seepage analysis between the flow net method and the finite element method (FEM).

The results showed a good match between the two approaches. The reason for the difference may be attributed to approaching used in the flow net method, proposed by Casagrande, which depends on plotting a square net of the flow lines and the equipotential lines to locate the phreatic surface inside the dam and is sensitive to the type of elements used. On the other hand, FEM analyzes the seepage problems mathematically by using the governing differential equation of seepage flow and may be considered more accurate.

### 3.5.2 Transient Case

This section presents a comparison of the experimental results from testing in the laboratory and the results from the modeling using GeoStudio using FEM. In 1941, Kellogg had constructed a physical model of an earth dam to predict the phreatic line and measure the total head inside the dam at various locations (Chang, 1986, 1987, 1988). The model was made of standard Ottawa sand with a typical permeability range of 0.0085 to 0.21 cm/sec. Seven pore pressure cells were embedded inside the dam to measure the total head. The height of the dam was 38 cm and the reservoir was filled up to level 38 cm. The experimental was initially maintained in a constant state until the steady-state flow conditions developed. **Figure 3.4a** shows the profile section of the experiment and the location of the pore pressure cells. Next, the reservoir water levels were dropped at a drawdown rate of 6.1 cm/sec. and the phreatic surface and corresponding total heads were measured.

The experiment is modeled using GeoStudio as a verification exercise. The permeability of the soil is considered to vary within a range of  $1 \times 10^{-6}$  to 0.1 cm/sec. The boundary conditions for the seepage analysis is presented in **Figure 3.4b**. The finite element mesh is carried out with elements

of 1525 and nodes of 4724 as shown in **Figure 3.5a**. The results of the phreatic line in the transient conditions are compared to the published experimental results in **Figure 3.5**. The phreatic line computed by the program is slightly higher than the measured at the upstream, while it is lower at the downstream as shown in **Figure 3.5b**.

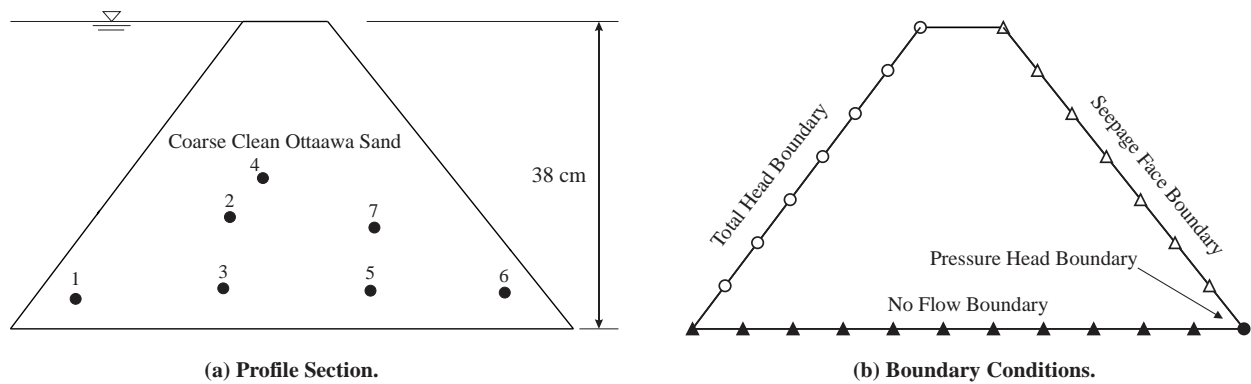


Figure 3.4: Profile section of the experiment and the boundary conditions of the model.

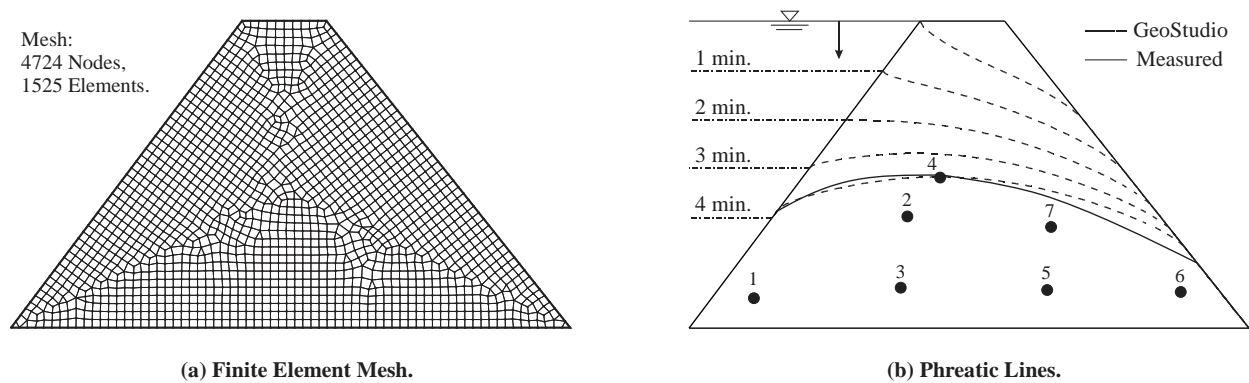


Figure 3.5: Finite element mesh and phreatic surfaces for the steady-state and transient conditions.

**Figure 3.6** shows the comparisons of measured and computed value of total head at the cell locations. The results showed no influence of the hydraulic conductivity on the total head when it is in a steady-state condition. Under drawdown conditions, the results for the total head showed a good match with the measured total head in most cells when using a hydraulic conductivity value of 0.011 cm/sec (**Figure 3.6**). There is a slight difference between the total head in some cells, for instance in cell 3 and cell 6. The reason may be because soil permeability of the dam used in the laboratory physical model is not uniform.

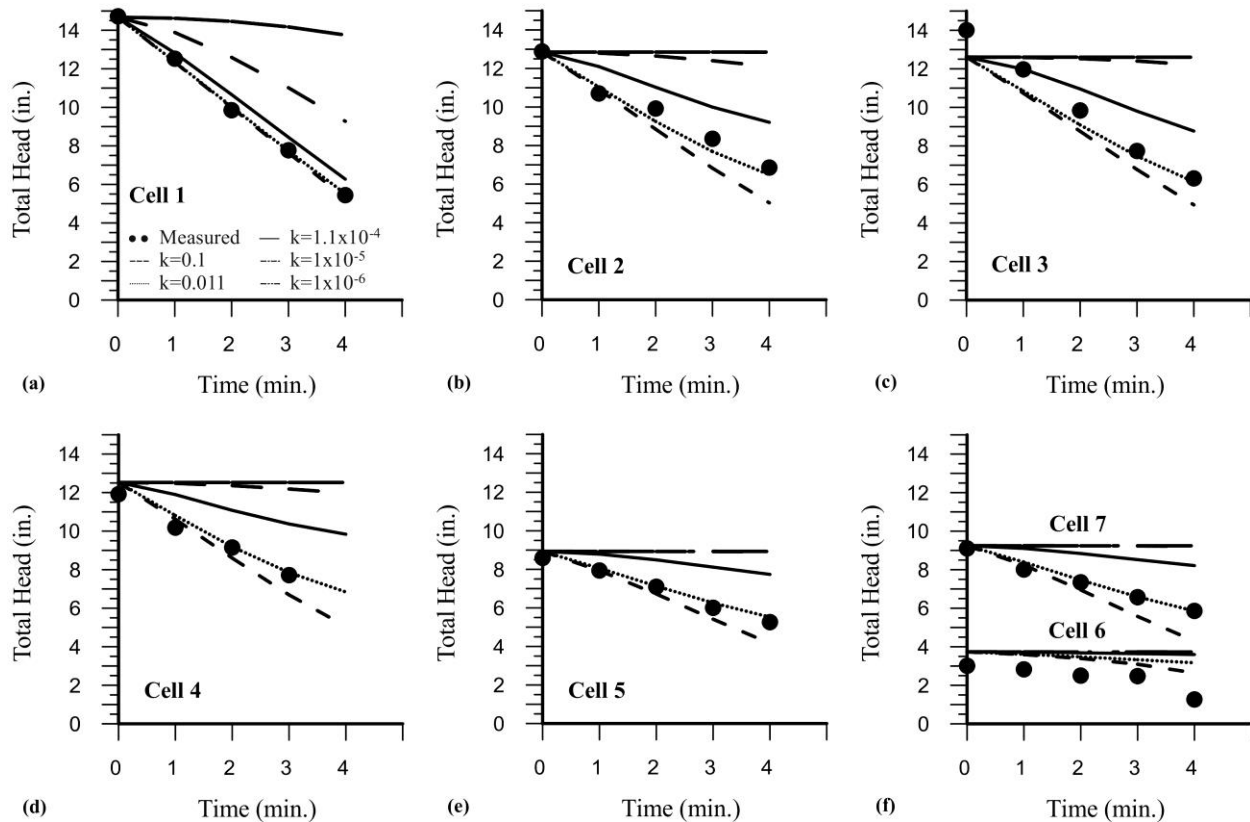


Figure 3.6: Comparisons of the total head in (in.) for the pore pressure cells.

In conclusion, the verification exercise conducted here showed a good match for the results when using the FEM program. Thus, GeoStudio 2012 will be used to model different cases of earth dams and simulate flow problems through porous media. The next four chapters will present results of the analysis of the earth dams under various drawdown conditions.



## **CHAPTER FOUR: EFFECT OF THE CORE ON INCREASING THE INTERNAL EROSION POTENTIAL UNDER DRAWDOWN CONDITIONS**

### **4.1 Introduction**

An earth dam is an earthen structure that is constructed for different applications, such as flood control and irrigation. Water transfer through the porous media (i.e. soil) from areas of the higher head to those of lower head. During the transfer, water loses energy due to the permeability of the soil. The magnitude of the energy loss is increased with the decreased permeability of the soil and a higher velocity of flow. There are many factors that put this structure at risk and may cause failure. One of the major challenges to earthen structures is internal erosion and seepage control is used to protect against this mode of failure. The fine soil grains within the matrix of coarse grains may be washed away under the drag forces of the seepage flow (D. S. Chang & Zhang, 2013). It is shown that about 50% of the earth dams failures are caused by the piping erosion (Fell et al., 2014). Suffusion occurs in non-plastic soils, such as silts, sands, silty sands and silt, sand, gravel mixtures when the water flow through the widely-graded soil or gap graded cohesionless soils causing erosion of fine particles exiting the coarse matrix of the soil (Fell et al., 2014; Sibille et al., 2015). During the drawdown condition, the hydraulic gradient inside the soil becomes higher than that in the reservoir, which causes a development of the seepage force toward the upstream slope.

The exit gradient is an important aspect of the seepage process that influences the stability of hydraulic structures. During the drawdown conditions, erosion and piping can occur at the upstream end of a hydraulic structure when hydraulic gradients are large enough to move soil

particles. Therefore, an exit gradient must be computed and compared with a critical gradient to ensure the safety of the soil mass.

#### 4.2 Seepage Force and the Exit Gradient

Seepage force develops due to the difference in the head between two locations. This force acts in the same direction as the water flow independent of the orientation of the soil mass. To show that, three orientations of the soil mass (upward, horizontal, and downward) are presented in **Figure 4.1**. In **Figure 4.1a**, no flow occurs through the soil mass when the hydraulic gradient is equal. In **Figure 4.1b**, water must flow from the left side toward the right side. When the head on the right side is higher than that on the left side, water must flow through the soil mass from the right to the left (**Figure 4.1c**).

**Figure 4.2** presents the seepage force ( $F$ ) acting on the slope and the body force of a saturated soil mass acting on the foundation surface. The stability of the soil mainly depends on its unit weight (**Figure 4.2**). Seepage force may increase or decrease the soil stability depending on the seepage direction. Seepage force increases the soil stability if its direction downward as shown in **Figure 4.2b**. When the seepage direction upward (opposite direction of the soil force), the stability of the soil is decreased (**Figure 4.2c**). The magnitude of the seepage force is calculated by using the equation:

$$F_s = i \cdot \gamma_w \cdot z \cdot A \quad (4.1)$$

where  $F_s$  is the seepage force,  $\gamma_w$  is the unit weight of water,  $z$  is the section length of the soil, and  $A$  is the area section of the soil. This seepage force per unit volume is found by dividing the

force in equation (4.1) by the soil volume ( $z.A$ ) as follows:

$$f_s = \frac{i \cdot \gamma_w \cdot z \cdot A}{z \cdot A} = i \cdot \gamma_w \quad (4.2)$$

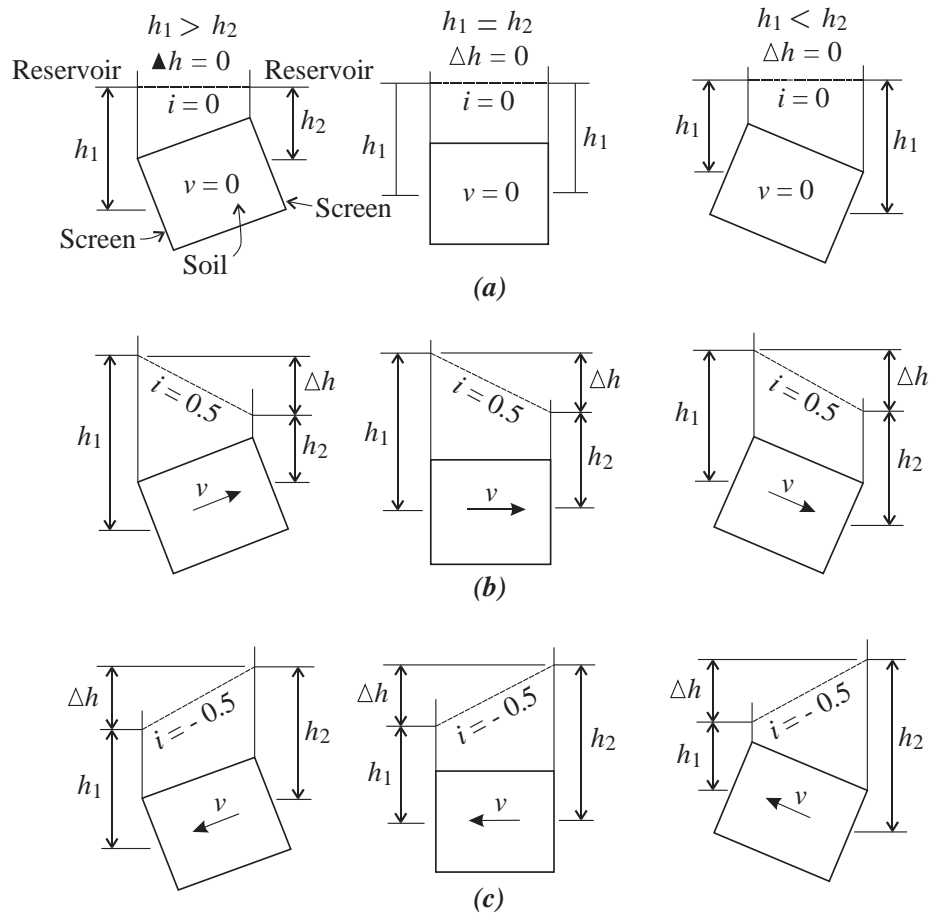


Figure 4.1: Flow of the water flux independent of soil direction (Cedergren, 1977).

This quantity is important in assessing the stability of the earth dams against piping that forms because of the action of the seepage force. The soil stability reaches the critical condition when

the seepage is equal to the effective stress. When the seepage force exceeds the combined forces from the submerged weight of soil, the soil behaves like a liquid and this condition is called “quicksand” or “boiling” resulting in enhanced erosion of the soil particles. The equation of the critical gradient is defined as:

$$i_c = \frac{\gamma_{sub}}{\gamma_w} = \left[ \frac{G_s - 1}{1 + e} \cdot \gamma_w \right] \cdot \frac{1}{\gamma_w} = \frac{G_s - 1}{1 + e} \quad (4.3)$$

where  $i_c$  is the critical gradient,  $\gamma_{sub}$  is the submerged unit weight of the soil,  $\gamma_w$  is the unit weight of water,  $G_s$  is the specific gravity of the soil, and  $e$  is the void ratio of the soil.

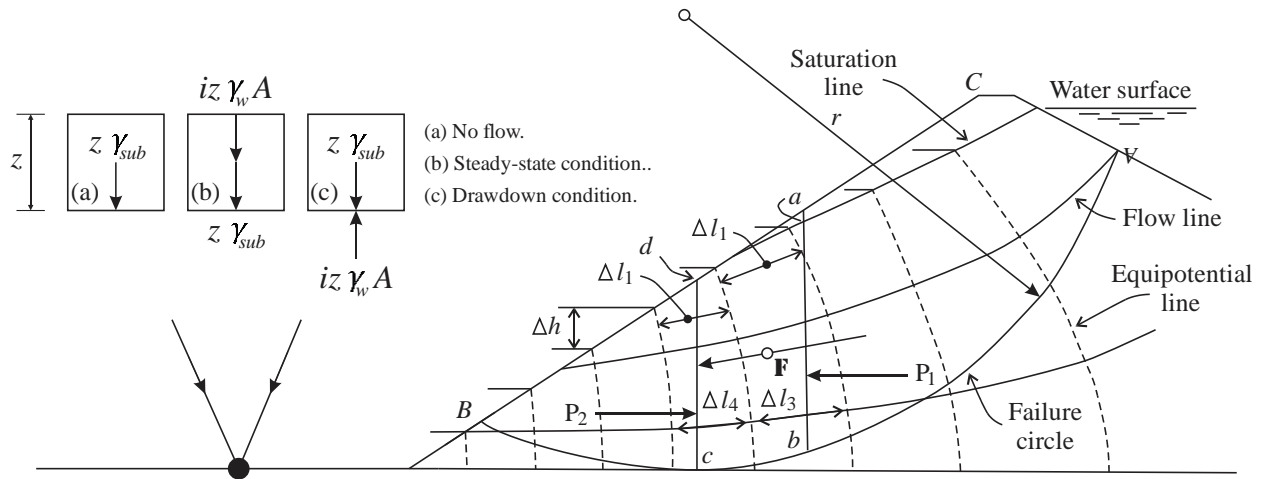


Figure 4.2: Seepage force acting on the dam slope and its foundation (Cedergren, 1977; Reddi, 2003).

Skempton and Brogan (1994) tested the initiation of piping in several sandy gravel specimens. They found that if the soil is internally unstable, the soil may, in fact, begin to erode at a gradient

lower than critical or zero effective stress gradient. They also found that, in a homogenous mass of unstable sandy gravels with the uniform porosity, the sandy soil may show piping behavior at hydraulic gradients one-third to one-fifth of the theoretical critical value. For stable sandy gravel, the sand particles begin to erode at a gradient close to the theoretical critical gradient.

Wan and Fell (2008) conducted laboratory tests to assess the potential of internal instability and suffusion in embankment dams and their foundations. They came to the same conclusion as Skempton and Brogan (1994) that the soil may begin to erode at a gradient lower than critical or zero effective stress gradient if it is internally unstable. All soils tested begin to erode with upward gradients of 0.8 or less, with several cases of less than 0.3. Soils with a higher porosity required lower gradients to begin to erode. With the same fines content, gap-graded soils begin to erode at gradients lower than non-gap-graded soils.

Ke and Takahashi (2012) studied the changes in cohesionless soil strength due to internal erosion caused by one-dimension upward seepage flow. Cone penetration tests were used to examine the mechanical properties of the soil during internal erosion. They found that the slope of the average hydraulic gradient is linear before erosion starts and changes to nonlinear after its inception. Internal erosion was found to occur at a hydraulic gradient one-fifth to one-third of the critical hydraulic gradient, based on Terzaghi's equation that is required for soil stability (Ke and Takahashi, 2012). The migration of the fine grains increases with hydraulic gradient and an increase of the hydraulic gradient beyond a value of 0.5 causes drastic changes in the soil strength. In addition, the angle of shearing resistance of a soil sample also decreases due to internal erosion.

### 4.3 Current Study

The findings of a study on the effect of the core with and without a low permeability cutoff on increasing the potential for the soil erosion at the upstream face of the dam are presented in this paper. Analysis of the seepage behavior before and after the water drawdown from the reservoir is carried out using FEM models. The influence of the drawdown rates in the water reservoir on the water flux that takes place between the soil mass within the dam and the reservoir is studied. The exit gradient, that may cause a migration of the soil particles and develop piping within both the dam and its foundation, is computed and compared to the critical values.

### 4.4 Description of the Earth Dam

In this chapter, a general case of an earth dam has been studied. It consists of three main materials: shell, foundation, and the downstream filter (**Figure 4.3a**). The core and the cutoff are additional components to the main dam based on each case shown below (**Figure 4.3 b-c**). The core is located at the center of the dam, and the cutoff has been added below the core. **Table 4.1** presents the soil properties for all dam cases.

The initial reservoir water level at the upstream is 8 m while the water level at the downstream is assumed to be zero, to model the worst-case scenario in the seepage analysis. The slope ratio of the upstream and the downstream is considered to be 1:2.5 and 1:2 respectively. The crest height of the dam is 10 m, while the height of the core is 9 m. The foundation is considered to be horizontal strata with a depth of 10 m. this general design of a typical dam provides insights into the behavior of the dam and the methodology can then be applied to modeling a specific dam in future efforts.

Three different dam profiles are modeled to investigate the behavior of the earth dam under

different drawdown conditions. The first case (Case 1) will assume that the dam is homogenous (**Figure 4.3a**). In Case 2, the dam is assumed to be a zoned earth dam with a core (**Figure 4.3b**). Lastly, Case 3 is a zoned earth dam with a core and a complete cutoff (**Figure 4.3c**).

The dam materials were modeled as follows: the shell and the core were modeled as a combination of saturated/unsaturated soil masses and the foundation, the cutoff, and the downstream filter are modeled as fully saturated materials. The material properties used in the modeling of each component are presented in **Table 4.1**. The boundary conditions and the finite element mesh are presented in **Figure 4.4 & 4.5** respectively. The number of elements used in Case 1 was 1033, for Case 2 was 1038, and 992 for Case 3 respectively. The upstream boundary condition is considered to be 8 m high water reservoir level and the downstream water level is considered to be zero. The potential seepage face was used as a boundary type on the downstream along the slope face to predict the seepage quantity discharging on the downstream face.

First, a steady-state analysis is used to compute the total head, the exit gradient, and the seepage magnitude through the earth dam. This step is necessary to determine the magnitude and the direction of the water flow through the earth dam. The steady-state results of the seepage analysis are then used in a transient analysis as an initial condition for the total applied head. The drawdown states of the water level in the reservoir are also modeled for two different levels – namely, 25% and 50% of the initial reservoir levels respectively. The drawdown conditions are simulated for four rates: entirely in one day, 1 m/day, 2 m/day, and 3 m/day for each of the drawdown cases.

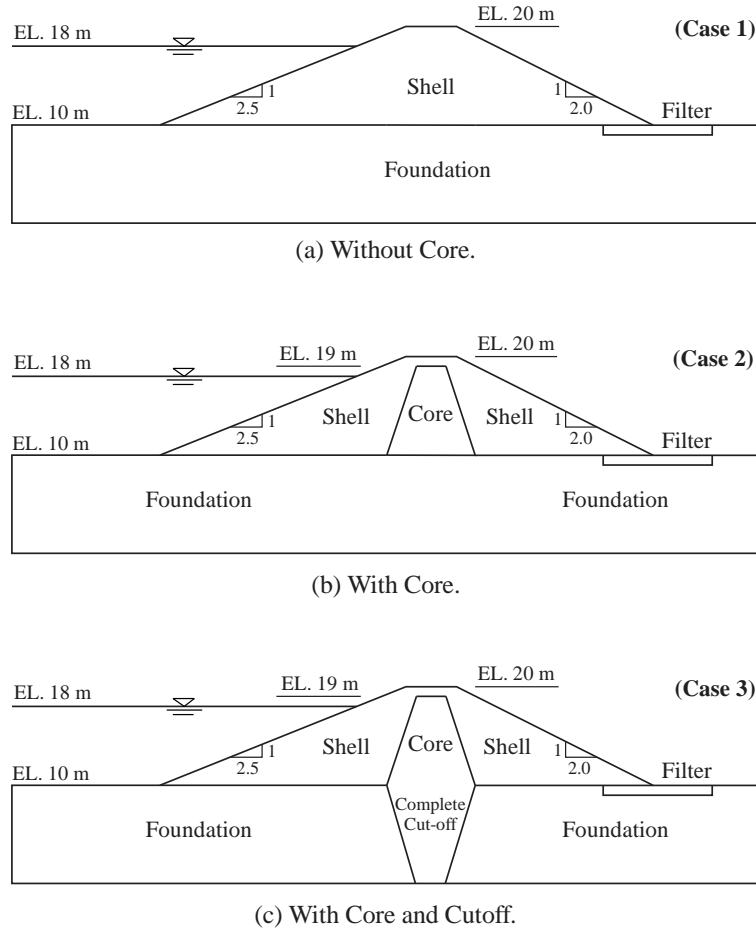


Figure 4.3: Profile Sections of the three dam cases; (a) without core; (b) with core; (c) with core and a complete cutoff.

Table 4.1: Material properties of the earth dam used for stresses and slope analysis.

	Symbols	Soil Materials			
		Shell <sup>a</sup>	Core <sup>b</sup>	Foundation <sup>c</sup>	Drain
Unit weight (kN/m <sup>3</sup> )	( $\gamma$ )	18	19	20	19
Hydraulic conductivity (m/day)	( $k$ )	0.1728	0.000864	0.1728	8.64
Cohesion (kPa)	( $c'$ )	5	14	5	0
Elastic Modulus (kPa)	( $E'$ )	3000	30000	5000-16515	5000
Friction angle	( $\phi'$ )	34°	14°	36°	35°

a: Compacted fill material used on the shell of Upper Fernando Dam (GEO-SLOPE, 2018).

b: Soil material used on the Dau Tieng reservoir (Fattah et al., 2015).

c: Alluvium material used on the foundation of Upper Francesco Dam (GEO-SLOPE, 2018).



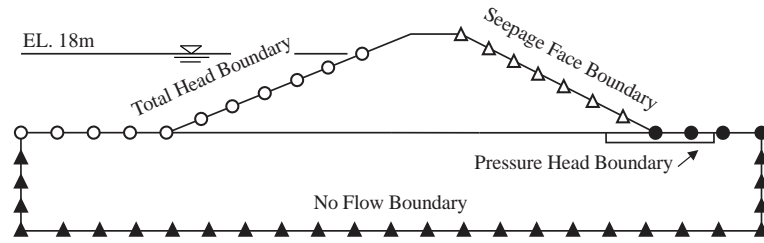
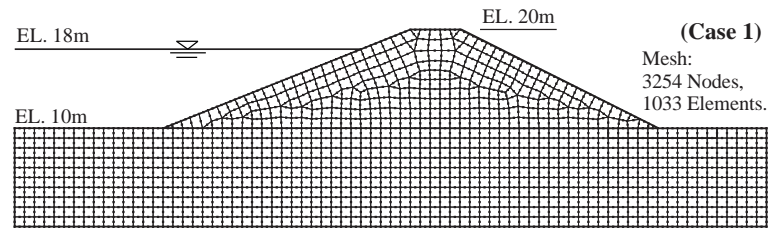
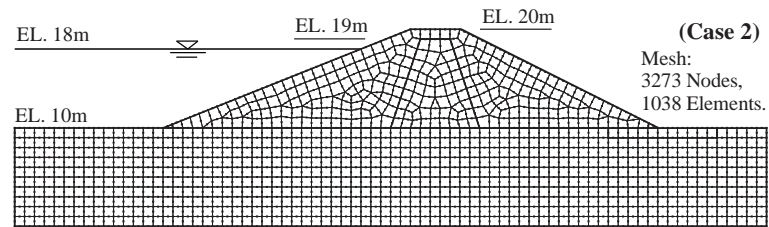


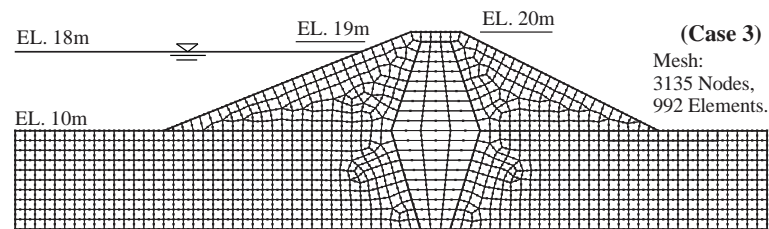
Figure 4.4: Boundary conditions for the dam model used for the seepage analysis.



(a) Without Core.



(b) With Core.



(c) With Core and Cutoff.

Figure 4.5: Finite element mesh for the three dam cases.

## 4.5 Results and Discussion

### 4.5.1 Homogenous Earth Dam (Case 1)

The permeability of the soil and the difference in energy between the upstream and the downstream ends drives the water in the reservoir to flow through the dam body toward the downstream. Water seeping out of the downstream face can be controlled by using a drain at the downstream end, as shown in the dam profile.

**Figure 4.6a** shows the result of the seepage analysis in the steady state. The result indicates that the total head decreases with the flow towards the downstream side due to the soil permeability and energy losses. The phreatic domain is drawn into the filter and away from the slope face. The total flux flowing through the dam soil and its foundation in the steady state is  $0.574 \text{ m}^3/\text{day}/\text{m}$ . In addition, the water flux rate through the soil mass is different than it is through the foundation surface. The results showed that the water flux through the upstream slope is  $0.5416 \text{ m}^3/\text{day}/\text{m}$ , contributed about 94.36% of the total flux, while the remainder of the flux ( $0.0324 \text{ m}^3/\text{day}/\text{m}$  or 5.64%) flows through the foundation surface at the upstream. The reason is that the flow paths from the upstream slope to the downstream is shorter than the flow paths from the foundation surface to the downstream end.

Next, as the drawdown of the reservoir takes place, it is seen that water occupying the soil voids flows out the dam through both the slope and the foundation surface due to the change of the total head between the reservoir and the dam developed under the drawdown event (**Figure 4.6b**). The water flowing in the upstream region is divided into two directions, one toward the upstream face, and the other continues flowing toward the downstream as shown in **Figure 4.6b**.

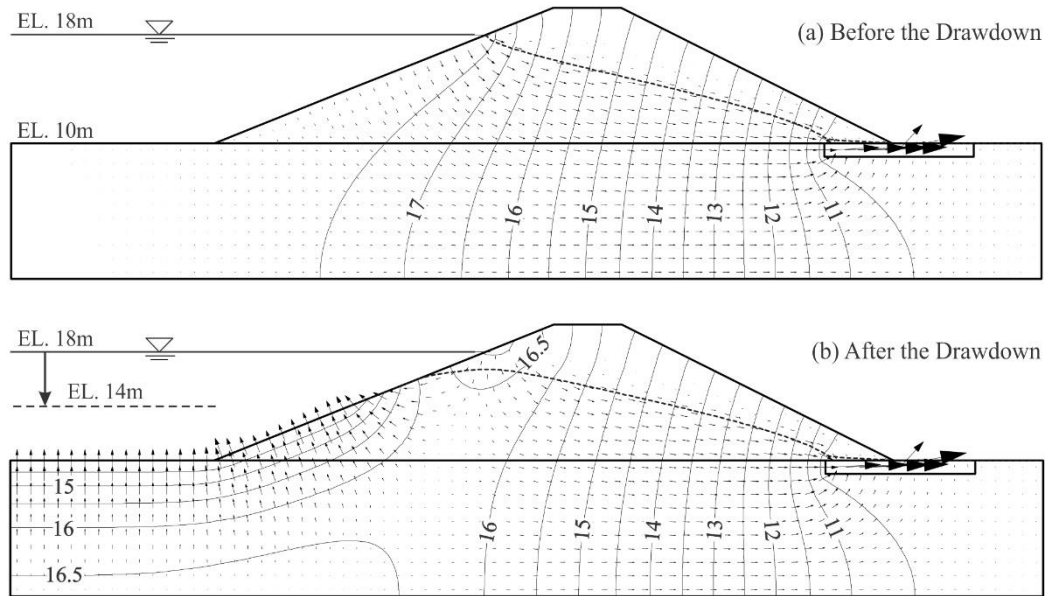


Figure 4.6: Total head contours (in m) and flow directions of the water flux for Case 1; (a) before the drawdown event, (b) after the reservoir is dropped to half in one day.

The behavior of the water flux that flows out of the dam under different drawdown depths and rates is shown in **Figure 4.7**, where the negative values indicate that the flow takes place *out* the dam. As shown in **Figure 4.7**, the exiting water flux is increasing with the drop of the reservoir level until it reaches a maximum value when the drawdown of the reservoir is stopped. Then, this flux rate starts to decrease until the seepage process is completed. The time period when the water flows out the dam is affected by the drawdown rate. It is seen that, for 25% drawdown case, the water flux flows out the dam for the duration of the drawdown event until the flux value returns to zero. For the 50% drawdown case, the behavior of the water flux is more interesting. The flux exiting the dam is higher in magnitude and the process continues beyond the end of the drawdown event until it eventually returns back to zero.

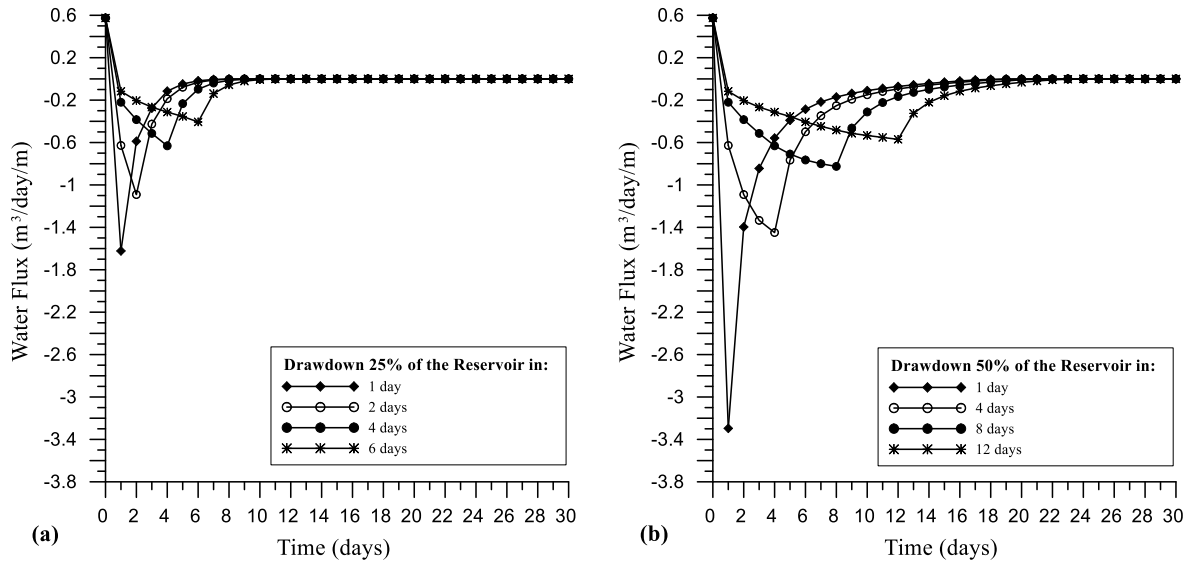


Figure 4.7: The behavior of the water flux flowing out of the upstream face after the drawdown conditions; (a) drawdown 25% of the reservoir, (b) drawdown 50% of the reservoir.

**Table 4.2** provides a summary of the water flux that flows out of the dam through the slope and the foundation surface over a period from one to 30 days after the drawdown to 25% and 50% of the initial reservoir height. The flux magnitude is impacted by the drawdown rate. The results showed that the flux is slower when the drawdown rate is lower. This may be due to some flow changing its direction toward the downstream for the slower rate of the drawdown. Through the foundation surface, the flux magnitude is not affected by the drawdown rate for both cases. After a period of time, the water flux that is flowing out of the dam through the slope begins to decrease depending on the percent and the period of the drawdown.

Table 4.2: Summary of the total flux (in  $m^3/m$ ) that flows out of the earth dam for a period of 30 days under the drawdown conditions.

	Total Flux	Flux through the slope		Flux through the foundation	
After Drawdown (25%) of the Reservoir					
Drawdown Rate	(m <sup>3</sup> /m)	(m <sup>3</sup> /period*/m)	(% of total)	(m <sup>3</sup> /period*/m)	(% of total)
1 day	2.67350	1.25779/6 days	47.05	1.41571/8 days	52.95
2 days	2.45419	1.05785/6 days	43.10	1.39634/9 days	56.90
4 days	2.13860	0.78145/7 days	36.54	1.35715/10 days	63.46
6 days	1.88416	0.56829/9 days	30.16	1.31587/11 days	69.84
After Drawdown (50%) of the Reservoir					
Drawdown Rate	(m <sup>3</sup> /m)	(m <sup>3</sup> /period*/m)	(% of total)	(m <sup>3</sup> /period*/m)	(% of total)
1 day	7.72925	4.48366/19 days	58.01	3.24559/18 days	41.99
4 days	7.16542	4.00117/20 days	55.84	3.16425/19 days	44.16
8 days	6.47936	3.41155/22 days	52.65	3.06781/21 days	47.35
12 days	5.84256	2.86827/24 days	49.09	2.97429/23 days	50.91

\*: The total period of the water flux to flow out the dam after the drawdown events.

It is hypothesized that lowering of the reservoir level at a significantly rapid rate may cause movement of the soil particles out the dam due to increased exit gradients. This can cause erosion of the soil inside the body of the dam and result in piping. To investigate the influence of the outlet water flux on the stability of the soil at the face of the dam, the exit gradient is estimated at two different levels. For the 25% drawdown case, the exit gradient is calculated at an elevation of 16 m and it is calculated at an elevation of 14 m for the 50% case. Also, it is necessary to estimate the exit gradient on the foundation surface to determine if any upheave take place at the bottom.

**Figure 4.8** shows the exit gradient for these different locations under various drawdown situations. The results showed that the slope surface has a higher magnitude of the exit gradient as compared to the foundation surface. The hydrostatic pressure of the water in the reservoir works against the upward seepage forces, which causes a lowering of the exit gradient on the foundation as shown in **Figure 4.8**.

Comparing **Figure 4.8a** and **Figure 4.8b**, it is clear that increasing the drawdown depth results in a higher difference in the gradient between the inside and the outside of the dam causing an increase in the exit gradient. It was observed that the exit gradient increases to critical levels when the drawdown of 50% of the initial reservoir height takes place in 1 day (**Figure 4.8b**). In comparison, the 25% drawdown cases of the reservoir (**Figure 4.8a**) do not exhibit this behavior. Slowing the drawdown rate gives additional time for the excess pore water pressure to dissipate which in turn decreases the exit gradient.

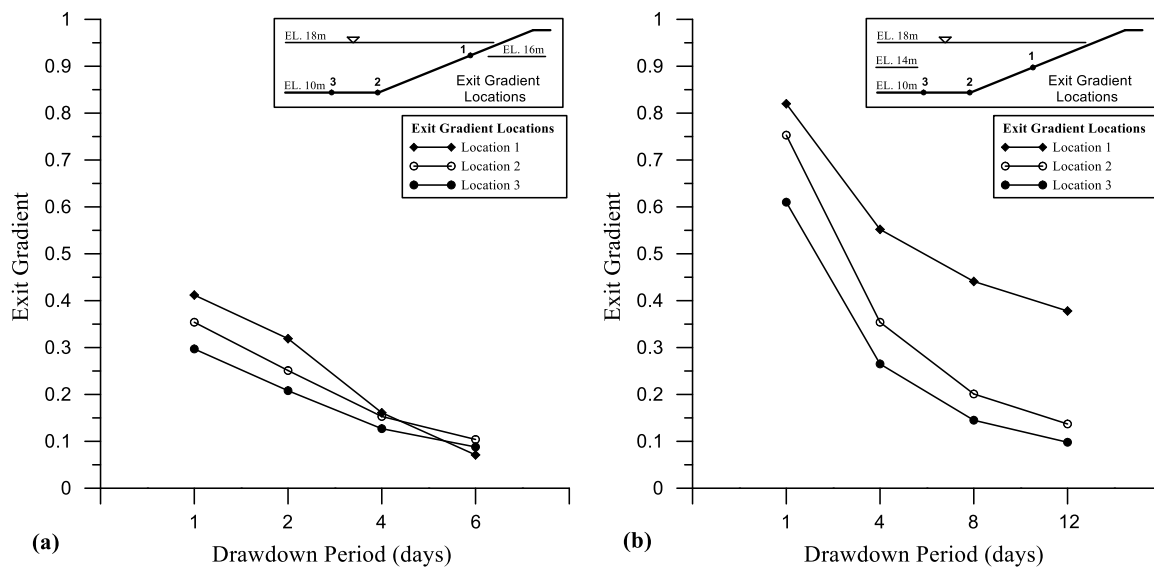


Figure 4.8: Maximum exit gradient on various locations of the upstream face due to the drawdown conditions; (a) drawdown a 25% of the reservoir, (b) drawdown a 50% of the reservoir.

#### 4.5.2 Earth Dam with a Core (Case 2)

The results of the seepage analysis under the steady-state condition, for the case when the dam is modeled with a core at the center, are shown in **Figure 4.9a**. The phreatic line and the water flux are both impacted by the presence of the core. The total head is decreased inside the core due to its lower permeability. For this reason, the core reduces the seepage velocity through the dam, which results in an increase in the submerged weight of the soil at the upstream side. Also, the total flux amount is decreased by about 23.59 % from  $0.574 \text{ m}^3/\text{day/m}$  to  $0.4386 \text{ m}^3/\text{day/m}$ . Similar to Case 1, a higher magnitude of the seepage,  $0.406 \text{ m}^3/\text{day/m}$  (92.57%), enters through the slope surface as compared to the magnitude through the foundation of  $0.0326 \text{ m}^3/\text{day/m}$  (7.43%). There is a significant amount of seepage that flows below the core base toward the downstream (**Figure 4.9a**).

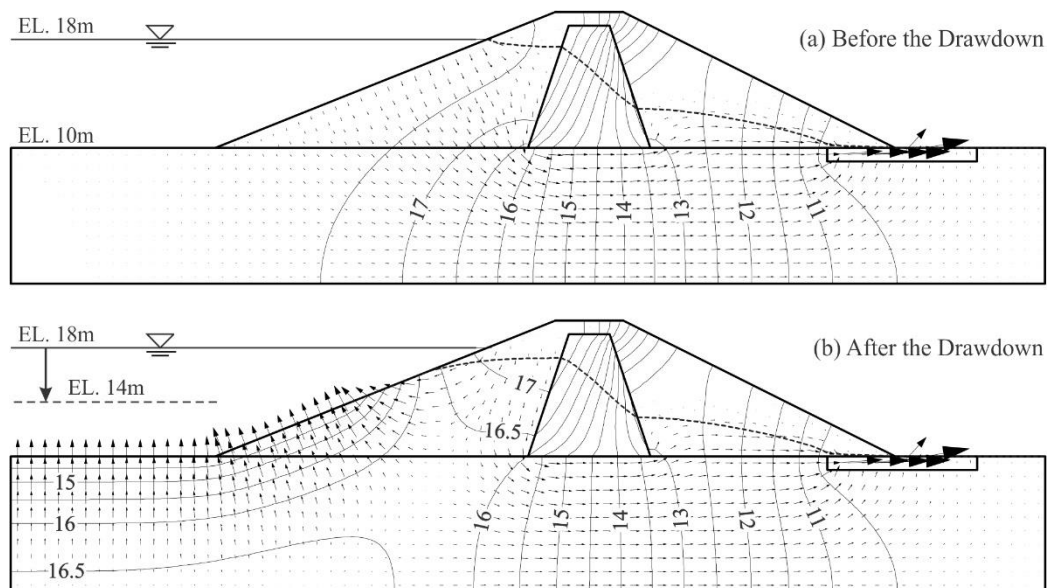


Figure 4.9: Total head contours (in m) and flow directions of the water flux for Case 2; (a) before the drawdown event, (b) after the reservoir is dropped to half in one day.

Again, as the reservoir level is lowered by drawdown, the seepage flows out of the dam through both the slope and the foundation on the upstream side (**Figure 4.9b**). The results show that a higher magnitude of the water flux exits the dam through the upstream slope compared to the flux in Case 1 without the core. However, the core has a very little effect on the water flux that flows through the foundation.

**Figure 4.10** presents the water flux during varied drawdown depths and periods as a function of time during and after the drawdown event. Once again, negative values indicate that the seepage is flowing *out* the dam. From **Figure 4.10**, it can be noted that more rapid drawdown causes higher water flux out the dam. While the behavior is similar to Case 1, it is observed that for both cases, the presence of the core causes a longer period of flux from the upstream side after the event is over and there is a delay in returning to the zero flux levels.

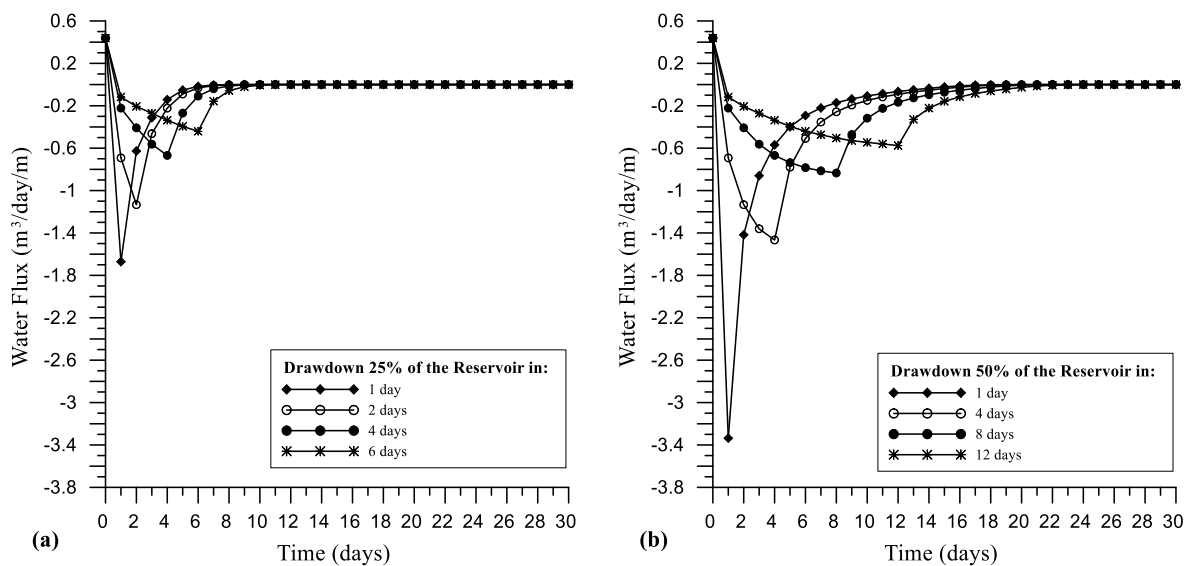


Figure 4.10: The behavior of the water flux flowing out of the upstream face after the drawdown conditions; (a) drawdown 25% of the reservoir, (b) drawdown 50% of the reservoir.



**Table 4.3** shows a summary of the values of the flux for the two drawdown cases considered - 25% and 50% of the reservoir. Similar to Case 1, the results showed that the seepage percentage through the upstream face depends on the drawdown depth. The seepage percentage on the slope face was lower than the foundation surface when 25% of the reservoir was drawn down. This percentage is higher on the slope when the reservoir is drawn down to 50%. The total length of time required for the seepage on the upstream face increases with the slowing of the drawdown of both 25% and 50% drawdown of the reservoir. The core does not have a major effect on the water flux that seeps through the foundation surface.

Table 4.3: Summary of the total flux (in  $\text{m}^3/\text{m}$ ) that flows out of the earth dam for a period of 30 days under the drawdown conditions.

	Total Flux	Flux through the slope		Flux through the foundation	
After Drawdown (25%) of the Reservoir					
Drawdown Rate	(m <sup>3</sup> /m)	(m <sup>3</sup> /period*/m)	(% of the total)	(m <sup>3</sup> /period*/m)	(% of the total)
1 day	2.82775	1.41257/6 days	49.95	1.41518/8 days	50.05
2 days	2.64505	1.24927/6 days	47.23	1.39578/9 days	52.77
4 days	2.29837	0.94171/7 days	40.97	1.35666/10 days	59.03
6 days	2.01006	0.69474/9 days	34.56	1.31532/11 days	65.44
After Drawdown (50%) of the Reservoir					
Drawdown Rate	(m <sup>3</sup> /m)	(m <sup>3</sup> /period*/m)	(% of the total)	(m <sup>3</sup> /period*/m)	(% of the total)
1 day	7.78598	4.55885/19 days	58.55	3.22713/16 days	41.45
4 days	7.31054	4.16345/20 days	56.95	3.14709/18 days	43.05
8 days	6.64488	3.59270/22 days	54.07	3.05218/20 days	45.93
12 days	6.02069	3.06145/24 days	50.85	2.95924/22 days	49.15

\*: The total period of the water flux to flow out the dam after the drawdown events.

The exit gradient during the drawdown period is calculated at three different locations on the slope and the foundation. **Figure 4.11** shows the maximum records of the exit gradient under different drawdown situations. The exit gradients are very close to Case 1 without the core except for

location 1, which is marginally higher. There is a very little impact of the core on the exit gradient which is consistent with the upstream exit flux rates in **Table 4.3**.

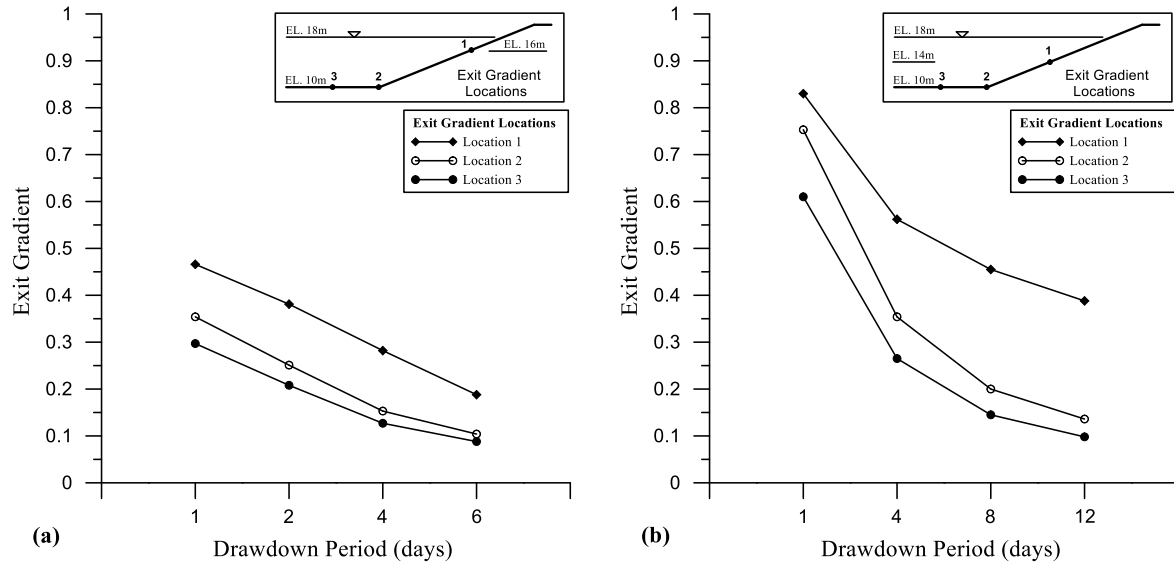


Figure 4.11: Maximum exit gradient on various locations of the upstream face due to the drawdown conditions; (a) drawdown 25% of the reservoir, (b) drawdown 50% of the reservoir.

#### 4.5.3 Earth Dam has a Core and a Complete Cutoff (Case 3)

The steady-state results for the third case of the earth dam with a core and a complete cutoff are shown in Figure 8a. The results show a raising of the phreatic line and an increase of the total head at the upstream zone of the dam when the dam was constructed with a core and a complete cutoff (**Figure 4.12a**). The low permeability of both the core and the complete cutoff reduces the magnitude and velocity of the seepage, which keeps the total head and the phreatic level at the upstream at a constant value. Inside the core, the total head is suddenly reduced to a very low

value, and the phreatic line drops. The total water flux under the steady state is  $0.0199 \text{ m}^3/\text{day}/\text{m}$ , made up of a rate of  $0.0188 \text{ m}^3/\text{day}/\text{m}$  (94.47%) through the slope face and  $0.0011 \text{ m}^3/\text{day}/\text{m}$  (5.53%) through the foundation surface. In contrast to previous cases, it is noted that a complete cutoff increases the efficiency of the core in reducing the seepage through it. The water flux is reduced by 96.53% and 95.46% compared to Case 1 and Case 2 respectively. The percent of the water flux that exits the dam through the slope again accounts for the bulk of the flow (about 93.52% in this case). Thus, the total flux in the high gradient area exits the dam.

Some of the water does find itself flowing over the core crest through the unsaturated soil of the shell although the water level in the reservoir and the associated phreatic line is lower than crest level. This is due to the capillarity rise of the water above the phreatic zone, where it may rise to and flow through unsaturated soil.

During the drawdown event, water occupying the soil voids begins to flow out of the dam. **Figure 4.12b** shows the arrows indicating the flow direction for the case where the reservoir level is dropped to half of its initial level in one day. The results showed that a substantial volume of water will seep out the dam starting from the core and the cutoff faces because of the low permeability of the core and the cutoff.

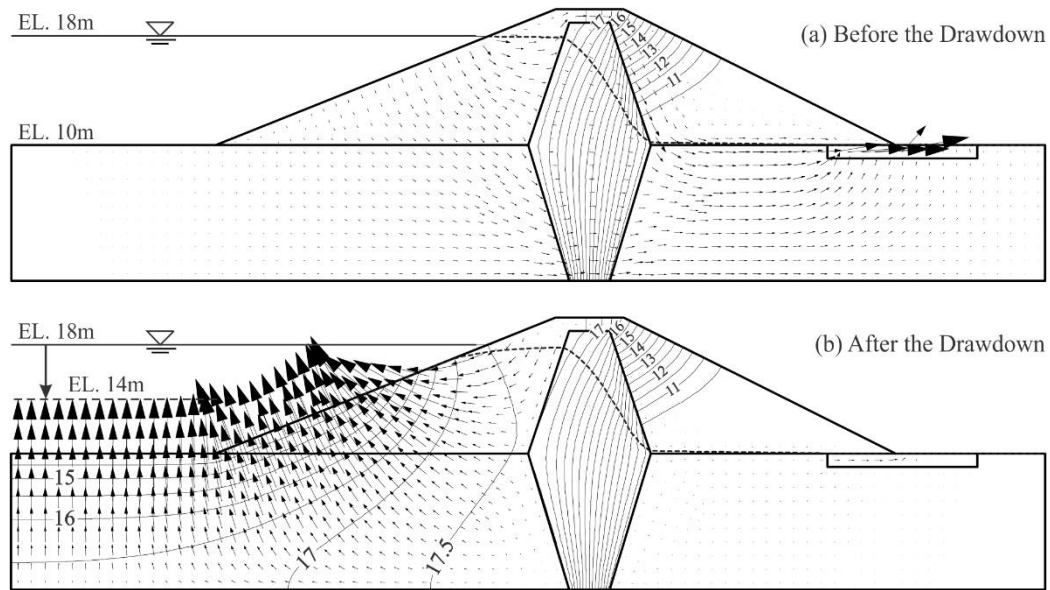


Figure 4.12: Total head contours (in m) and flow directions of the water flux for Case 3; (a) before the drawdown event, (b) after the reservoir is dropped to half in one day.

**Figure 4.13** presents the water flux that flows out of the dam under different drawdown conditions, as a function of time during and after the drawdown event. Unlike the previous cases, the seepage now starts to exit the dam immediately after the drawdown starts for all the drawdown periods. Also, the seepage period is further prolonged and lasts for more than thirty days for both drawdown depth cases.

A summary of the flux through the soil slope and foundation is presented in **Table 4.4** for various rates and periods of drawdown. It is observed that a higher percentage of flux takes place through the face than the foundation in this case. For the 25% drawdown case, the average flux is around  $6.1 \text{ m}^3/\text{day}$  with about 71% flowing through the slope, while the average for 50% drawdown case is about  $12.5 \text{ m}^3/\text{day}$  with about 69% through the slope.

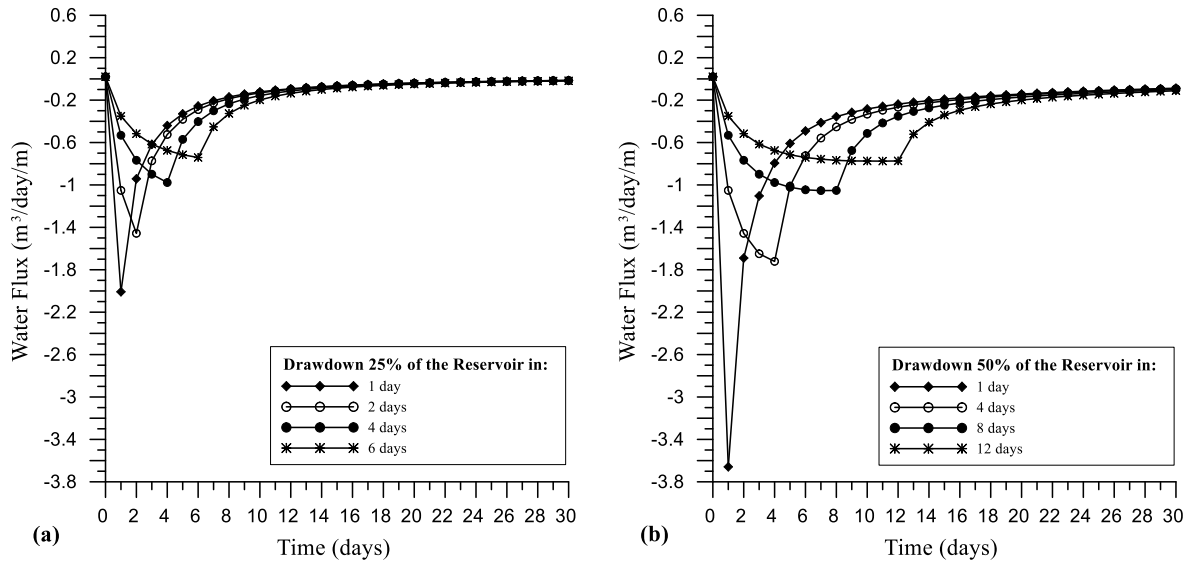


Figure 4.13: The behavior of the water flux flowing out of the upstream face after the drawdown conditions; (a) drawdown 25% of the reservoir, (b) drawdown 50% of the reservoir.

Table 4.4: Summary of the total flux (in  $\text{m}^3/\text{m}$ ) that flows out of the earth dam for a period of 30 days under the drawdown conditions.

	Total Flux	Flux through the slope		Flux through the foundation	
After Drawdown (25%) of the Reservoir					
Drawdown Rate	(m <sup>3</sup> /m)	(m <sup>3</sup> /30 days/m)	(% of the total)	(m <sup>3</sup> /30 days/m)	(% of the total)
1 day	6.12433	4.37483	71.43	1.7495	28.57
2 days	6.11141	4.36600	71.44	1.74541	28.56
4 days	6.08137	4.34204	71.40	1.73933	28.60
6 days	6.04816	4.31429	71.33	1.73387	28.67
After Drawdown (50%) of the Reservoir					
Drawdown Rate	(m <sup>3</sup> /m)	(m <sup>3</sup> /30 days/m)	(% of the total)	(m <sup>3</sup> /30 days/m)	(% of the total)
1 day	12.72093	8.81622	69.30	3.90471	30.70
4 days	12.60112	8.75081	69.44	3.85031	30.56
8 days	12.40068	8.61083	69.44	3.78985	30.56
12 days	12.16226	8.43115	69.32	3.73111	30.68

Next, the exit gradient at different points on the slope and the foundation is studied. **Figure 4.14** shows the maximum exit gradient during various drawdown conditions. It was observed that the

exit gradient is higher for location 1 in both cases and reaches the critical value if the reservoir level is dropped by 50% in one day. This has a significant impact on the internal erosion-related safety of the dam and may initiate the phenomenon of piping.

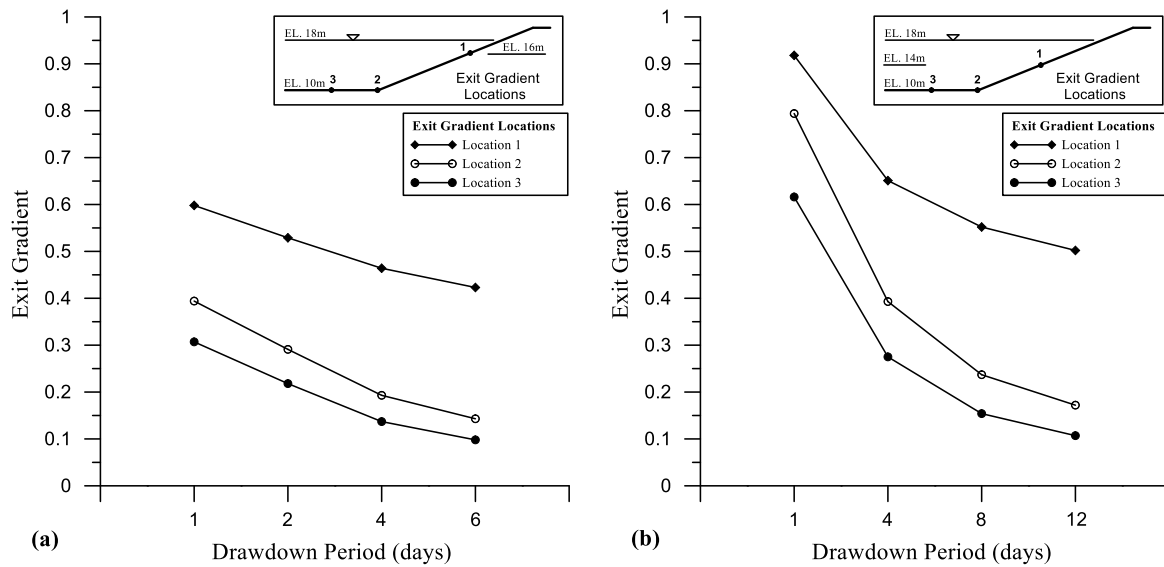


Figure 4.14: Maximum exit gradient on various locations of the upstream face due to the drawdown conditions; (a) drawdown a 25% of the reservoir, (b) drawdown a 50% of the reservoir.

#### 4.6 Comparison of the Three Cases

Three typical designs of the earth dam, a homogeneous dam (Case 1), a dam with a core (Case 2), and a dam with a core and a complete cutoff (Case 3), were modeled to study the effect of the core, without and with a complete cutoff, on the seepage behavior inside the dam and its impact on the dam stability before and after drawdown conditions. The drawdown rates are simulated to be rapid

drawdown (in one day), 1 m/day, 2 m/day, and 3 m/day for both 25% and 50% drawdown of the reservoir. The water flux, seepage behavior, and the exit gradient are tested for each case before and after the drawdown events.

Seepage through earth dams depends on the soil permeability and may be reduced by using a core in the center of the dam or using a core with a complete cutoff inside the foundation. Water flows through a homogeneous dam at a rate higher than in case the dam has a core with/without complete cutoff. As shown in **Figure 4.15**, the magnitude of the seepage flowing through the dam is reduced by 23.59% when the dam is constructed with a low permeability core, while it is reduced by 96.53% when the dam is constructed with a core and a complete cutoff.

The presence of an impermeable core alters the nature of the flow through the dam-foundation system. In contrast to the homogenous dam, the core helps decrease the water flowing through the dam body and at the same time results in development a concentrated flow through the foundation below the core base. The results showed that water can flow through the foundation toward the downstream when the dam has a core only. A zoned dam with a complete cutoff, in contrast, is a very effective design to control the seepage through the dam and its foundation (**Figure 4.15**). However, this design is certainly not a safer design from the perspective of upstream stability related to erosion potential due to higher exit gradients under the drawdown conditions. The results of this study showed that a zoned dam with and without a complete cutoff raises the phreatic line on the upstream side which causes an increase in the water flux flowing out the dam slope face, as shown in **Figure 4.16**.

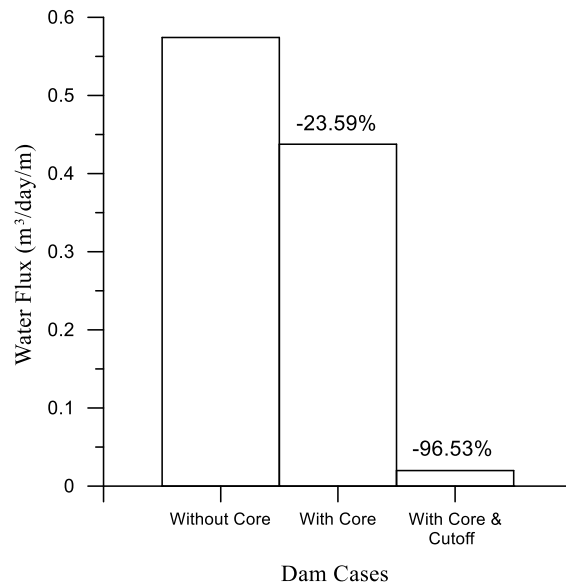


Figure 4.15: Comparison of the water flux and the reduced percent for all dam cases in the steady-state analysis.

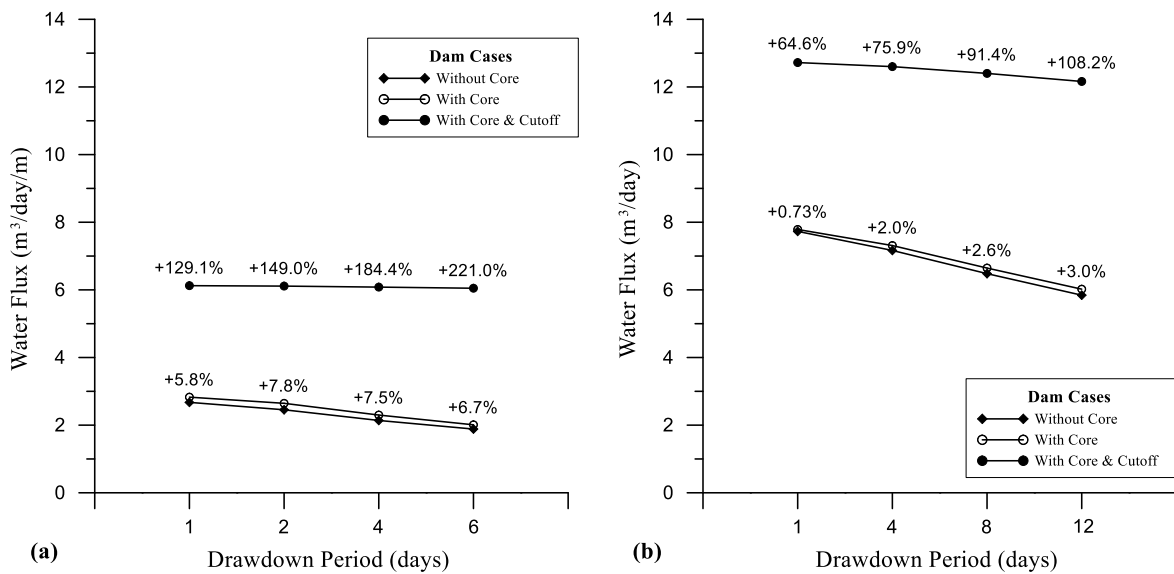


Figure 4.16: Comparison of the water flux that flows out of the dam body through the upstream face for the dam cases under different drawdown conditions; (a) drawdown 25% of the reservoir, (b) drawdown 50% of the reservoir.



Another major difference between the three cases is the exit gradient due to the drawdown. Lowering the reservoir level results in a difference in the total head between the dam and the reservoir, which can cause water to seep towards the reservoir instead of away from it. **Figure 4.17** presents the maximum exit gradient at two different elevation levels, 16 m and level 18 m, for the three cases under 25% and 50% drawdown of the reservoir. The results show that a homogeneous dam has a lower magnitude of the exit gradient, while a zoned dam with a complete cutoff is the worst case. In contrast to a homogenous dam, the results also showed that the case with a core causes an increase of between 13% and 165% at 25% drawdown and between 1.2% and 2.6% for the 50% drawdown scenario. The dam with a core and a complete cutoff results in an increase of between 45% and 496% for 25% and between 12.0% and 33% for the 50% drawdown cases respectively (**Figure 4.17**). This may be attributed to the increase in the submerged weight of the soils which causes higher seepage forces on the slope face and the foundation surface. Also, it is clear the magnitudes of the exit gradient are very similar between a homogeneous dam and a dam with a core when the reservoir level is reduced by half. The reason is that the difference of the total head at the exit gradient is similar although the difference of the phreatic line between the both cases.

#### 4.7 Influence of Foundation Impermeability

As seen in the previous section, the water flux flows through the foundation from the higher head at the upstream toward the lower head at the downstream in the steady state. Under the drawdown condition, the water flux starts to exit the dam through the slope face and the foundation surface due to the difference in the hydraulic gradient after dropping the water level in the reservoir. To

investigate the influence of the foundation on the seepage behavior before and after the drawdown event, the extreme case of an impermeable foundation material is considered. This may reflect the case of dense soils or impermeable rock.

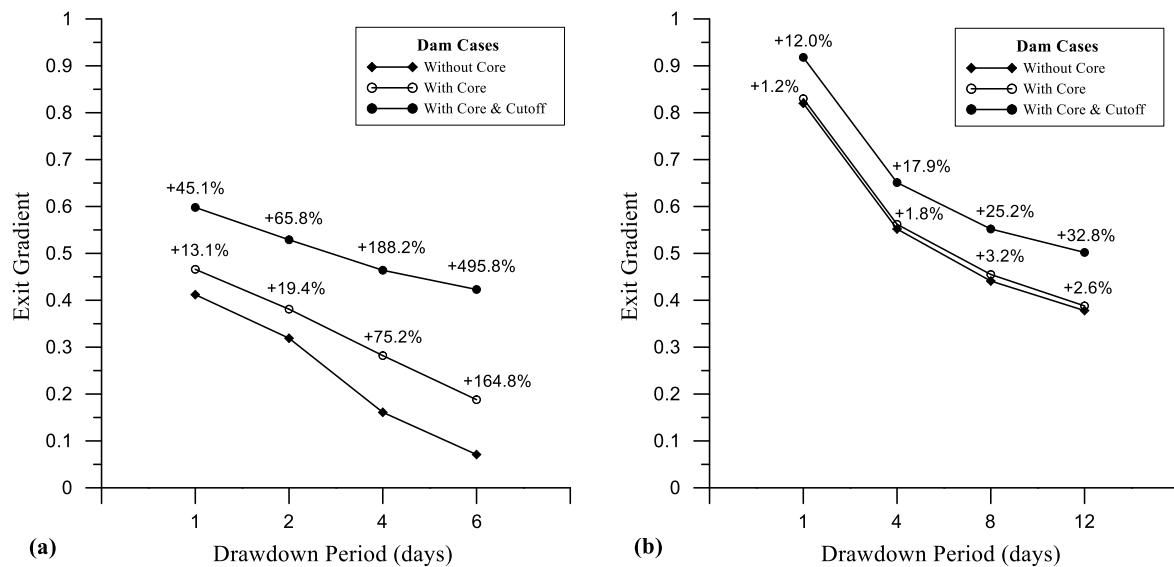


Figure 4.17: Comparison of the maximum values of the exit gradient for the dam cases under different drawdown conditions; (a) drawdown 25% of the reservoir, (b) drawdown 50% of the reservoir.

Two designs of the dam are modeled for this purpose; dam without a core, titled as Case 4, and dam with a core, titled as Case 5, as shown in **Figure 4.18**. The seepage results are presented in **Figure 4.19** under the steady-state condition. The results showed a concentrated flow is developed at the downstream side when the dam is constructed with a core (**Figure 4.19b**) as the impermeability of the foundation drains all of the water flux toward the downstream drain. When the foundation soil is impermeable, the seepage pressure is raised, and concentrated flow is

developed between the core and the downstream filter. The magnitude of the water flux in the steady state is  $0.22015 \text{ m}^3/\text{day}/\text{m}$  for the homogenous dam (Case 4), and  $0.00744 \text{ m}^3/\text{day}/\text{m}$  for the dam with a core (Case 5). In comparison with Case 1 and Case 3, the water flux is decreased by 61.65% and 62.61% respectively when the dam is constructed on an impermeable foundation.

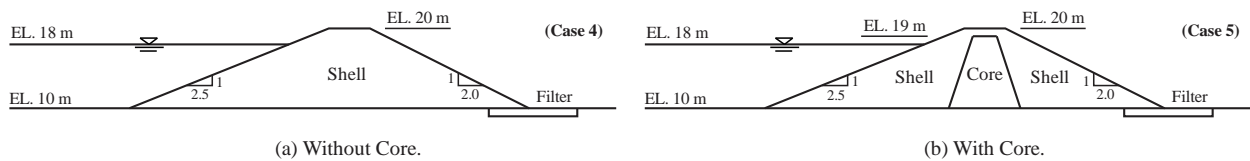


Figure 4.18: Profile section of the dam models applied on impermeable foundation.

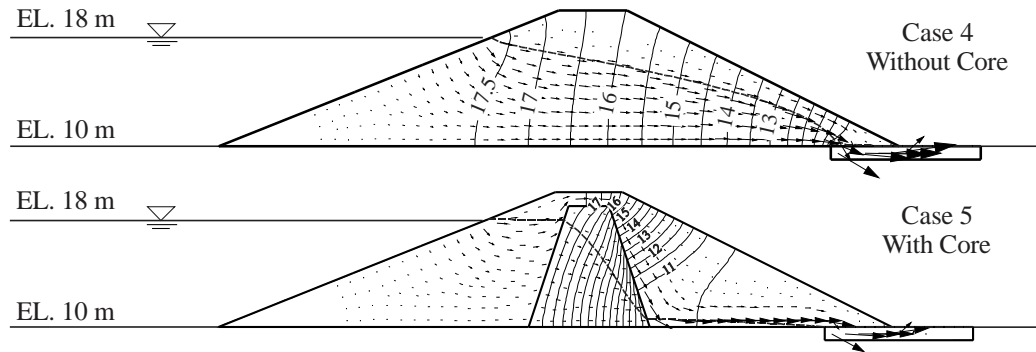


Figure 4.19: The results of the seepage analysis for Case 4 and Case 5.

Under the drawdown conditions, the water flux again begins to exit the dam through the upstream slope face. **Figure 4.20** shows the change of the total head and the flow direction after the water level on the reservoir is dropped to half at a rate of 4 m/day. As seen in the figure, the maximum

magnitude of the water flux is concentrated at the middle of the slope and reduced gradually toward the lowest point of the slope, i.e. the toe.

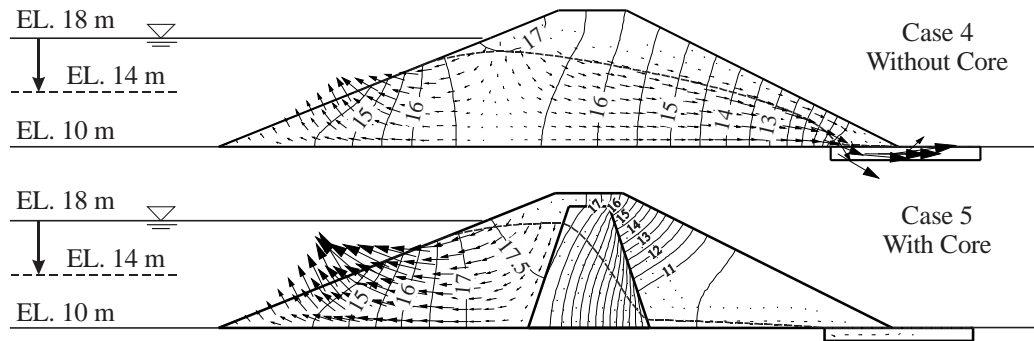


Figure 4.20: The results of the seepage analysis for Case 4 and Case 5 after the drawdown event.

The behavior of the seepage after the drawdown condition is still the same in comparison to previous cases as shown in **Figure 4.21 & 4.22**. The seepage magnitude on the slope face is increasing with the drawdown process until it reaches a maximum value when the drawdown is completed. Then, it decreases with the time due to the dissipation the excess pore water pressure. However, the results showed an interesting influence of the foundation permeability on the magnitude of the water flux. The water flux actually decreased when the foundation soil is impermeable. The reason is that the high permeability of the foundation soil provided a state of storage a higher magnitude of the water flux inside the soil voids of the foundation. When the total head is changed between the reservoir and the dam, the water flux begins to transfer from the foundation to the upstream region and, in turn, begins leaving the dam through the slope face. This process causes an increase of the water flux (seepage) through the slope.

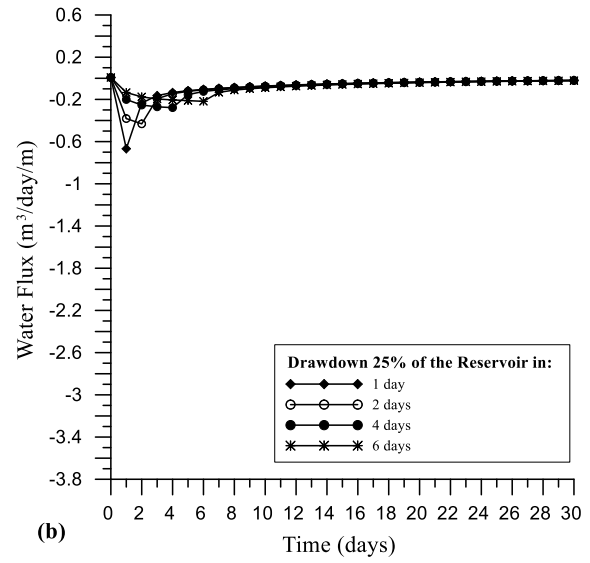
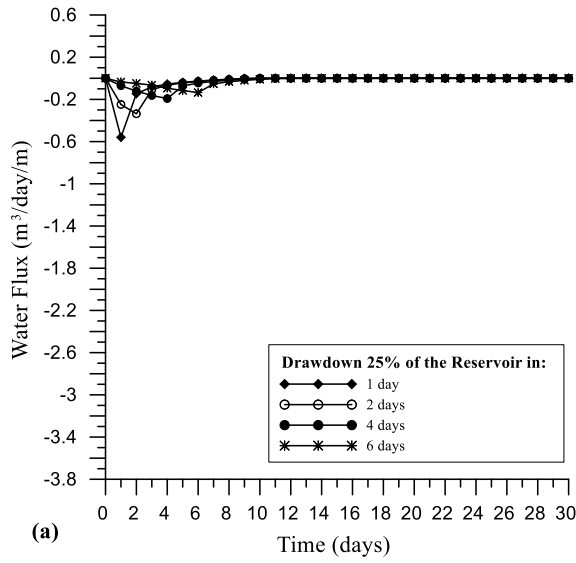


Figure 4.21: The behavior of the water flux flowing out of the upstream face after drawdown 25% of the reservoir at various rates; (a) without core case, (b) with core case.

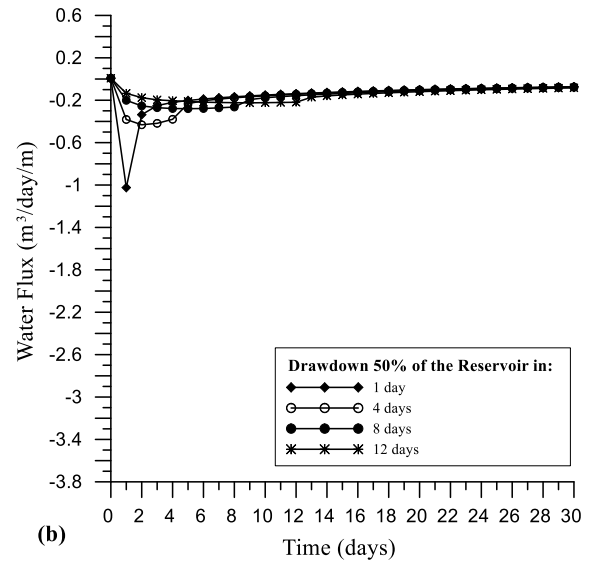
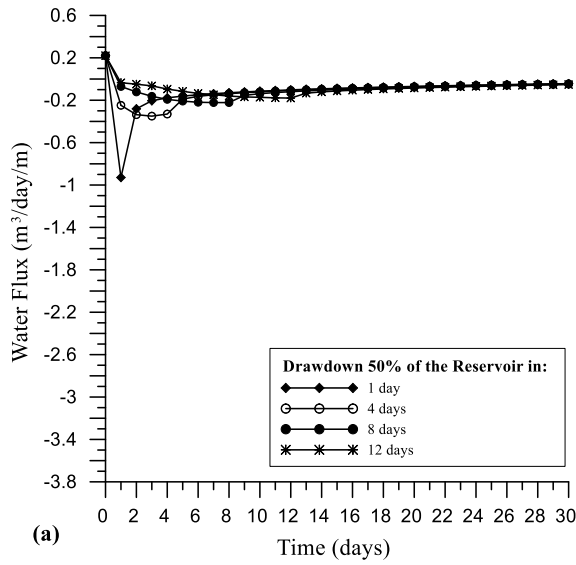


Figure 4.22: The behavior of the water flux flowing out of the upstream face after drawdown 50% of the reservoir at various rates; (a) without core case, (b) with core case.

**Table 4.5** shows a summary of the total flux flowing out of the dam and the percent of change under different drawdown conditions. The influence of the presence of an impermeable foundation is a decrease of the drawdown rate for Case 4, while it stays almost the same for Case 5 (**Table 4.5**).

Table 4.5: Summary of the total flux (in  $\text{m}^3/\text{m}$ ) that flows out of the earth dam for a period of 30 days under the drawdown conditions.

<i>Water Flux Flowing through the Slope Face</i>				
<i>After Drawdown (25%) of the Reservoir</i>				
<i>Case 4: Without Core</i>			<i>Case 5: With Core</i>	
Drawdown Rate	( $\text{m}^3/\text{m}$ )	% of Changing <sup>1</sup>	( $\text{m}^3/\text{m}$ )	% of Changing <sup>1</sup>
<b>1 day</b>	0.93308/30 days	-25.82	2.51714/30 days	-42.46
<b>2 days</b>	0.86595/30 days	-18.14	2.50820/30 days	-42.55
<b>4 days</b>	0.72700/30 days	-6.97	2.48592/30 days	-42.75
<b>6 days</b>	0.61156/30 days	+7.61	2.46081/30 days	-42.96
<i>After Drawdown (50%) of the Reservoir</i>				
<i>Case 4: Without Core</i>			<i>Case 5: With Core</i>	
Drawdown Rate	( $\text{m}^3/\text{m}$ )	% of Changing <sup>2</sup>	( $\text{m}^3/\text{m}$ )	% of Changing <sup>2</sup>
<b>1 day</b>	3.82306/30 days	-14.73	4.92364/30 days	-44.15
<b>4 days</b>	3.62842/30 days	-9.32	4.85639/30 days	-44.50
<b>8 days</b>	3.31104/30 days	-2.95	4.73098/30 days	-45.06
<b>12 days</b>	2.99863/30 days	+4.54	4.58226/30 days	-45.65

1, 2: Percent of decrease of the water flux in comparison to Case 1 and Case 3 respectively.

**Figure 4.23** and **Figure 4.24** show the maximum record of the exit gradient on the *upstream* slope face after the drawdown events. As seen in the figure, the exit gradient is also reduced due to the permeability of the foundation. At the drawdown 25% of the reservoir, the core causes an increase of the exit gradient on the slope face, while there is no change on the exit gradient at the toe (**Figure 4.23**). At the drawdown 50% of the reservoir, the results showed no observing influence of the core on the exit gradient on both the slope face and the toe (**Figure 4.24**).

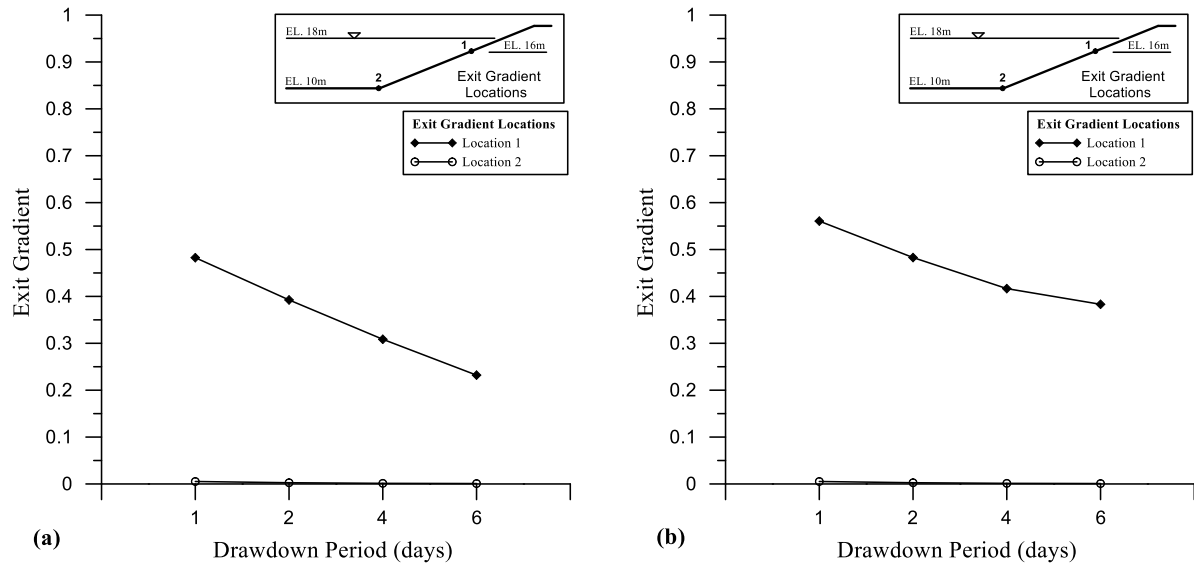


Figure 4.23: Maximum exit gradient on various locations of the upstream face due to draw down 25% of the reservoir; (a) without core case, (b) with core case.

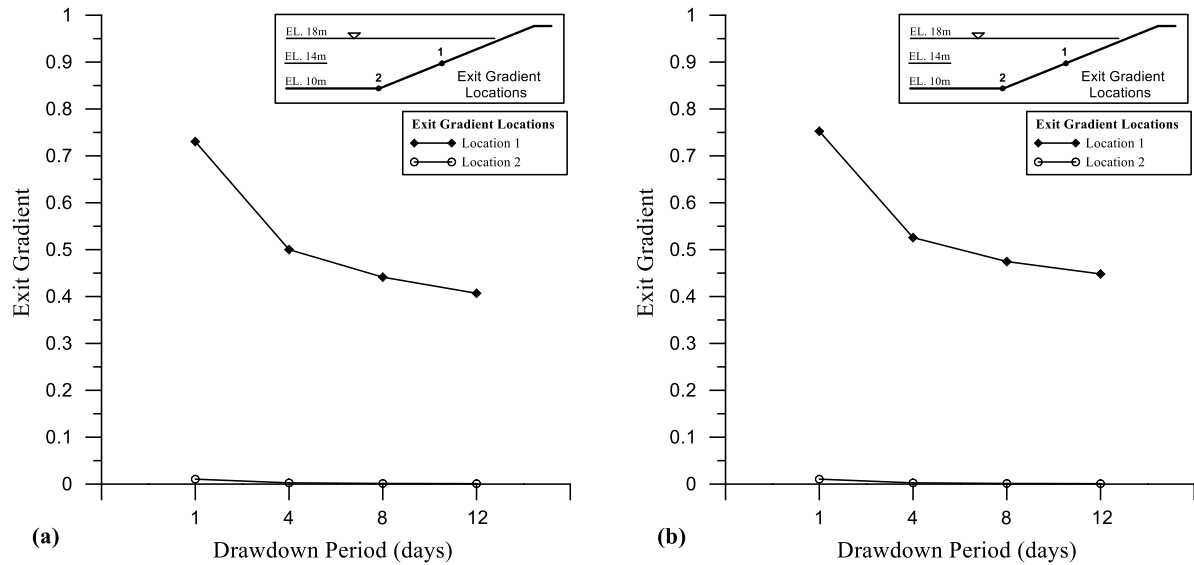


Figure 4.24: Maximum exit gradient on various locations of the upstream face due to draw down 50% of the reservoir; (a) without core case, (b) with core case.

In summary, three typical designs of earth dams, with and without the core, and incorporating two locations of the upstream filters, are used to study the seepage behavior before and after the drawdown event in the reservoir. A similar analysis is carried out for the erosion potential of typical dam designs constructed on an impermeable foundation. Water flux, flow direction, and exit gradient are calculated in each case.

The results show that the core is important in reducing the flux through the dam. Constructing a cutoff under the core increases the efficiency of the core and lowers the phreatic line. However, it is seen that the submerged weight increases when the earth dam is constructed with a core or with a complete low permeability cutoff. This increase in the submerged weight, in turn, causes higher water flux to flow out of the dam under the drawdown condition which increases the exit gradient.

The permeability soil of the foundation has a significant influence on the behavior of the flux during the drawdown event. The water flux begins to flow from the foundation to the dam slope and then exit the dam through the drawdown process, which causes an increase in the magnitude of the water flux on the slope face and rise in the value of the exit gradient, especially on the dam toe.



## **CHAPTER FIVE: EFFECT OF THE UPSTREAM FILTER IN INCREASING THE STABILITY OF THE DAM**

### 5.1 Introduction

The fine grains of the soil in the dam are typically the limiting element for the flow of water that is the result of high gradient development due to any changes in the external boundary conditions of the dam (i.e. dropping of the water level in the reservoir). Seepage forces develop inside the soil and act in the flowing direction, which tends to migrate of the soil grains and increase the rate and volume of erosion of the soil. Dangers of a rapid drawdown of upstream water on the stability of the slope can be controlled by using soil filters at the upstream side of the dam. Filters can improve the dam stability by accommodating the seepage forces resulting from the high gradient zones and reducing them to acceptable levels. In addition, the well-graded nature of the filter soil can prevent any migration of the fine particles of the soil between different zones and beneath the dam. The U.S. Department of the Interior explained four main requirements for the use of filter soils (Reddi, 2003):

- The soil permeability of the filter should be higher than the protected material (base soil) to prevent any hydraulic pressure from building up.
- The soil voids of the filter must be sufficiently small to prevent any migration of the base soil particles through the filter.
- The filter layer must be thick enough to allow a uniform distribution of all soil particles and, in turn, prevent any gap inside the filter.
- Soil particles of the filter must have the strength to stop any movement into the drainage pipes, which may require an additional layer of the coarser filter or using a small slot

opening for the pipes.

**Figure 5.1** presents the interface between the protected soil (base soil) and the filter soil. Terzaghi suggested an early filter design criteria(Fannin, 2008; Reddi, 2003) as follows:

$$4d_{85} > D_{15} > 4d_{15} \text{ or } \frac{D_{15}}{d_{85}} < 4 < \frac{D_{15}}{d_{15}} \quad (5.1)$$

where  $D_{15}$  is the particle size of the filter soil corresponding to 15% finer,  $d_{85}$  is the base soil corresponding to 85% finer and  $d_{15}$  is the base soil corresponding to 15% finer.

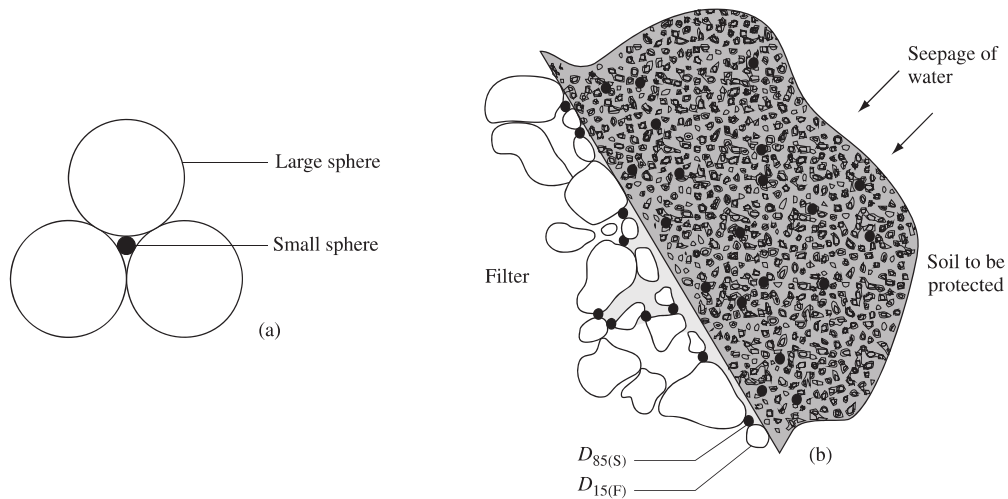


Figure 5.1: Profile section of the base soil and the filter soil (Das & Sobhan, 2014).

As discussed in the previous chapter, the zoned dam with a completed cutoff (Case 3) causes a critical condition of the dam stability with respect to exit gradient and erosion potential, under the sudden drawdown events. In this chapter, three effective factors of the upstream filter: namely, the effect of the filter location, effect of the filter permeability and effect of the transition zone, are studied under the drawdown conditions. All the filter cases are applied to the most critical design

case (Case 3) which was described in detail in Chapter 4.

### 5.2 Effect of the Filter Location

In general, the hydraulic conductivity of chimney drains on the downstream end may be evaluated by using Darcy's law:

$$k = \frac{Q}{i \cdot A} \quad (5.2)$$

where  $k$  is the hydraulic conductivity of the soil using in the filter (L/T),  $Q$  is the discharge (L<sup>3</sup>/T),  $i$  is the hydraulic gradient, and  $A$  is the area section of the filter (L<sup>2</sup>). The hydraulic conductivity of the horizontal filter is larger than the hydraulic conductivity of the vertical filter because of the additional seepage discharge coming from the vertical filter (Cedergren, 1977; Reddi, 2003; U.S. Army Corps of Engineers, 1993). Under drawdown conditions, the seepage discharge on the upstream face depends on both the rate and the depth of the drawdown.

In this section, two different possible locations of the upstream filter are tested for the critical condition. These are used to study the behavior of the excess pore water pressure at the upstream face after the drawdown takes place. The first location is assumed to be in the middle of the upstream shell, titled Central Filter, while the second location is assumed to be on the face of the upstream slope, titled Slope Filter. **Figure 5.2** shows two options for the filter location. The hydraulic conductivity of the filter is considered to be 4.32 m/d at a ratio  $k_{\text{filter}}/k_{\text{shell}} = 25$ . The location of the filter on the core face is neglected to prevent a sudden lowering of the phreatic surface at the core face, which may cause a buildup of the excess pore pressure and lead to the development of the piping inside the core.

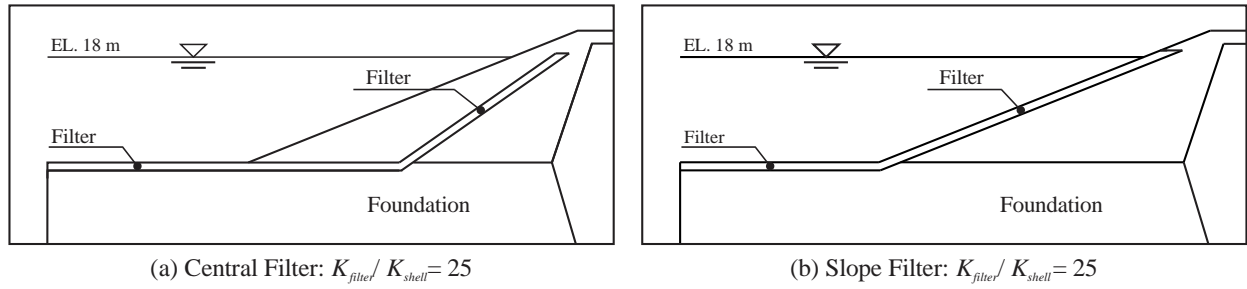


Figure 5.2: Location of the upstream filter; (a) central filter, (b) slope filter.

When the upstream drawdown occurs, excess pore pressure is developed and the water that fills the soil voids starts to flow out the dam. The drop of the phreatic surface is affected by the filter location as shown in **Figure 5.3**. It is seen that a higher drop occurs at the slope face when using a central filter because water can exit through the slope face and through the slope filter. The low permeability of the filter does not have a significant impact on the phreatic surface.

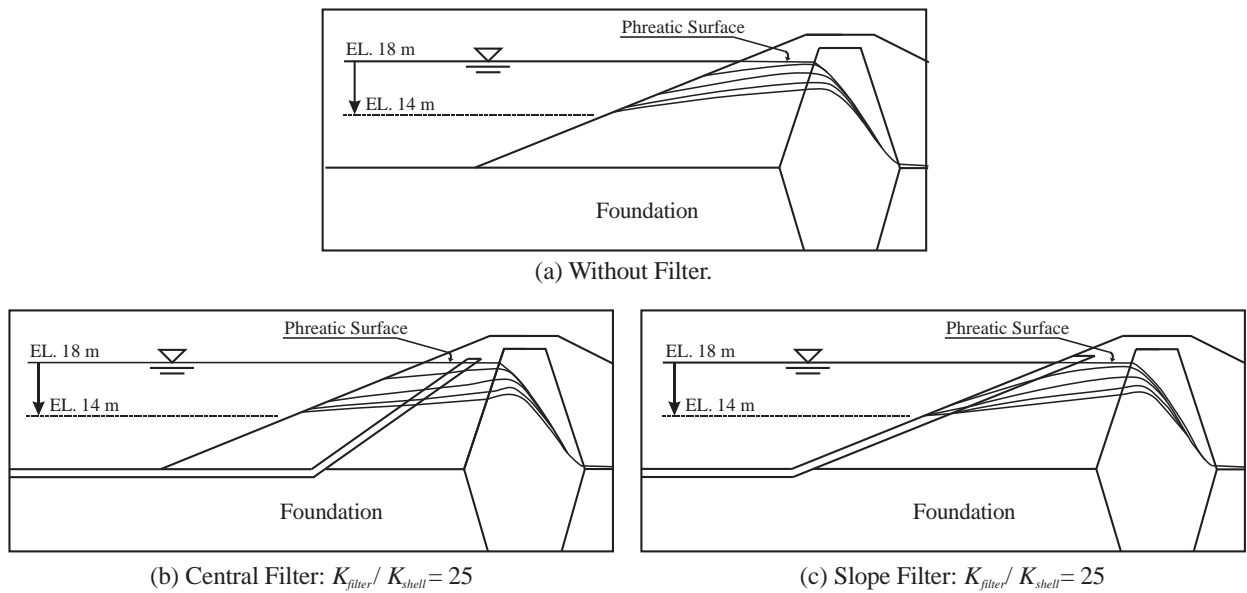


Figure 5.3: Comparison of the effect of the upstream filter on the phreatic surface in the 1<sup>st</sup>, 4<sup>th</sup>, 8<sup>th</sup>, and 12<sup>th</sup> days when the drawdown of the reservoir occurs in one day.

A comparison of the water flux that flows out of the dam through the slope face and its foundation surface for a period of 30 days is depicted in **Figure 5.4**. As shown in **Figure 5.4**, it is noted that for a period up to one day, the seepage increases to the maximum magnitude. The maximum water flux occurs immediately when the drawdown is stopped when the highest gradient between the dam and the reservoir is present. The total period of the water flux that flows out of the dam lasts for a period over 30 days. The central filter reduces the flux through the slope and drains it to the reservoir through the horizontal filter. On the other hand, the slope filter pulls more flux and drains it through the vertical filter instead of the horizontal filter.

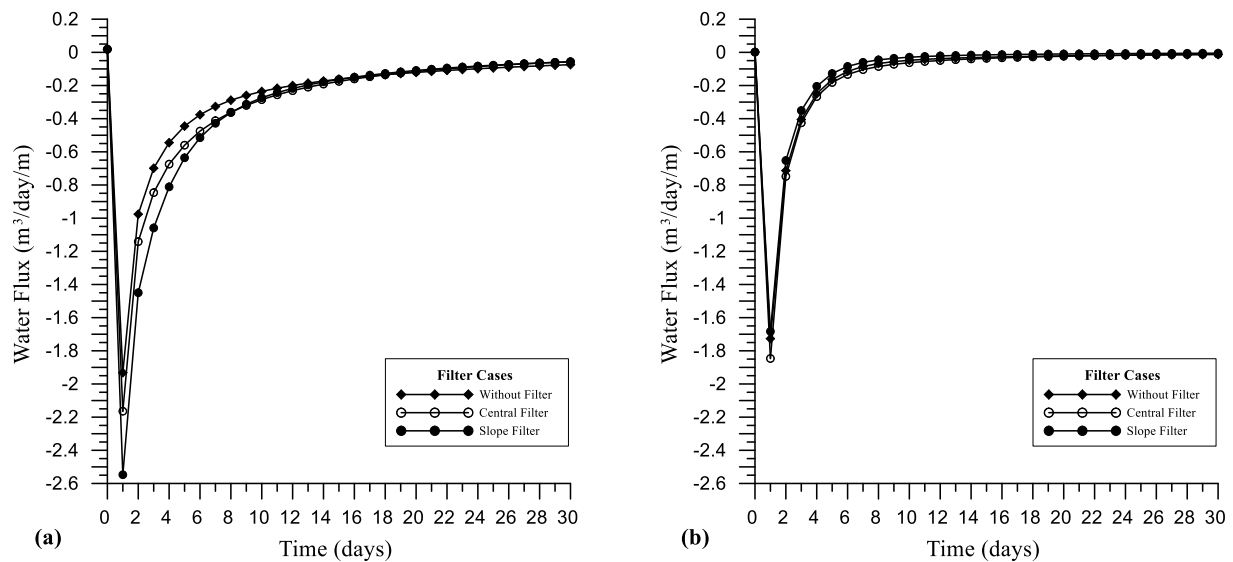


Figure 5.4: Comparison of the water flux behavior that flows out of the dam for different filter location under the drawdown condition at a rate of 4 m/day; (a) through the slope face, (b) through the foundation surface.

**Table 5.1** shows a summary of the total flux that flows out the dam and the amount of water flux that exits through the slope face and through the foundation surface. It is clear that there is an

increase of the water flux flowing out of the dam when using upstream filter cases due to an increase of the submerged weight of the upstream soil. This increase is due to the higher permeability of the filter as compared to the shell soil, which causes a reduction in the energy loss of the water flowing through the soil. The water flux through the foundation surface is increased in the central filter case because the water continues to flow from the upstream shell center toward the foundation surface through this filter.

Table 5.1: Summary of the total flux (in  $m^3/m$ ) that flows out of the earth dam for a period of 30 days under the drawdown conditions.

<i>Reservoir Drawdown in 1 Day</i>					
<b>Dam Cases</b>	<b>Total Flux</b> ( $m^3/m$ )	<b>Flux through the slope</b>		<b>Flux through the foundation</b>	
		( $m^3/30 \text{ days}/m$ )	(% of the total)	( $m^3/30 \text{ days}/m$ )	(% of the total)
<b>Without Filter</b>	12.72092	8.81622	69.30	3.90471	30.70
<b>Central Filter</b>	13.83052	6.19878	44.82	7.63174	55.18
<b>Slope Filter</b>	14.53097	11.08701	76.30	3.44396	23.70
<i>Reservoir Drawdown in 4 Days</i>					
<b>Dam Cases</b>	<b>Total Flux</b> ( $m^3/m$ )	<b>Flux through the slope</b>		<b>Flux through the foundation</b>	
		( $m^3/30 \text{ days}/m$ )	(% of the total)	( $m^3/30 \text{ days}/m$ )	(% of the total)
<b>Without Filter</b>	12.60112	8.75081	69.44	3.85031	30.56
<b>Central Filter</b>	13.75029	6.35130	46.19	7.39899	53.81
<b>Slope Filter</b>	14.45787	11.0550	76.46	3.40287	23.54

Estimating the exit gradient is important to study the possibility of the occurrence of quick conditions when the drawdown happens. **Figure 5.5** and **Figure 5.6** show the results of the exit gradient computations on the slope face and on the foundation surface under various drawdown rates.

For a central filter, the results showed that the exit gradient value on the slope face is close to the case without a filter. This may be due to the permeability of the filter not being high enough to

change the flow direction from flowing towards the slope to flowing towards the filter. On the foundation surface, the results were different. They showed that the horizontal filter reduced the exit gradient about 96%. For a slope filter, the results showed a significant decrease in the exit gradient before and after the filter face under drawdown rates of 4 m/day and 1 m/day as shown in **Figure 5.5** and **Figure 5.6** respectively. The presence of the filter prevents the excess pore pressure buildup. On the foundation surface, the exit gradient is similar to the central filter case. Therefore, the slope filter is more effective in lowering the exit gradient.

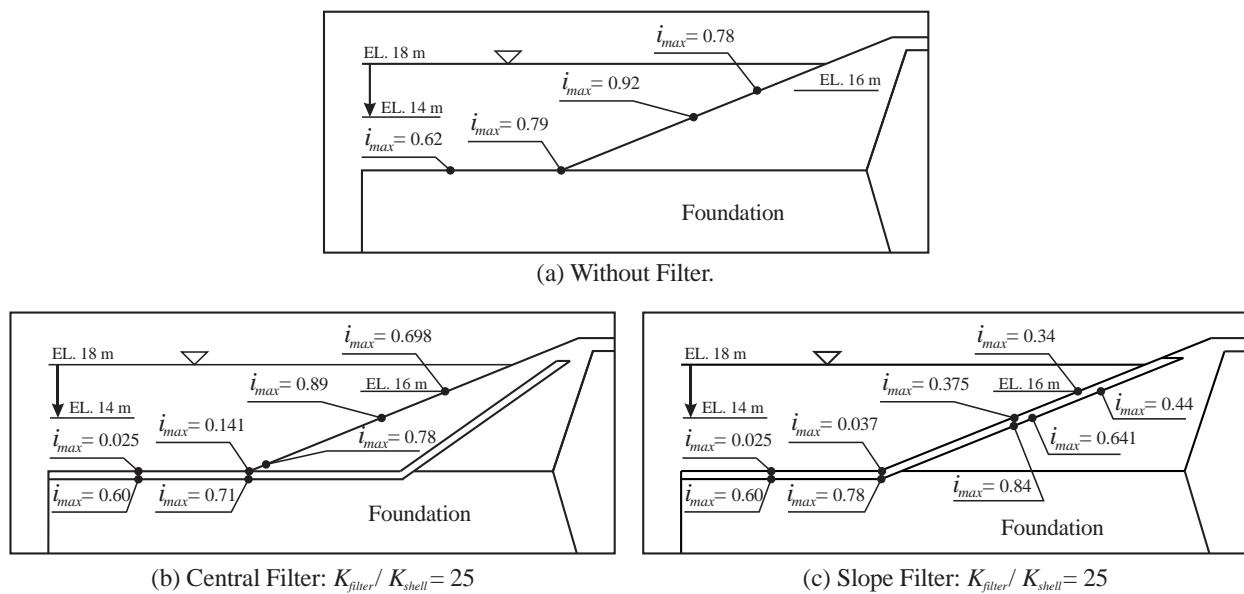


Figure 5.5: Comparison of the effect of the location of the upstream filter on the exit gradient when the reservoir level is dropped to 14 m at a rate of 4 m/day.

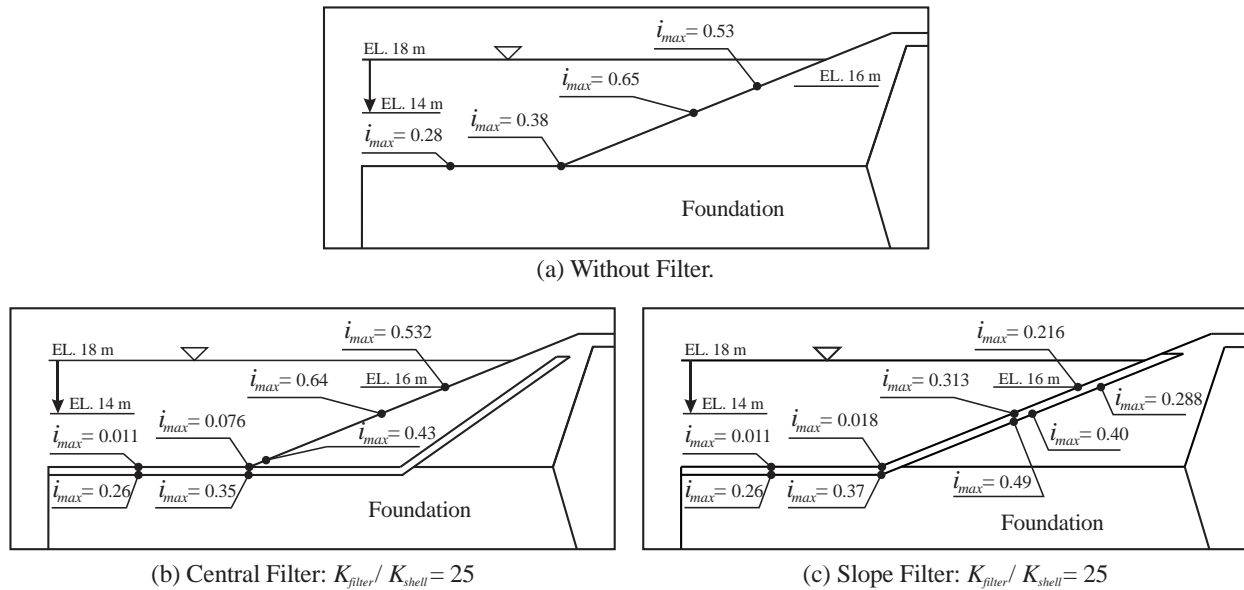


Figure 5.6: Comparison of the effect of the location of the upstream filter on the exit gradient when the reservoir level is dropped to 14 m at a rate of 1 m/day.

### 5.3 Effect of the Filter Permeability

The efficiency of the filters as a functional drain can be improved by increasing its permeability to an optimum level. Various ratios of the filter to shell permeability are tested to study the effect of the filter permeability on the flux that flows out of the dam and the exit gradient at different locations. To model the drawdown event, the reservoir level is dropped from its initial elevation of 18 m to an elevation of 14 m at rates of 1 m/day and 4 m/day. **Table 5.2** shows a summary of the results of the water flux that seeps out of the dam for both central and slope filter cases when the drawdown occurs at various rates.

As shown in the table, the filter permeability has a small effect on the total magnitude of the water flux under various drawdown rates. The fast drawdown causes a higher seepage volume than the



slow drawdown as the slow case allows more time for the water to flow towards the downstream and a decrease in the total flux that flows out the dam.

The central filter causes a reduction in the water flux through the slope with higher filter permeability. The reason is that the filter function as a drain is improved in moving water from the center of the upstream shell toward the reservoir through the horizontal filter.

In contrast to the central filter, the results of the water flux in the slope filter were different. Increasing the filter permeability causes an increase of the seepage through the slope. This increase was on account of the seeping through the horizontal filter which caused a decrease in the water flux through the foundation surface. Increasing of the filter permeability helps to pull additional magnitude of water from inside the dam toward the reservoir as shown in **Table 5.2** for a slope filter case.

Table 5.2: Summary of the total flux (in m<sup>3</sup>/m) that flows out of the earth dam for a period of 30 days under the drawdown conditions.

<i>Reservoir Drawdown in 1 Day</i>						
Water Flux (m <sup>3</sup> /m)	Central Filter			Slope Filter		
	$K_{filter}/K_{shell}$			$K_{filter}/K_{shell}$		
	50	75	100	50	75	100
Through the Slope	6.76719	5.73176	4.96137	11.0940	11.2104	11.2714
Through the Foundation	7.89071	9.12077	9.9962	3.43014	3.40402	3.38913
Total Flux	14.6579	14.85253	14.95757	14.52414	14.61442	14.66053
<i>Reservoir Drawdown in 4 Days</i>						
Water Flux (m <sup>3</sup> /m)	Central Filter			Slope Filter		
	$K_{filter}/K_{shell}$			$K_{filter}/K_{shell}$		
	50	75	100	50	75	100
Through the Slope	6.85497	5.86128	5.11418	11.0551	11.1692	11.2297
Through the Foundation	7.72499	8.92265	9.78056	3.40280	3.37954	3.36658
Total Flux	14.57996	14.78393	14.89474	14.4579	14.54874	14.59628

The maximum exit gradient at different points of the upstream is shown in **Figure 5.7** through **Figure 5.10** under different drawdown rates. The filter efficiency increases with the increase of the filter permeability. For the central filter, the increase of the filter permeability did not result in a significant decrease of the exit gradient. The results showed a high value of the exit gradient on the upstream slope, especially at level 16 m and 14 m. The slope filter showed better results. They showed a high efficiency of the filter in reducing the exit gradient on the upstream slope. Thus, the slope becomes safer against the quick conditions/erosion that may occur during the drawdown of the reservoir.

On the foundation surface, the maximum exit gradient decreases substantially for both central and slope filters as shown in **Figure 5.7** through **Figure 5.10** during the drawdown at different rates. The higher the filter permeability, the lower the exit gradient. The results show the lowest level of the exit gradient when using a slope filter. In contrast to the slope filter, the exit gradient was higher at the intersection between the slope and the foundation surface when using a central filter because of the additional magnitude of the flux coming from the vertical filter.

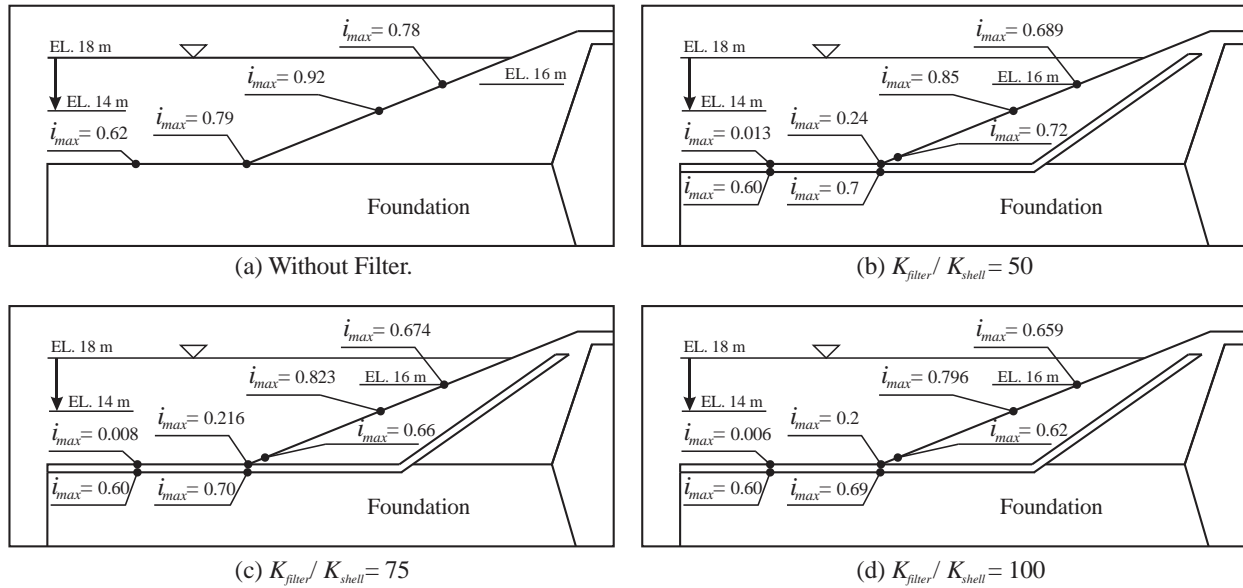


Figure 5.7: Comparison of the effect of the permeability of the central filter on the exit gradient when the drawdown of the reservoir occurs in one day.

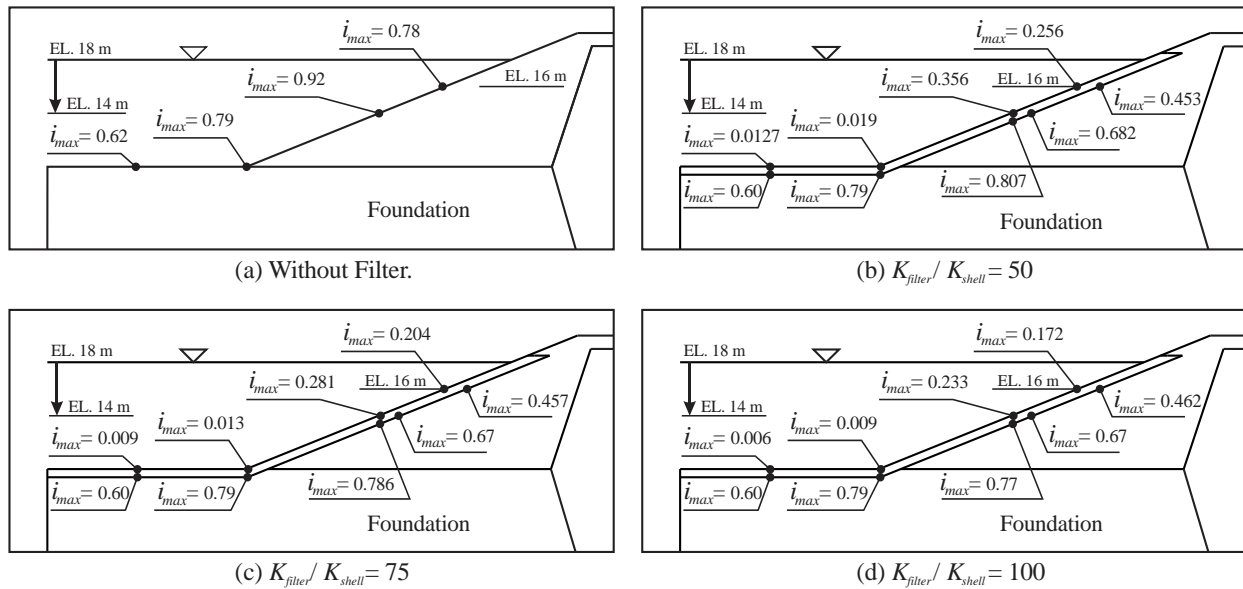


Figure 5.8: Comparison of the effect of the permeability of the slope filter on the exit gradient when the drawdown of the reservoir occurs in one day.

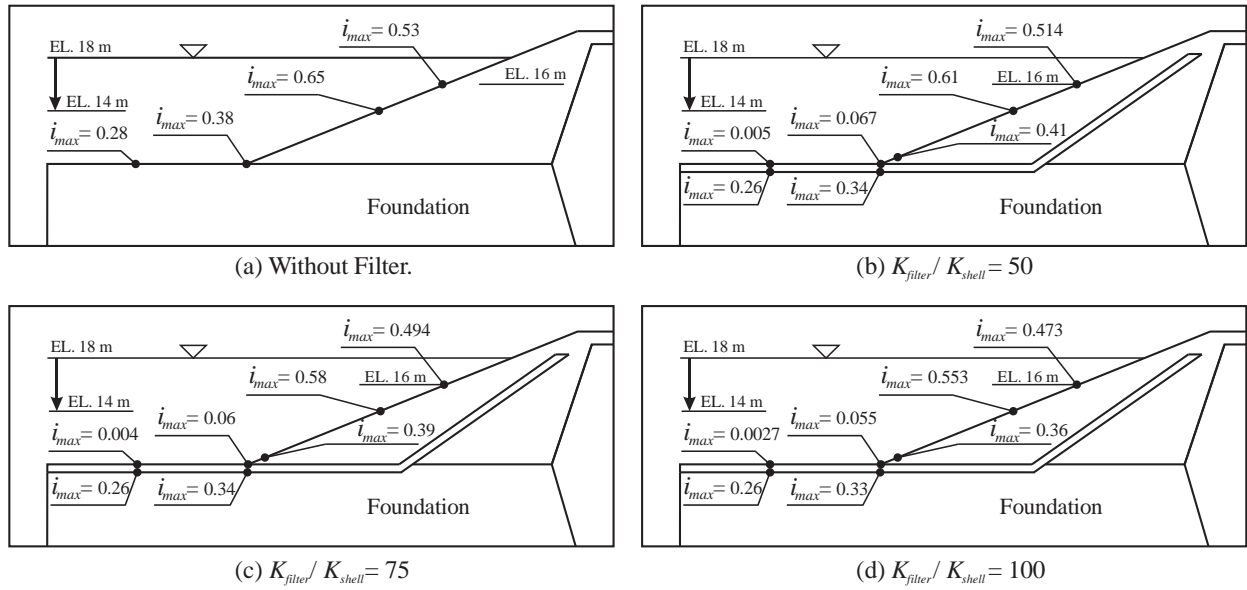


Figure 5.9: Comparison of the effect of the permeability of the central filter on the exit gradient when the drawdown of the reservoir occurs in four days.

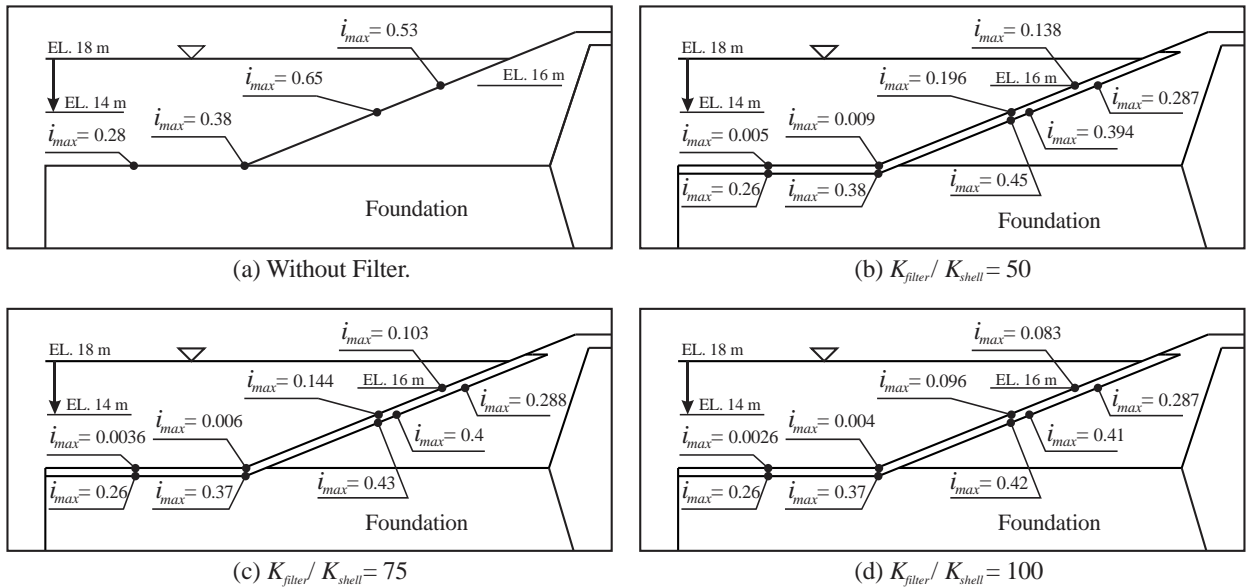


Figure 5.10: Comparison of the effect of the permeability of the slope filter on the exit gradient when the drawdown of the reservoir occurs in four days.

#### 5.4 Effect of the Transition Zone

The purpose of the transition zone in the design of an earth dam is to prevent the finer particles from moving into the filter and then developing piping conditions. As discussed in the previous section on the effect of the filter permeability, the results showed that the function of the filter is improved with an increase in the filter permeability. But, at the same time, it has been reported that it may cause piping inside the dam body (Fannin, 2008). So, it is necessary to add a transition layer around the filter of a suitable permeability to minimize the possibility of piping development.

For the modeling in this section, the hydraulic conductivity of the filter is increased to 216 m/day, while the hydraulic conductivity of the newly introduced transition zone is 8.64 m/day. The permeability ratio of the transition soil to the shell soil is 50, while the permeability ratio of the filter soil to the transition soil is 25. These magnitudes of the hydraulic conductivity fall under the recommended ratio between the filter permeability to the soil permeability ( $K_{filter}/K_{base} = 25$  to 100) (Reddi, 2003). The drawdown of the reservoir to an elevation level 14 m is simulated at rates 1 m/day and 4 m/day by using a transient seepage analysis. The initial groundwater level results from the steady-state analysis are once again used as initial conditions for the transient analysis.

For erosion protection, two layers are used for the central filter; one is on the right and below the filter and one is on the left and above the filter (see **Figure 5.11 a**). The slope filter is modeled using one layer on the right and below of the filter as shown in **Figure 5.11b**. To investigate the effect of using transition layers on the phreatic surface when the drawdown happened, the reservoir is dropped at a rate of 4 m/day and the phreatic surface is observed after the 1<sup>st</sup>, 2<sup>nd</sup>, 3<sup>rd</sup>, and 4<sup>th</sup> days as shown in **Figure 5.12**.

The results show a sudden drop of the phreatic surface in the central filter immediately after the first day of the drawdown (**Figure 5.12a**). The efficiency of the central filter is improved in draining the water from inside the upstream shell toward the reservoir compared to central filter case presented in sections 5.2 and 5.3. Also, the phreatic surface in the slope filter abruptly drops after the drawdown near the transition layer, but it is still slightly higher at the core face (**Figure 5.12b**).

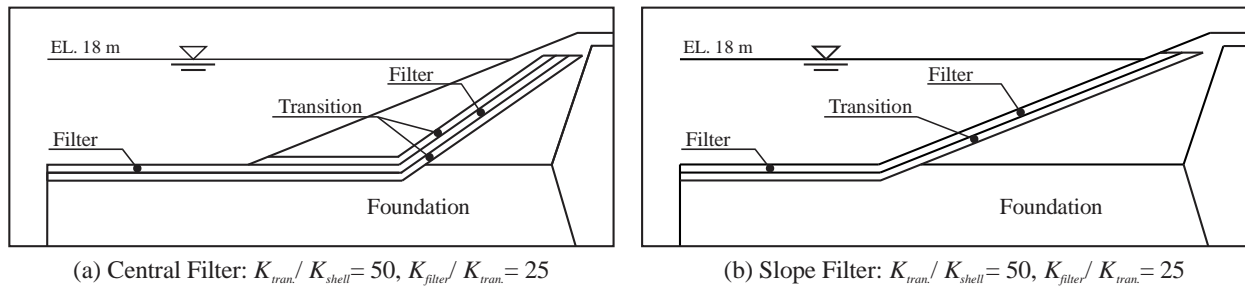


Figure 5.11: Location of the transition layer for the central filter and the slope filter.

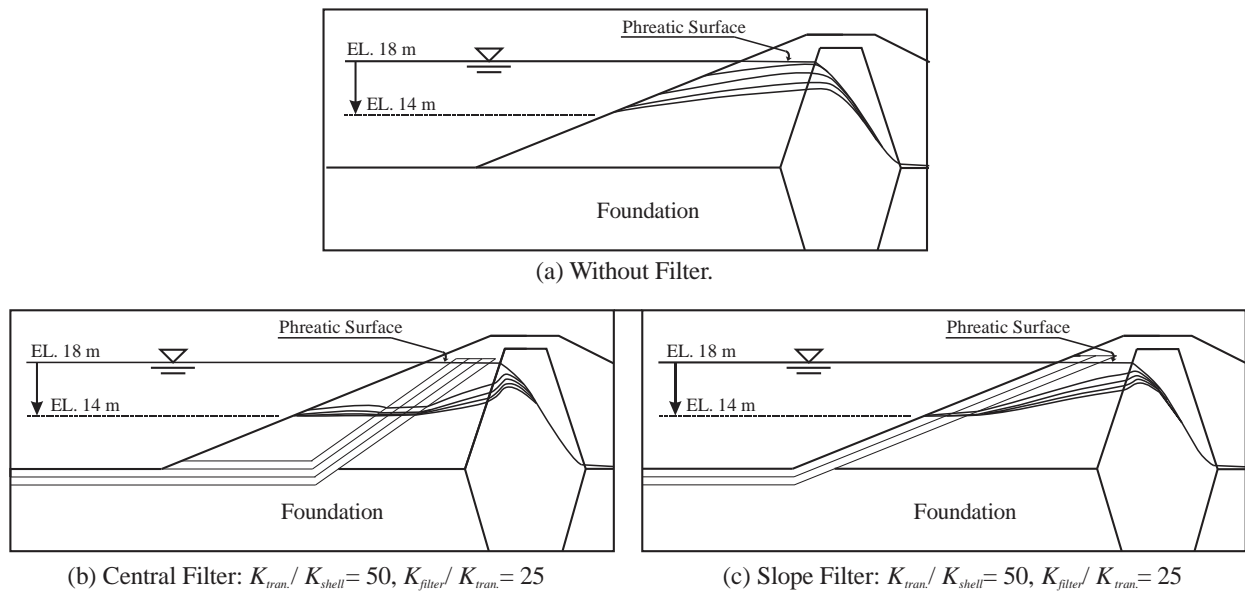


Figure 5.12: Comparison of the effect of the upstream filter on the phreatic surface in the 1<sup>st</sup>, 2<sup>nd</sup>, 3<sup>rd</sup>, and 4<sup>th</sup> days of the drawdown of the reservoir at a rate of 4 m/day.

**Table 5.3** presents a summary of the water flux for a period of 30 days under different drawdown rates. As shown in the table, the drawdown rate has a slight effect on the flux. In the central filter, the water flux through the slope face is reduced to less than 9% of the total flux, while it increases through the foundation surface by more than 91% of the total flux. The transition layer can work as a water drain if the permeability is sufficiently high. The results also showed that, when a central filter is added, the upper horizontal transition layer drained for a period of 30 days is about 3.49 m<sup>3</sup> and 3.44 m<sup>3</sup> of the water flux at a drawdown rate of 4 m/day and 1 m/day, respectively.

Table 5.3: Summary of the total flux (in m<sup>3</sup>/m) that flows out of the earth dam for a period of 30 days under the drawdown conditions.

<i>Reservoir Drawdown in 1 Day</i>					
<b>Dam Cases</b>	<b>Total Flux</b> (m <sup>3</sup> /m)	<b>Flux through the slope</b> (m <sup>3</sup> /30 days/m) (% of the total)		<b>Flux through the foundation</b> (m <sup>3</sup> /30 days/m) (% of the total)	
<b>Without Filter</b>	12.72092	8.81622	69.30	3.90471	30.70
<b>Central Filter</b>	12.30245*	0.963851	7.83	11.3386	92.17
<b>Slope Filter</b>	15.73601	12.6516	80.40	3.08441	19.60
<i>Reservoir Drawdown in 4 Days</i>					
<b>Dam Cases</b>	<b>Total Flux</b> (m <sup>3</sup> /m)	<b>Flux through the slope</b> (m <sup>3</sup> /30 days/m) (% of the total)		<b>Flux through the foundation</b> (m <sup>3</sup> /30 days/m) (% of the total)	
<b>Without Filter</b>	12.60112	8.75081	69.44	3.85031	30.56
<b>Central Filter</b>	12.31964*	1.09064	8.85	11.229	91.15
<b>Slope Filter</b>	15.73199	12.6575	80.46	3.07449	19.54

\*: There is an additional water flux coming from the transition face.

The comparison results of the maximum exit gradient are presented in **Figure 5.13** and **Figure 5.14** for the drawdown rate 4 m/day and 1 m/day, respectively. As shown in the figures, the higher exit gradient is recorded on the slope face at an elevation of 14 m for both dam cases and drawdown rates. The efficiency of the filter in reducing the exit gradient is improved when the filter

permeability is increased, and a transition layer is used around the filter as a protective layer against the soil erosion that may occur during and after the drawdown.

The slope filter showed a higher efficiency in preventing the buildup of excess pore pressure. The exit gradient at a level of 14 m, the critical condition, is decreased by about 37.5% when using a central filter, while it is reduced by about 95.4% when using a slope filter (**Figure 5.13**).

The slow drawdown of the reservoir gives more time for the excess pore water pressure to dissipate resulting in a decrease in the exit gradient, as shown in **Figure 5.14**. The exit gradient on the foundation surface is also affected when using a transition layer with the filter. The foundation surface becomes safer against the quick condition/erosion potential. The exit gradient becomes almost zero on the foundation surface and less than 0.35 on the transition base as shown in **Figure 5.14**.

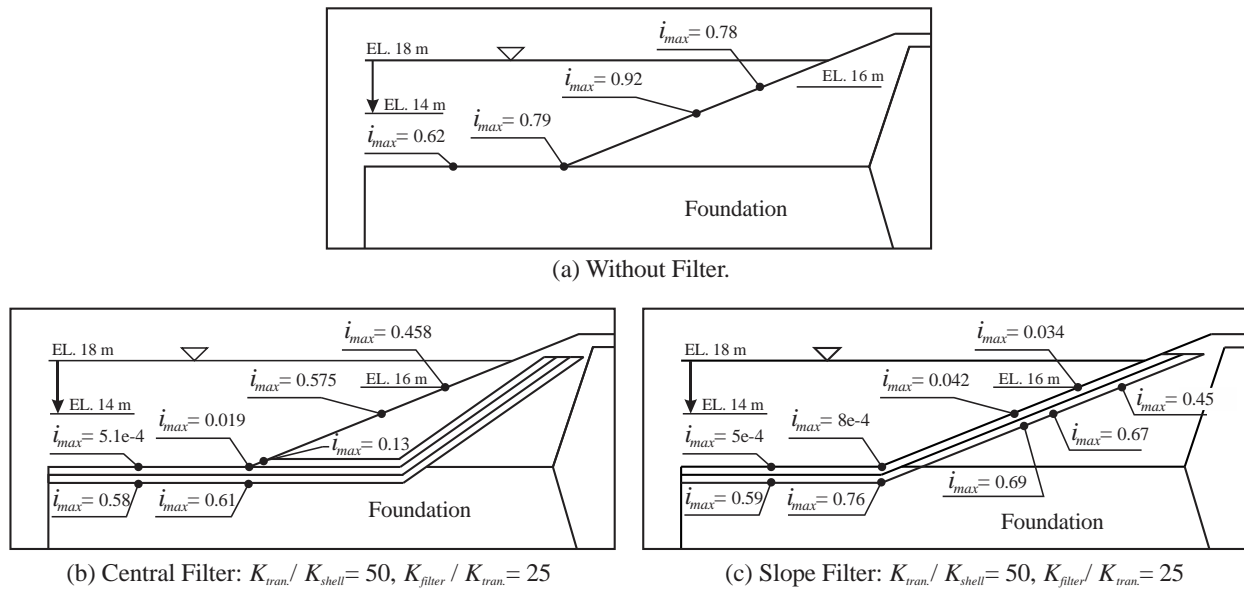


Figure 5.13: Comparison of the effect of both the upstream filter and the transition layer on the exit gradient for different hydraulic conductivities when the drawdown of the reservoir occurs in one day.



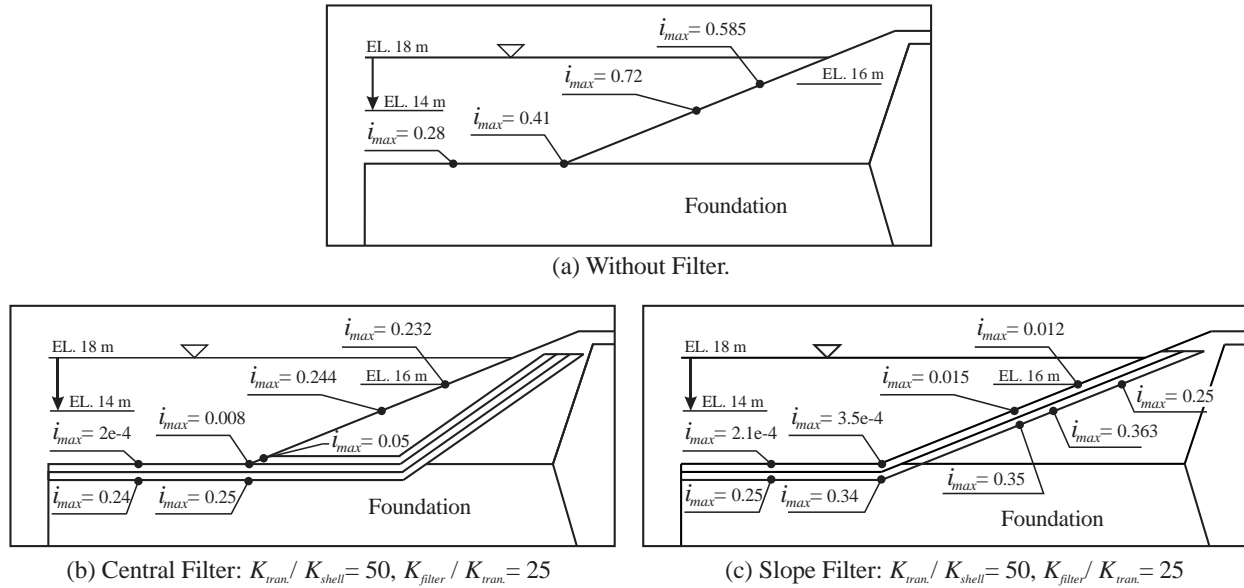


Figure 5.14: Comparison of the effect of both the upstream filter and the transition layer on the exit gradient for different hydraulic conductivities when the drawdown of the reservoir occurs in four days.

In conclusion, constructing an upstream filter is very important in preventing the buildup of excess pore water pressure. It significantly decreases the exit gradient on the upstream slope face of the dam and its foundation surface. The efficiency of the filter improves with higher filter permeability. Amongst the various configurations, the upstream slope filter configuration showed the best results in reducing the exit gradient at the upstream face. Increasing the filter permeability and using a transition zone around the filter further improves the filter function of lowering the phreatic surface inside the dam and decreasing the exit gradient on the slope surface under different drawdown conditions.

## **CHAPTER SIX: ANALYSIS OF THE EARTH DAMS UNDER DRAWDOWN CONDITIONS FOR SLOPE AND DEFORMATION STABILITY**

### **6.1 Introduction**

The stability of the upstream slopes of hydraulic structures such as earth dams may be affected when water flows through the soil from higher head locations to a lower head. The purpose of this paper is to study the slope stability behavior of the earth dam before and after the water level in the reservoir is drawn down in a rapid manner. Also, this paper presents the results of the deformation field of the dam due to the sudden development of excess pore water pressure within the soil voids and its dissipation. This study also includes an investigation of the effect of a low permeability core, the effect of the foundation type on the dam stability, and any improvement in the stability by using an upstream filter.

This chapter is organized into two parts: the first part presents the investigation of the deformation of the dam which including estimating the movement of the soil particles in the  $x$ - and  $y$ - directions displayed in the form of contours lines. The second part shows the influence of the upstream water level under rapid drawdown conditions as compared to the normal steady-state flow condition, on the factor of safety against sliding slope failure.

### **6.2 Numerical Models**

Three typical designs are formulated to study the effect of the core on the slope stability under various drawdown conditions. The base design of the dam consists of a shell, foundation, and downstream filter. An impervious core and a complete foundation cutoff are then added as case

studies to compare the effect of these features on the upstream slope stability. In summary, three cases are studied – namely, Case 1 consisting of a dam without core, a dam with a core only, titled Case 2, and a dam with a core and a cutoff, titled Case 3. **Figure 6.1** shows the profiles of the dams for these three cases. The properties of the soil used in all modeling applications are presented in **Table 6.1**.

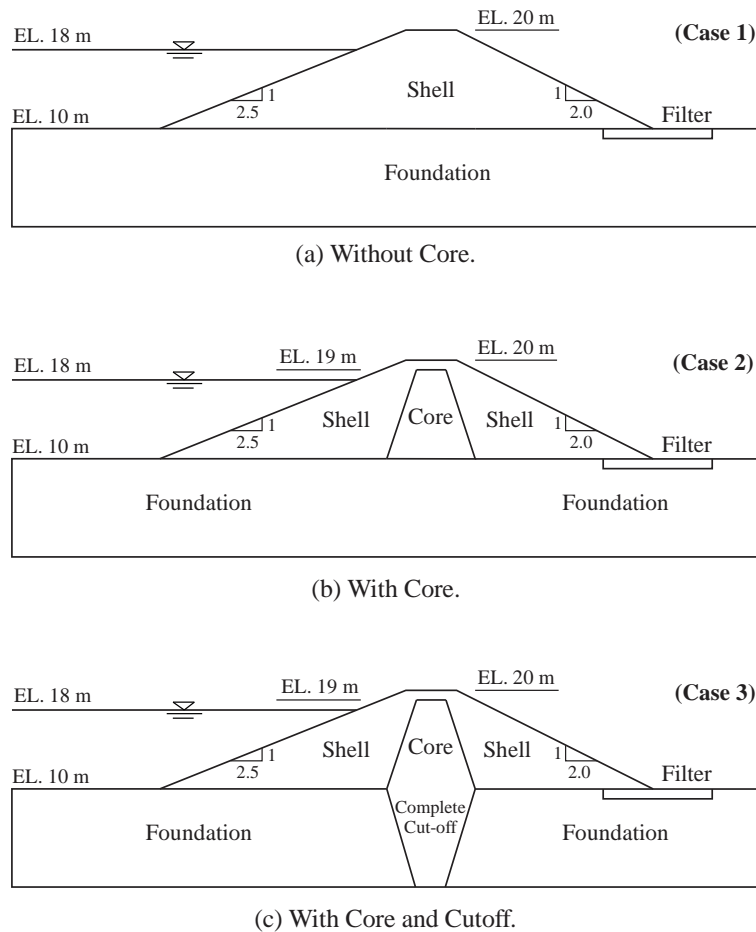


Figure 6.1: Profile sections of the three dam models.

Table 6.1: Material properties of the earth dam used for seepage, stresses and slope analysis.

	Symbols	Soil Materials			
		Shell <sup>a</sup>	Core <sup>b</sup>	Foundation <sup>c</sup>	Drain
Unit weight (kN/m <sup>3</sup> )	( $\gamma$ )	18	19	20	19
Hydraulic conductivity (m/day)	( $k$ )	0.1728	0.000864	0.1728	8.64
Cohesion (kPa)	( $c'$ )	5	14	5	0
Elastic Modulus (kPa)	( $E'$ )	3000	30000	5000-16515	5000
Friction angle	( $\phi'$ )	34°	14°	36°	35°

a: Compacted fill material used on the shell of Upper Fernando Dam (GEO-SLOPE, 2018).

b: Soil material used on the Dau Tieng reservoir (Fattah et al., 2015).

c: Alluvium material used on the foundation of Upper Francesco Dam (GEO-SLOPE, 2018).

Once again, the finite element method (FEM) was used for analysis. GeoStudio 2012 is a software program that uses FEM to solve the governing equations. This family of programs has several software tools that are applicable to the present study, such as SEEP/W for the seepage modeling, SIGMA/W for the stresses/deformation modeling and SLOPE/W for the slope stability. The material models used for the shell and the core soils was a combination saturated/unsaturated system, while the foundation and the filter soils were modeled as fully saturated layers. Quad and triangle elements were used to mesh the dam and other parts in the FEM models. The number of elements used in Case 1 was 1033, for Case 2 was 1038, and 992 for Case 3.

The boundary condition for the seepage analysis in the steady state is specified as the total head on the upstream and downstream sides. The total head is specified as elevation of 18 m on the upstream and 10 m on the downstream side which coincides with the foundation surface. The boundary condition on the downstream slope face cannot be specified as the pore water pressure will depend on the location of the phreatic surface. For this reason, the boundary condition on the

downstream slope surface is modeled as a potential seepage surface.

For the concurrent stress analysis, the boundary condition is specified as a hydrostatic pressure for the water reservoir. The hydrostatic pressure is 18 m on the upstream side and zero on the foundation surface at the downstream side. The displacement in the x-direction is specified as a fixed boundary condition on the left and the right of the ends of the foundation, while a fixed x and y displacement condition is specified at the bottom of the dam model. For the transient analysis, the boundary condition for the seepage analysis is varying values of the head versus time, while it is varying hydrostatic pressure versus time for the stress analysis. The sudden drawdown of the upstream water is simulated by lowering the water level from 18 m to 14 m in one day. Lastly, the Spencer's Method is used to calculate the slope factor of safety. This method includes both interslice shear and normal forces and satisfies both moment and force equilibrium fully (SLOPE/W, 2012).

### 6.3 Deformation Analysis of the Earth Dams

The stability of the dam is impacted the settlement that can occur during the phase when the water level of the reservoir is changed drastically. The water in the soil is bearing some of the weight of the soil and thereby reducing the effective stress in the soil. The ultimate response of the soils depends on the effective stresses. During the drawdown condition, the hydraulic gradient inside the soil becomes higher than the reservoir, which results in the development of seepage forces toward the upstream slope. This generates a force that can either push the particles apart or pull them closer together; as would be the case if the water in the soil was in a capillary state. The deformation state of the earth dam under various seepage conditions is studied in this section.

Several dam designs are modeled to investigate the effect of the core and the foundation soil on the deformation of the dam under steady-state and sudden drawdown condition.

### 6.3.1 With a Permeable Foundation

The voids in the soil foundation are completely filled with water (saturated) through the service period of the earth dams. However, dropping the water level in the reservoir can cause a flow of water toward the reservoir and the development of the seepage force in the direction of the flow. **Figure 6.2** shows the vectors and the shapes of the soil deformation after the reservoir is drawn down to half (i.e, to an elevation of 14 m) at a rate of 4 m/day. As seen in the figure, the soil moves with the seepage flow towards the reservoir, which causes deformation of the earth dam. The maximum deformation of the soil is concentrated on the slope face where the higher magnitude of the water flux was recorded. The drawdown causes *settlement* of the dam soil around the crest and *swelling* of the foundation soils and the below some portion of the upstream slope. The core is also influenced by the drawdown. The major movement of the core soil occurs at the core crest and decreases with the core depth.

**Figure 6.3** shows the deformation contours of the soil for all three cases after the reservoir is dropped to elevation of 14 m (50% of the reservoir) at a rate of 4 m/day. The results showed an increase in the soil deformation when the core permeability is low. The difference in the volume change of the soil depends on the soil properties. The soil movement at the center of the dam was different when using the core as compared to without or with the cutoff, because of the different properties of the core and the cutoff soils.

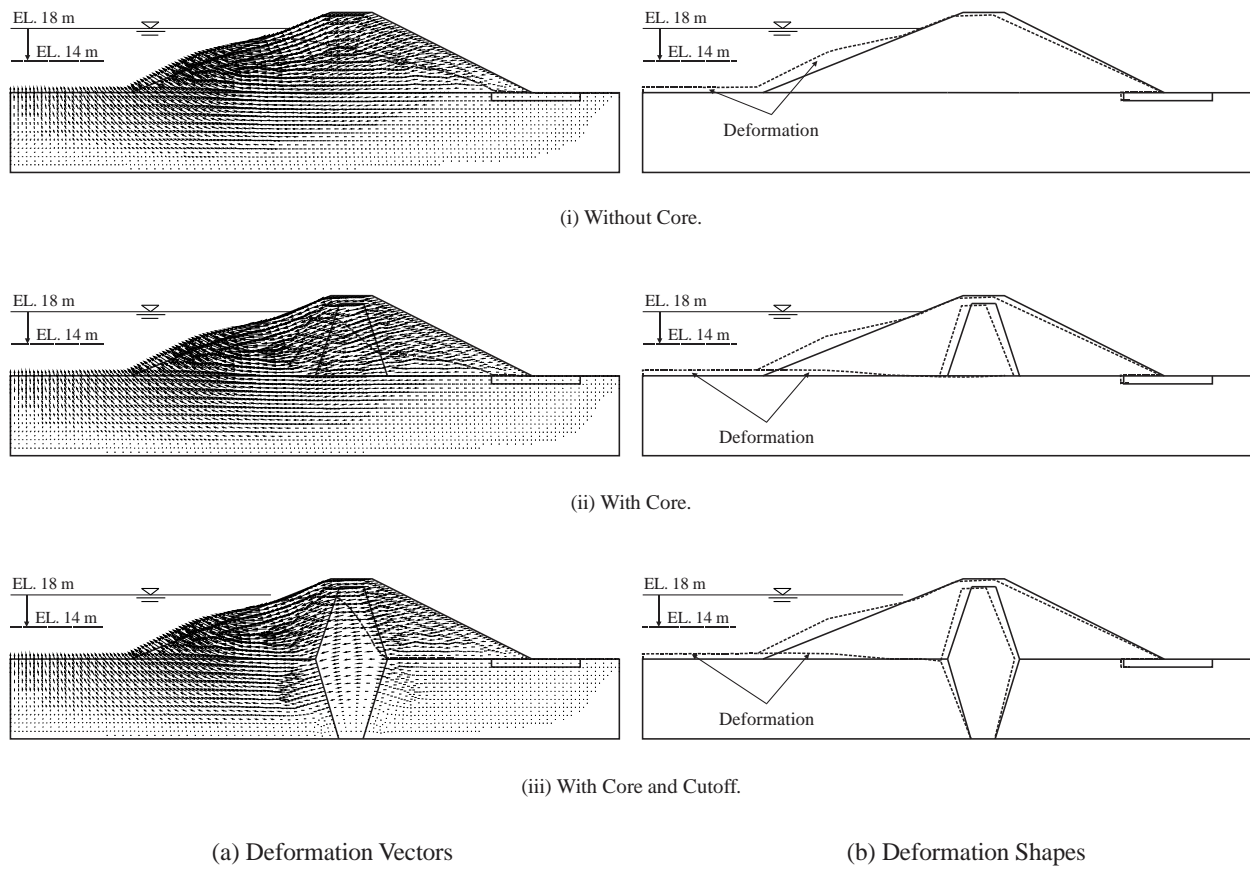


Figure 6.2: Vectors and shapes of the soil deformation for the dam cases under sudden drawdown condition (at a scale of 50x).

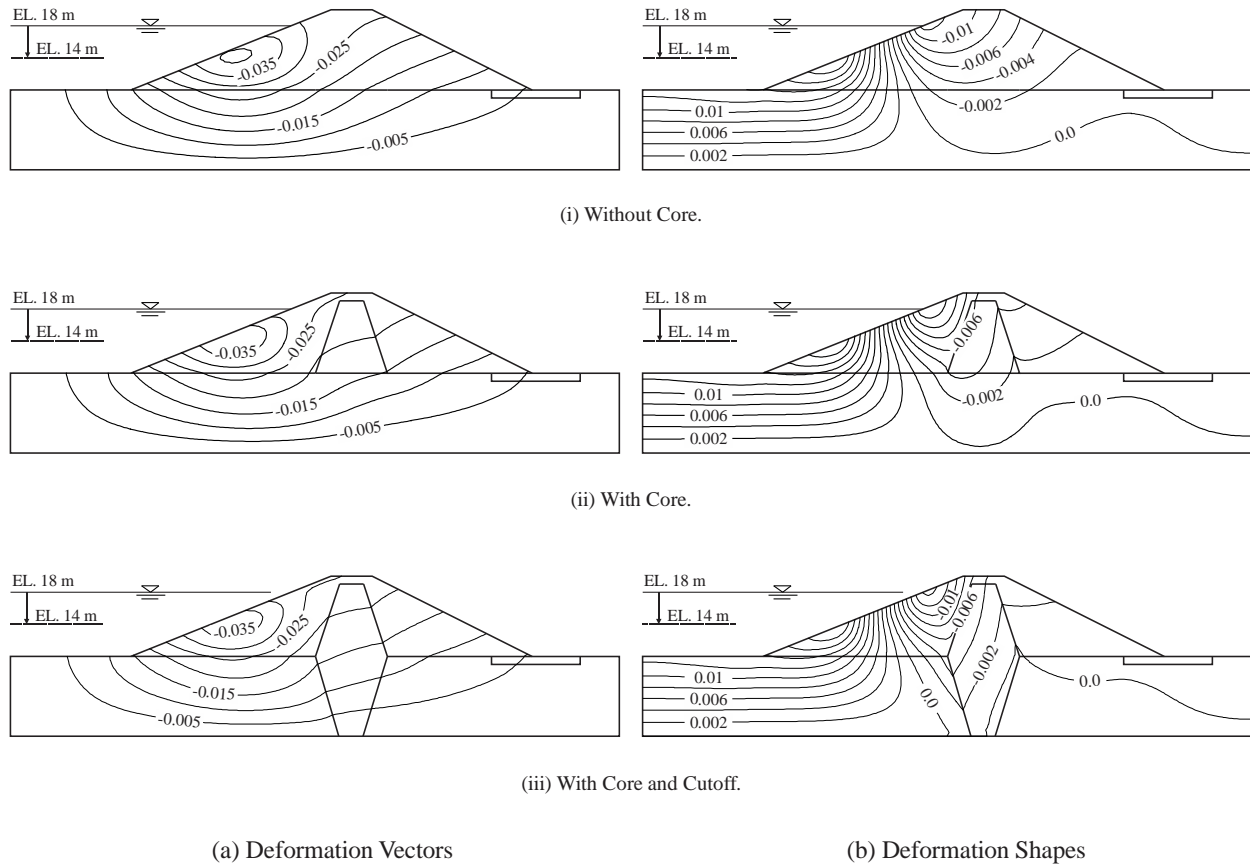


Figure 6.3: Contour lines of the maximum soil displacement (in m) for the dam cases under sudden drawdown condition.

### 6.3.2 With an Impermeable Rigid Foundation

The impermeable nature of the foundation soil may increase the stability of hydraulic structures by preventing the water flux from flowing through its mass. Such soil prevents any influence of the seepage force when the reservoir is drowned down. In addition, the high strength capacity of the foundation soil prevents any further movement of the soil particles after the drop in the level



of the reservoir. To investigate the influence of the foundation soil on the deformation field in the dam, two typical design are modeled; one without a core while the other with a core.

The deformation boundary condition for the foundation is specified as fixed in both  $x$ - and  $y$ -directions. **Figure 6.4** presents the particle movement vector field and the deformation shape of the soil for the case of a drawdown of 50% of the reservoir in one day. The results showed a marked reduction of the deformation in comparison with the permeable foundation case shown in **Figure 6.2**. The movement of the soil particles is reduced near the foundation and on the slope toe. In addition, the swelling deformation state of soil is concentrated on the slope face at the new water level. The calculated values of settlement are presented in **Figure 6.5**. Once again, there is an observed reduction of the deformation when the foundation is rigid. At the downstream side, the movement of the soil particles is also lower for both the without and with core cases in comparison with the low strength permeable foundation case of **Figure 6.3**.

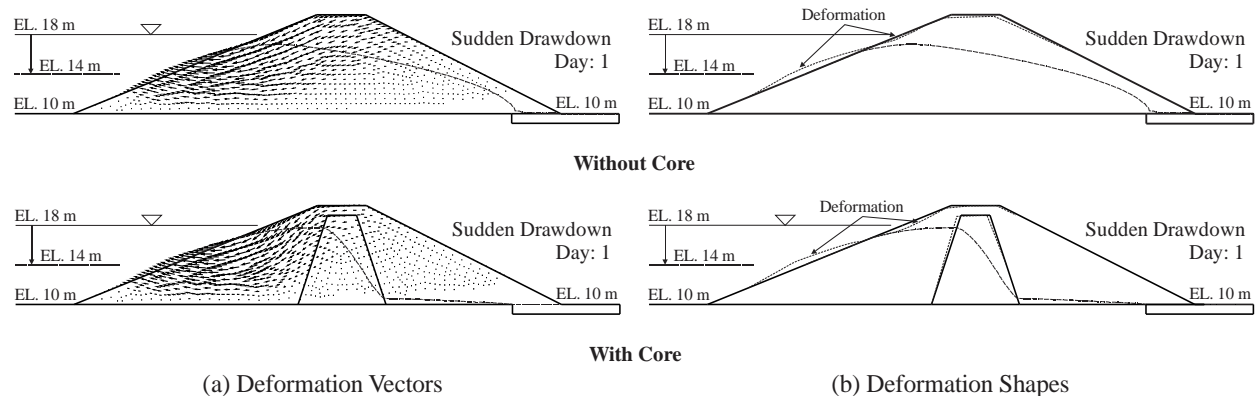


Figure 6.4: Vectors and shapes of the soil deformation for the dam cases under sudden drawdown condition (at a scale of 50x).

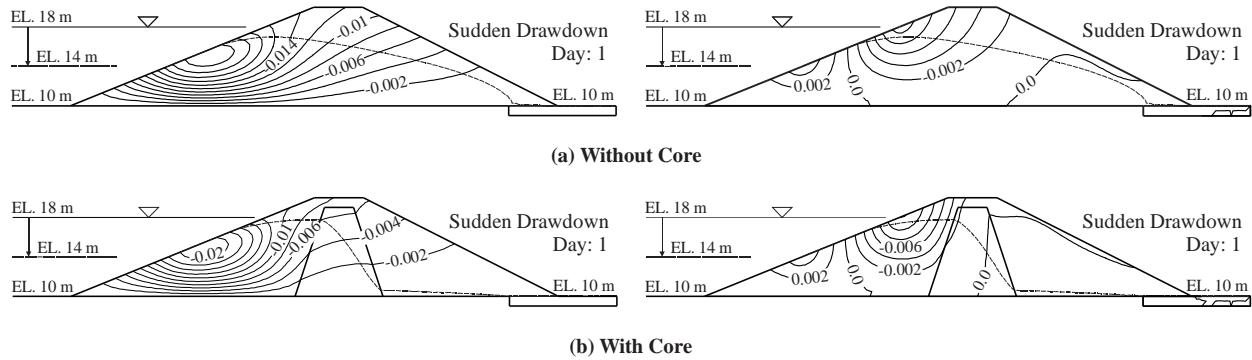


Figure 6.5: Contour lines of the maximum soil displacement (in m) for the dam cases under sudden drawdown condition.

#### 6.4 Slope Stability Analysis of the Earth Dams

The slope stability against failure is discussed in this section. Slope behavior is affected when additional seepage is developed within the dam due to an abnormal situation. Such seepage produces additional pore water pressure which causes a reduction of the effective stress and therefore the shear strength of the soil. In addition, seepage increases the driving shear force by producing added seepage forces. Lastly, seepage may also cause a change in overall soil strength properties by either reducing or eliminating the cohesive strength.

Water waves acting on the upstream face of the dam can also lead to erosion of the slope soil. Further erosion causes cracking on the slope which extends to the dam crest and, in turn, reduces the crest width increasing the risk of collapse. One of the common methods to protect the upstream slope against wave erosion is placing a layer of the rock riprap over a bedding layer and a filter material. The additional weight of the rock increases the slope stability of the dam. However, this type of protection is not included in the current research for the stability analysis.

The stability analysis of the finite slope has been studied in much detail. The current research uses Spencer's Method for slope stability analysis against sliding failure considering seepage. **Figure 6.6** shows a typical assumed slip surface and the balance of forces acting on an element of this finite slope. As seen in the figure, the element  $ABCD$  consists of the self-weight, the seepage force  $J_s$ , the lateral forces ( $U_j$ ,  $U_{j+1}$ ,  $E_j$ , and  $E_{j+1}$ ), and the reaction force ( $T_j$ ) from the soil at the bottom of the element. The flow gradient is also different at different regions in the element. The location of the seepage force is on the center of gravity of the element in the same direction as the flow.

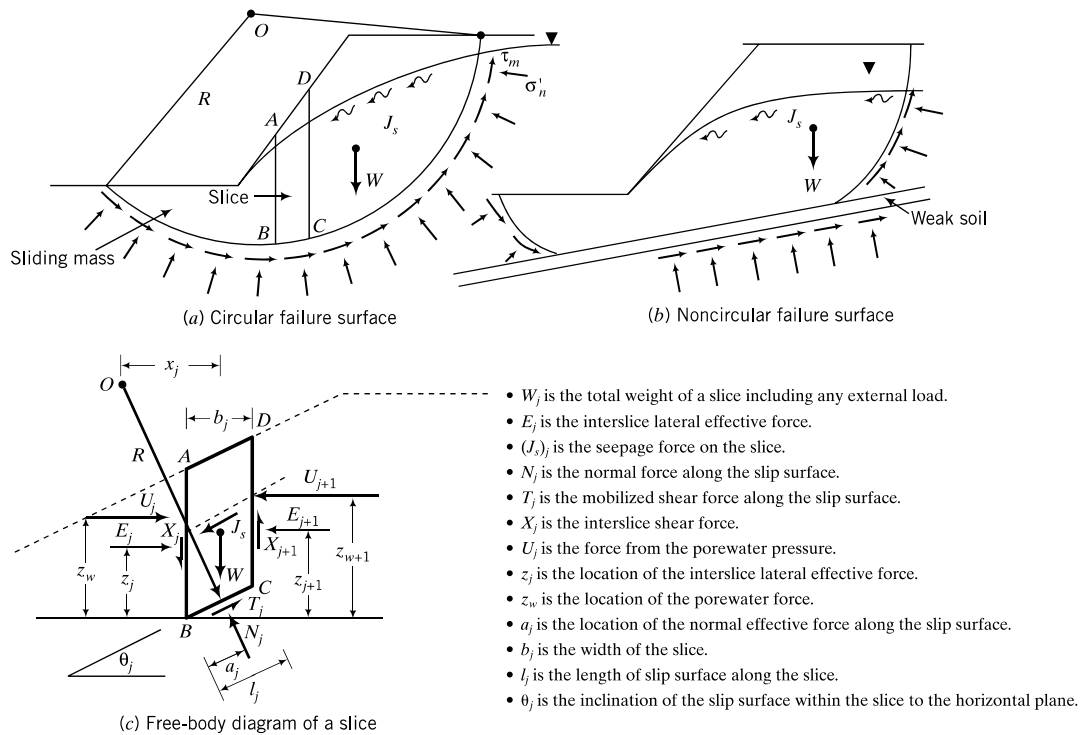


Figure 6.6: Circular and non-circular slip surface in an earth slope and the force diagram in an element (Budhu, 2011).

#### 6.4.1 Factor of Safety Against Sliding

The computation of the factor of safety against sliding failure depends on the driving shear forces and the shear strength of the soil. The components of the driving shear forces are self-weight of soils while the shear strength of soils is based on the Mohr-Coulomb failure criterion with components of cohesion and friction resistance of soils. The shear strength is defined as:

$$\tau = c + \sigma' \tan \phi \quad (6.1)$$

The critical surface in the finite slope could be the interface between the top soil mass and a cylindrical base. The sliding failure of the critical surface takes place when the driving shear forces are larger than the shear strength of soils. Therefore, the factor of safety (FS) against sliding is defined as:

$$FS = \frac{\text{Moment due to } \tau}{\text{Moment of } T} \quad (6.2)$$

Where  $\tau$  is the shear strength of soils, and  $T$  is the net driving shear force. U.S. Army Corps of Engineers (2003) specifies the following: a minimum required a factor of safety against sliding failure for the upstream slope of 1.1 for a rapid drawdown from the maximum surcharge pool; 1.3 for the rapid drawdown from the maximum storage pool; and a minimum of 1.4-1.5 for routine drawdown conditions.

#### 6.4.2 Driving Forces in the Finite Slope

Taylor (1948) described some important concepts to different sets of slope conditions; the dry condition, the submerged condition, the drawdown condition, and the steady-state condition. The

force balance of finite slope under dry condition consists of the dry weight of soil ( $V\gamma_d$ ), the resultant normal force on the failure plan ( $P_B$ ), and the shear strength available on the failure plan, as shown in **Figure 6.7**. The force required for equilibrium is not necessarily equal to the shear strength available on the failure plan. The dry weight of the soil alone contributes to the resultant normal force on the failed plane and is the force required for equilibrium.

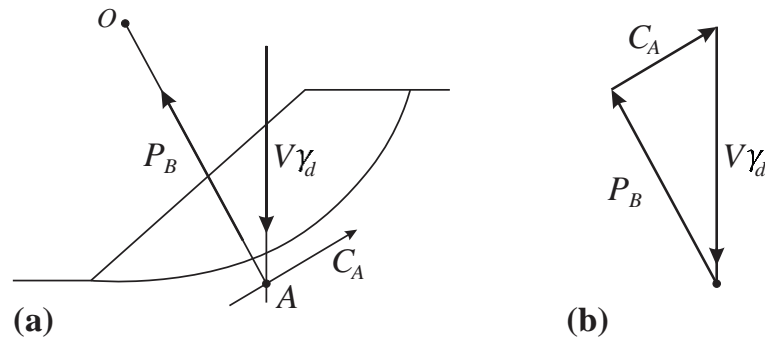


Figure 6.7: The dry case of the slope (Reddi, 2003; Taylor, 1948).

When the reservoir is filled with water (**Figure 6.8**), the presence of water under submerged condition leads to two hydrostatic forces, one from the reservoir ( $U_2$ ) and the other from the water filled the soil voids ( $U_1$ ). The combination of these hydrostatic forces effectively reduces the dry weight of soil ( $V\gamma_d$ ) to the submerged weight ( $V\gamma_b$ ). The weight of water filling the soil voids ( $V\gamma_w$ ) is just supported by the hydrostatic forces. For this case, the factor of safety can be calculated by using the equation:

$$(F_H) = \frac{Ca}{C_B a} = \frac{Ca}{V\gamma_b m - P_B R \sin \phi_d} \quad (6.3)$$

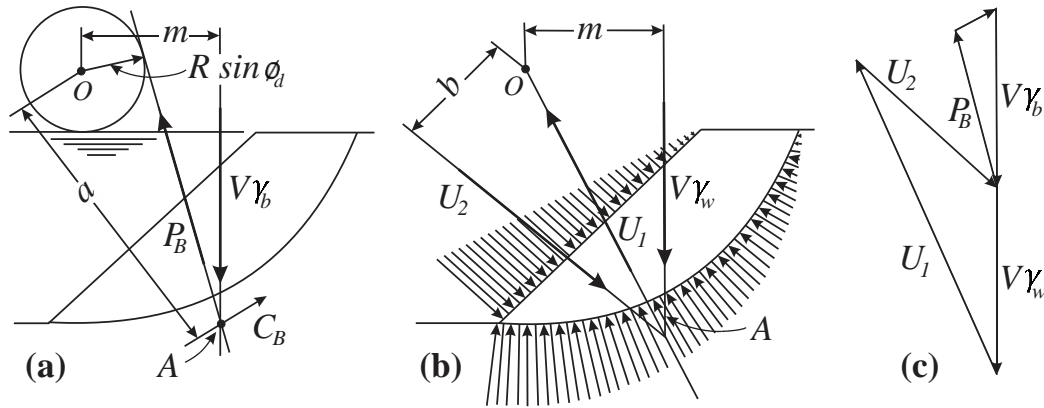


Figure 6.8: The submerged case (Taylor, 1948).

In the sudden drawdown condition (**Figure 6.9**), the analysis of forces is the combination of the same force in the submerged case (**Figure 6.8a**) and the required force for the equilibrium (**Figure 6.9a**). The hydrostatic force of the water reservoir ( $U_2$ ) is eliminated while the hydrostatic force of the water filling the voids ( $U_A$ ) remains the same for a long period of time because of permeability of the soil. The hydrostatic force ( $U_2$ ) forms a balanced force with the water weight ( $V\gamma_w$ ) and the elimination of this force can cause critical loading condition. The hydrostatic force ( $U_A$ ) becomes a natural force acting across the failure plane and must pass through the point  $O$  (**Figure 6.9a**). the force ( $U_A$ ) is a combination force of the submerged weight ( $V\gamma_b$ ) and the water weight ( $V\gamma_w$ ), (**Figure 6.9b**). An additional cohesion ( $C_A$ ) is required in the drawdown case for the equilibrium, which is larger than the force ( $C_B$ ) in the submerged case. The total required cohesion force for equilibrium is ( $C_T$ ) which is the result of the force ( $C_B$ ) and the force ( $C_A$ ).

The slope stability at the upstream side of the earth dam depends on several factors, such as soil properties, slope grading, and the pore water pressure developed when the reservoir level is

changed. The difference in the total head between the reservoir and inside the earthen structural will cause a flowing of the water between the slope face at the upstream. The factor of safety is estimated by using the equation:

$$(F_H) = \frac{Ca}{C_T a} = \frac{Ca}{V\gamma_b m - P_T R \sin \phi_w} \quad (6.4)$$

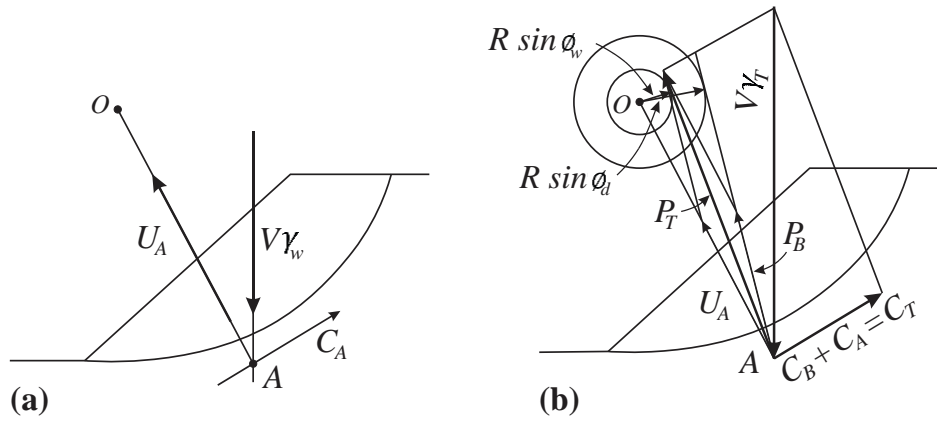


Figure 6.9: Friction circle method for the drawdown case (Taylor, 1948).

After the drawdown event, the excess pore water pressure begins to dissipate until it reaches a steady-state condition after a certain period, depending on the soil permeability. **Figure 6.10** presents the force balance diagram for the steady-state condition at the dam slope. The magnitude and the direction of the neutral force ( $U_{III}$ ) are changed leading to a more stable force ( $B$ ) incorporation to the drawdown case. In addition, the required cohesion ( $C_{III}$ ) become smaller (more favorable) than that in the drawdown case. Thus, the factor of safety against sliding becomes higher than that in the drawdown case.

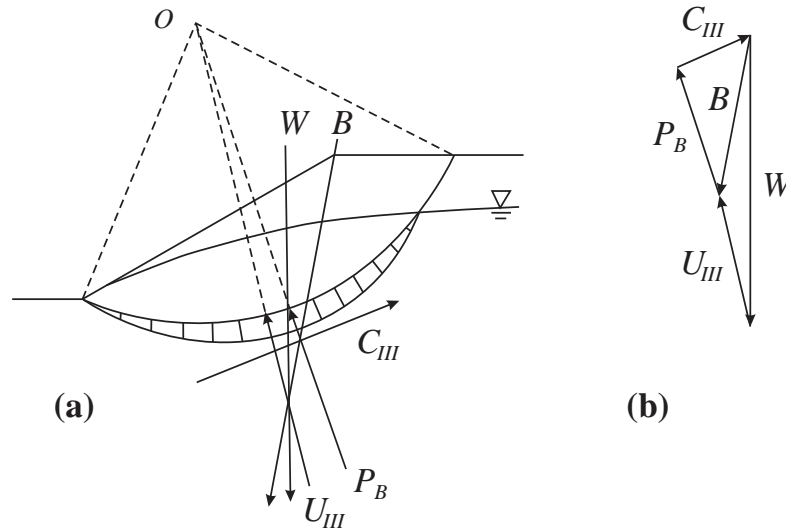


Figure 6.10: Analysis of the steady seepage case (Reddi, 2003; Taylor, 1948).

## 6.5 Analysis of the Slope Stability

### 6.5.1 Effect of the Core

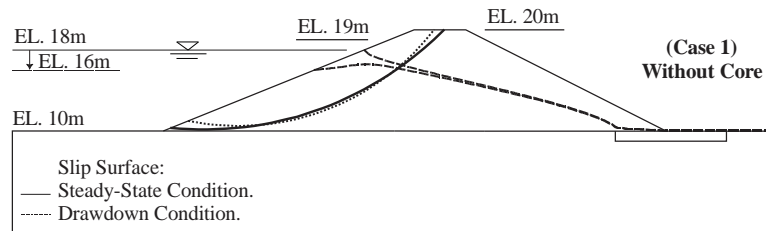
#### 6.5.1.1 Homogenous Earth Dam (Case 1)

The hydrostatic pressure (i.e. water weight) on the slope provides an additional stabilizing effect for the upstream slope. The factor of safety against sliding failure in the steady-state condition is found to be 2.737. If the water level is dropped, the boundary neutral force is decreased, and excess pore water pressure develops toward the upstream face causing an increase in the buoyancy force.

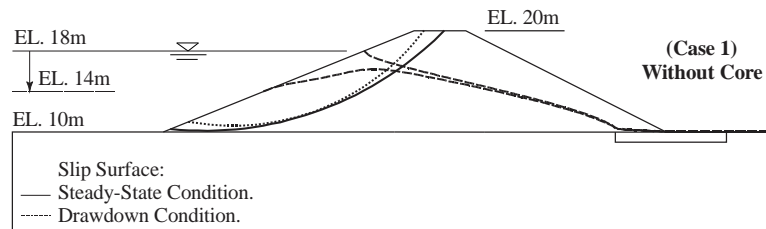
**Figure 6.11** shows the result for the critical slip surface. To investigate the effect of the drawdown on the slope stability, the relationship between the factor of safety and the drawdown rate is plotted in **Figure 6.12** for a period of 30 days after the start of the drawdown event. The results showed a reduction in the factor of safety after the drawdown event. The factor of safety for the upstream



slope decreases until it reaches the lowest level when the drawdown is completed. After this level, the excess pore water pressure begins to dissipate with the time, and the factor of safety starts to increase until it reaches to a new value depending on the new water level of the reservoir and the driving force after the drawdown. The magnitude and the rate of the water drawdown are the primary factors influencing the factor of safety. The slower the drawdown rate, the higher the factor of safety. The pore pressure needs a longer period to dissipate because of the lower porosity of the soil. There is evidence that the pore water pressure does not dissipate through the first 30 days of the drawdown as presents in **Figure 6.12b**. The factor of safety does not reach the steady-state level after 30 days of the drawdown event.



(a) Drawdown 25% of the reservoir.



(b) Drawdown 50% of the reservoir.

Figure 6.11: Critical slip surface for Case 1 under sudden drawdown of 4 m/day.

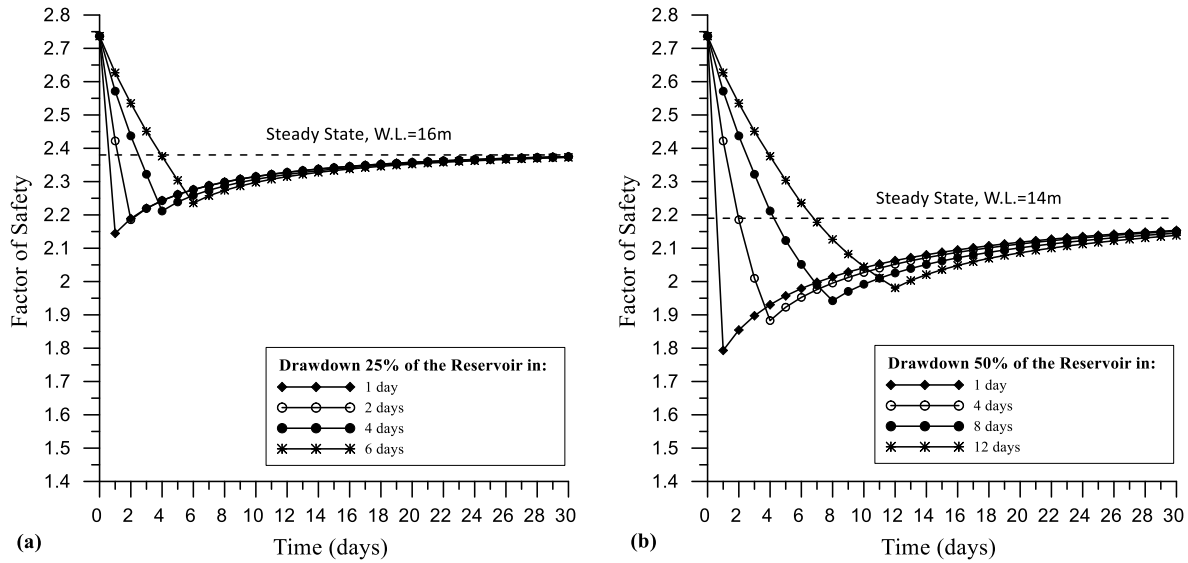


Figure 6.12: Influence of the upstream slope stability for Case 1 under different drawdown rates; (a) drawdown 25% of the reservoir, (b) drawdown 50% of the reservoir.

#### 6.5.1.2 Earth Dam with a Core (Case 2)

**Figure 6.13** shows the critical slip surface at various water levels. The results show a slightly different slip surface shape in comparison with Case 1 which may be attributed to the presence of the core. **Figure 6.14** shows the influence of the core on the factor of safety against sliding under various drawdown conditions. It is seen that the factor of safety under the steady-state condition is lower by about 6.76% compared to Case 1. The reason is that the core increases the buoyancy of the mass of the soil causing a decrease in the effective stress.

During the drawdown condition, the reduction of the neutral boundary force (i.e. water weight in the reservoir) developed a higher level of the non-equilibrium condition between the dam soil and the reservoir. This approach causes an additional decrease in the factor of safety in comparison with Case 1. The slip surface is also slightly changing after the drawdown. In comparison with

Case 1, the critical condition on the slope stability also occurred under sudden drawdown (**Figure 6.13**). At this condition, the factor of safety is decreased up to 18.61% when the reservoir is drawdown 25% of the reservoir, and up to 30.09% under drawdown 50% of the reservoir.

The results of the slow drawdown conditions showed a decrease in the factor of safety for all rates. The low permeability of the core prevents the excess pore water pressure from dissipating toward the downstream, which slows the process of dissipation post drawdown. The factor of safety begins to increase after a period of time because of the increase in the effective stress due to the dissipation of excess pore water with time. However, the excess pore water pressure needs a period of more than 30 days to completely dissipation under both drawdown 25% and 50% of the reservoir (**Figure 6.14**).

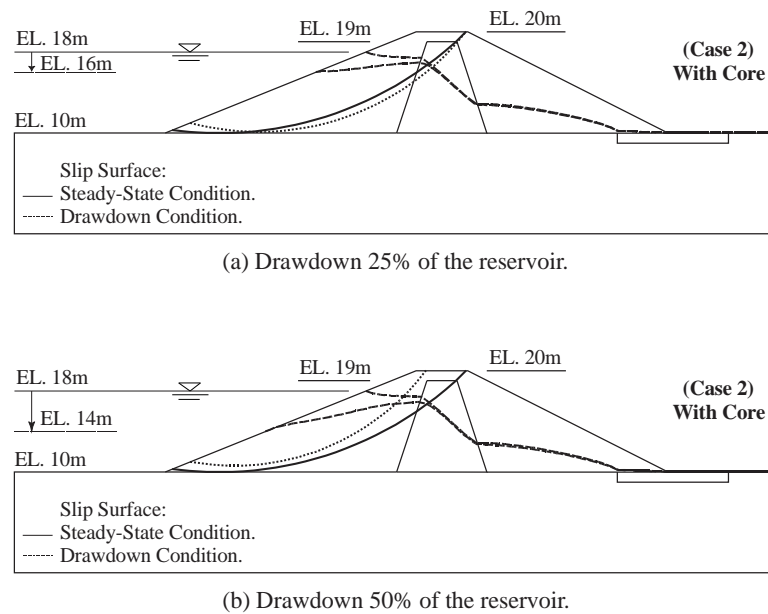


Figure 6.13: Critical slip surface for Case 2 under sudden drawdown of 4 m/day.

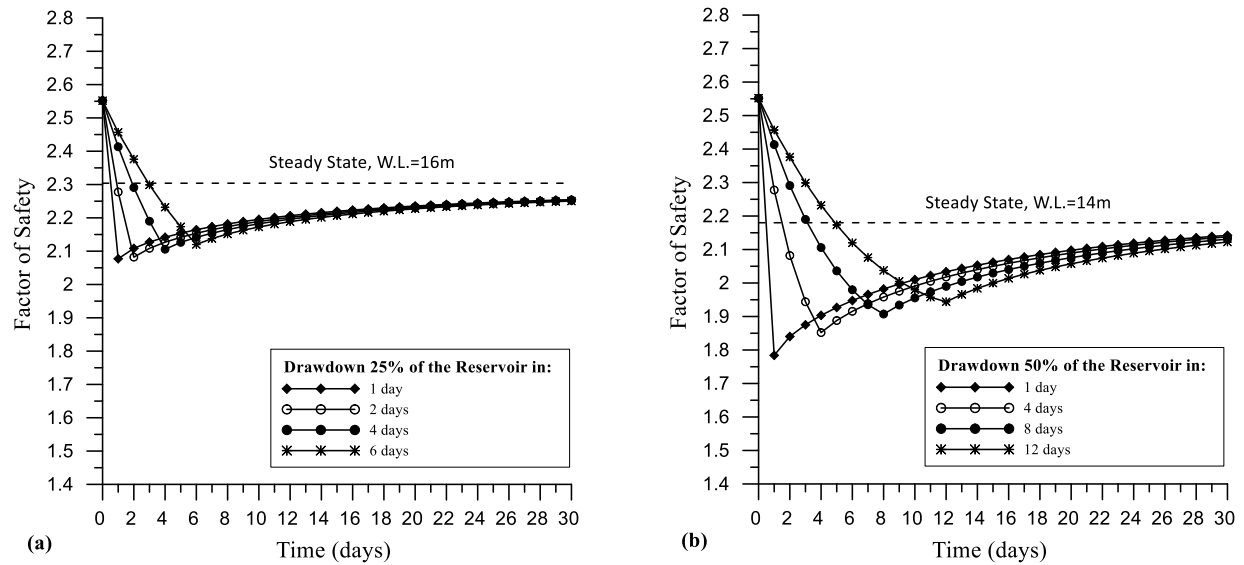


Figure 6.14: Influence of the upstream slope stability for Case 2 under different drawdown rates; (a) drawdown 25% of the reservoir, (b) drawdown 50% of the reservoir.

### 6.5.1.3 Earth Dam has a Core and a Complete Cutoff (Case 3)

The slip surface of the for the Case 3 with both core and complete cutoff is shown in **Figure 6.15**. **Figure 6.16** shows the factor of safety against sliding of the upstream slope at varies drawdown depths and rates. As shown in the figure, the factor of safety at the steady state is decreased by 14.65% and 8.46% in comparison with Case 1 and Case 2, respectively. The reason is that the low permeability of the core and the cutoff acts as a wall causing a large reduction of the flux velocity at the upstream side, which causes an increase the buoyancy of the soil (i.e. decrease in the soil weight) and thus a decrease in the effective stresses.

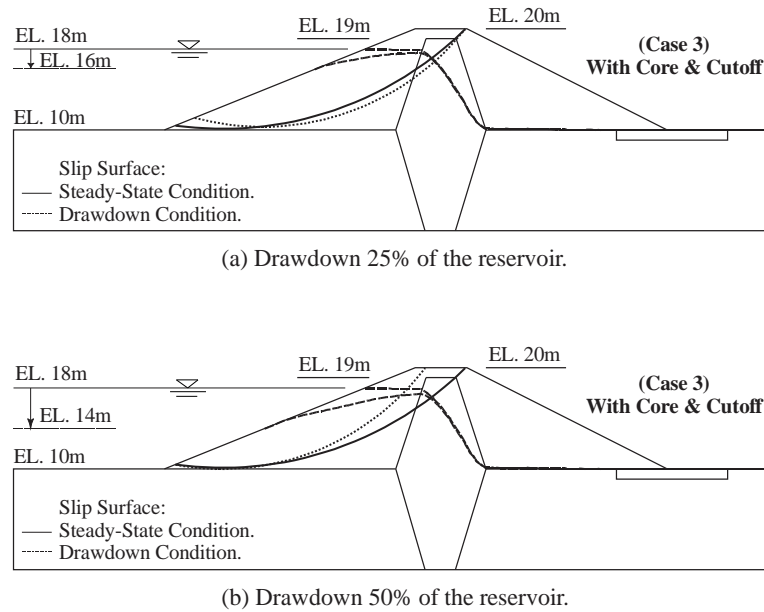


Figure 6.15: Critical slip surface for Case 3 under sudden drawdown of 4 m/day.

During the drawdown conditions, higher driving forces develop inside the slope soil resulting in a critical condition of the instability due to the need for longer time to dissipate all the excess pore pressure. This condition caused a higher reduction in the factor of safety in comparison with Cases 1 and 2. The slower rate of the drawdown does not improve the slope stability against sliding in this case. The results of the factor of safety showed a lower level of the stability in comparison with both other cases. Depending on the drawdown speed, the factor of safety will decrease up to 18.49% when drawdown 25% of the reservoir, and up to 30.05% when drawdown 50% of the reservoir.

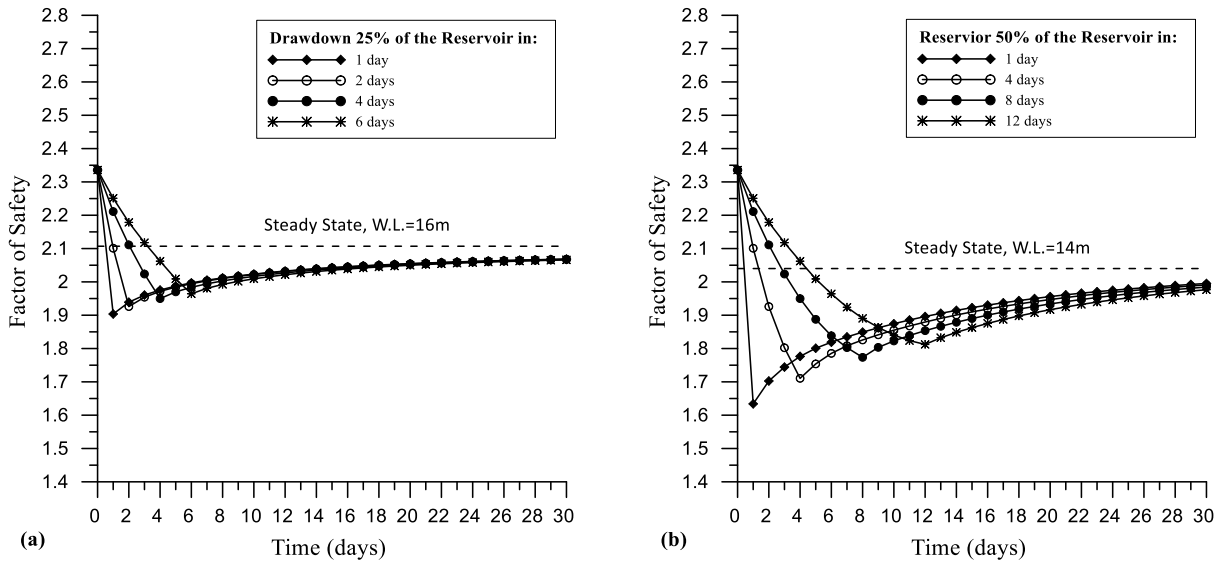


Figure 6.16: Influence of the upstream slope stability for Case 3 under different drawdown rates; (a) drawdown 25% of the reservoir, (b) drawdown 50% of the reservoir.

#### 6.5.1.4 Summary of Comparisons

Three typical designs of the earth dam, a homogeneous dam (Case 1), a dam with a core (Case 2), and a dam with a core and a complete cutoff (Case 3), are modeled to study behavior of the soil properties and seepage rates on stability under drawdown condition. Water flux, exit gradient, and the factor of safety are computed for each case before and after the drawdown at various periods: fast drawdown, drawdown at a rate 1, 2, and 3 m/day for both 25% and 50% drawdown of the reservoir.

**Table 6.2** shows the upstream slope factor of safety against sliding for the three cases at various steady-state conditions. Constructing the dam with the core or with a core and a cutoff reduces the upstream slope stability against sliding. The low permeability of the core soil reduced the seepage

velocity inside the core and, in turn, increase the saturated area (i.e. the buoyancy) of the soil mass. This decreases the effective stresses in the upstream region.

The slope stability is decreased with lowering of the water level in the reservoir as shown in **Table 6.2**. The hydrostatic pressure coming from the water in the reservoir provides an additional stabilizing effect for the upstream slope. The factor of safety for Case 1 in the steady state is 2.737, while it is decreased to 2.552 for Case 2 at a decreasing percentage of 6.76%. The reason is that the core increases the buoyancy of the soil which in effect is a decrease in its weight. In Case 3, the factor of safety at the steady state reduces to 2.336 compared to other cases present in the previous sections. This may due to the core and a complete cutoff holding a large amount of water at the upstream side, which causes an increase the buoyancy of the soil and reducing the effective stresses.

Table 6.2. Factor of safety in the steady-state analysis for all dam cases at different reservoir levels

Dam Cases	<i>Factor of Safety Against Sliding</i>		
	Reservoir Level		
	At Level 18 m	At Level 16 m	At level 14 m
<b>Case 1</b>	2.737	2.384	2.192
<b>Case 2</b>	2.552	2.304	2.182
<b>Case 3</b>	2.336	2.107	2.039

Under drawdown conditions, the boundary neutral force in the form the water weight in the reservoir will decrease *faster* than the buoyancy force of the soil due to the low permeability of the soil. In addition, excess pore water will develop toward the upstream face causing an increase of the buoyancy force. This combination results in a decrease in the stability of the upstream slope.

To investigate the effect of the drawdown, the relationships between the minimum values of the factor of safety against sliding and the drawdown rates are plotted in **Figure 6.17** for a period of 30 days after the beginning of the drawdown. The percentage reduction of the factor of safety caused by the core and the core with a cutoff is also presented in the figure.

The results showed that the factor of safety for the upstream slope decreases rapidly through the drawdown event until reach its lowest value when the drawdown is completed. Then, it starts to increase with time because of the dissipation of the excess pore pressure until a steady-state condition is reached. The depth and the period of the drawdown are the main factors affecting the change in the factor of safety.

The most critical condition impacting the slope stability is sudden drawdown (**Figure 6.17**). In this condition, the factor of safety is decreased by 21.63% for Case 1, 18.61% for Case 2, and 18.49% for Case 3 when the drawdown is 25% of the reservoir. The factor of safety is additionally decreased by 34.49% for Case 1, 30.09% for Case 2, and 30.05% for Case 3 when the drawdown is 50% of the reservoir. The percentage reduction in the factor of safety caused by the core (Case 2) or the core with a cutoff (Case 3) is presented in **Figure 6.17** in comparison with Case 1. The rest of the drawdown conditions showed a lesser drop in the factor of safety compared to the rapid drawdown case. This may be attributed to the process where the slow drawdown gives an additional period for the excess pore water pressure to dissipation. After a period of time, the factor of safety starts to increase because of the dissipation of the excess pore water with the time which turns causes an increase of the effective stress in the slope soil. The factor of safety does not return



to the original value before the drawdown because of a permanent alteration of the force balance between the dam and the reservoir.

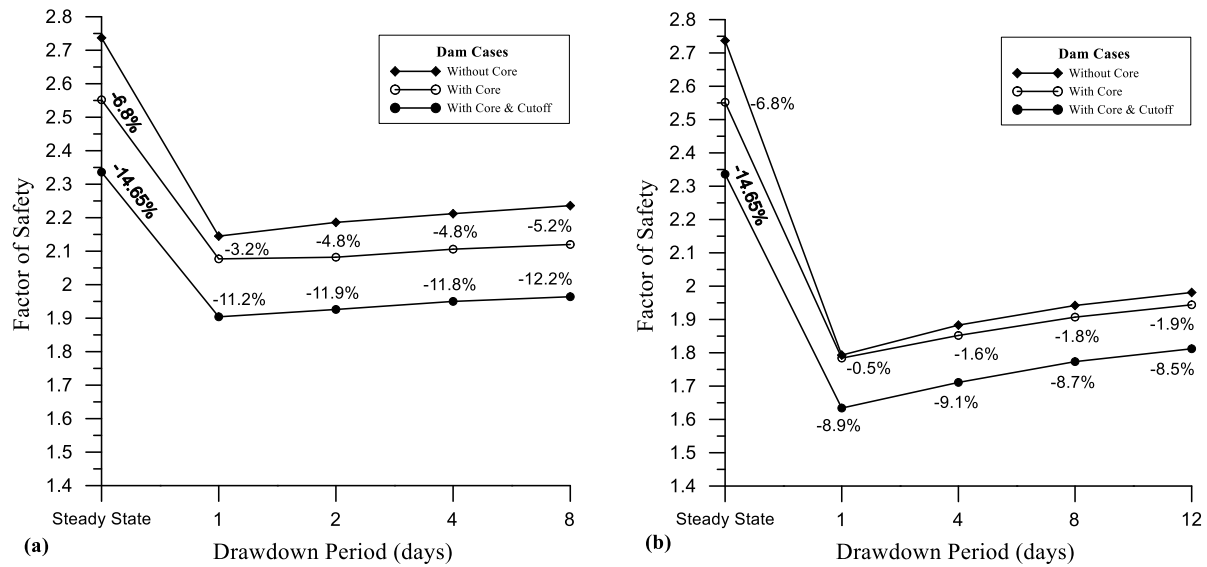


Figure 6.17: Comparison of the factor of safety for the dam cases under different drawdown conditions; (a) drawdown 25% of the reservoir, (b) drawdown 50% of the reservoir.

### 6.5.2 Influence of the Foundation Material

The factor of safety depends on the soil properties of both the dam and the foundation. In this section, the earth dams are assumed to be constructed on a rigid foundation to investigate the influence of the foundation on the dam stability. The results of the stability analysis showed a change of the slip surface to become non-circular as shown in **Figure 6.18**. **Table 6.3** summarizes the factor of safety at various water level under steady-state conditions. The results showed a reduction in stability of the slope. The factor of safety for the case without core is reduced by 6.69%, 5.66%, and 4.84% at level 18m, 16 m, and 14 m, respectively in comparison to Case 1

(presented in section 6.5.1.1). The stability is also decreased when constructed with a low permeability core. The factor of safety is reduced by 0.43%, 1.8%, and 0.93% at level 18m, 16m, and 14 m respectively in comparison with Case 3 (presented in section 6.5.1.3). The reason is that the permeability of the foundation soil increases the draining process of the water flux toward the downstream. An impermeable foundation causes a raising of the phreatic surface at the upstream region and, in turn, reduce the stability of the upstream slope.

Table 6.3. Factor of safety in the steady-state analysis for all dam cases at different reservoir levels

Dam Cases	<i>Factor of Safety Against Sliding</i>		
	Reservoir Level		
	At Level 18 m	At Level 16 m	At level 14 m
<b>Without Core</b>	2.554	2.249	2.086
<b>With Core</b>	2.326	2.069	2.020

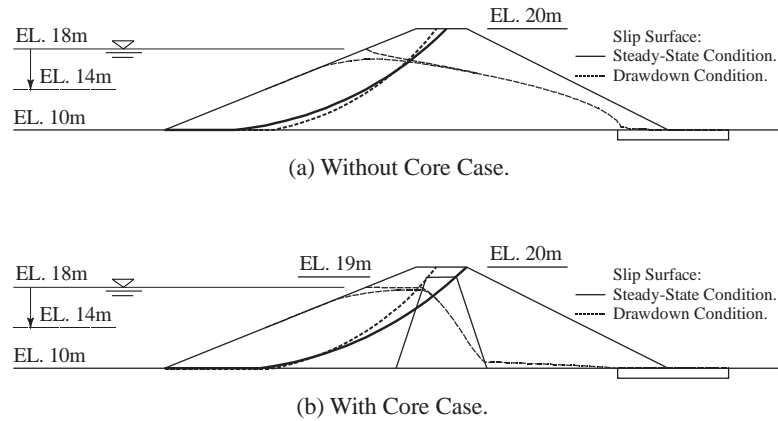


Figure 6.18: Critical slip surface for the dam cases after drawdown 50% of the reservoir at a rate of 4 m/day.

The results of the factor of safety against sliding are presented in **Figure 6.19**. As seen in the figure, the factor of safety is slightly increased during the drawdown process because of the

foundation material. In addition, the excess pore water pressure is not totally dissipated from the dam. It needs a period of more than 30 days to completely dissipation for both dam cases under drawdown 25% (Figure 6.19 a,b) and 50% (Figure 6.19 c,d) of the reservoir.

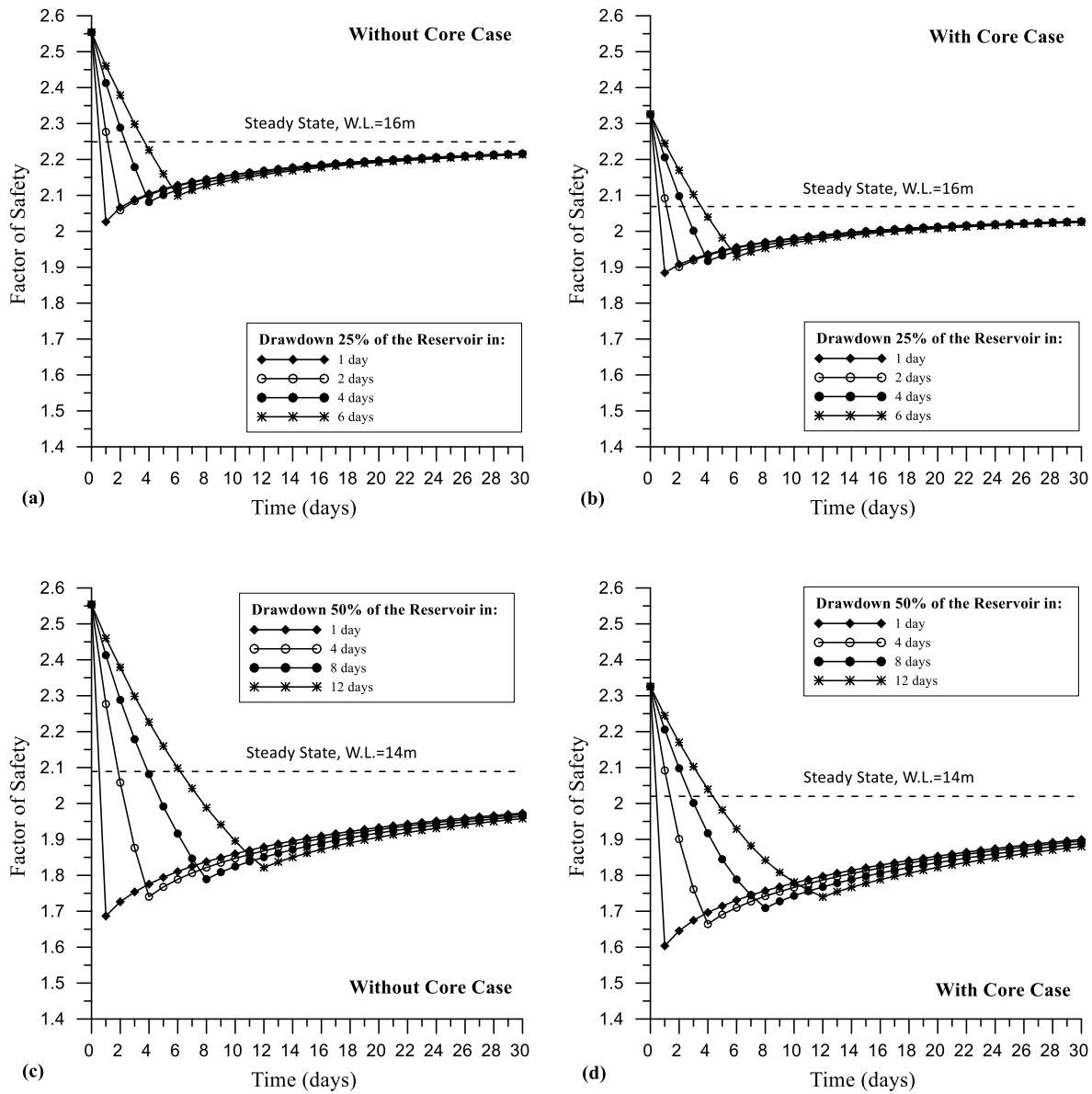


Figure 6.19: Influence of the dam foundation on the upstream slope stability under different drawdown conditions.

### 6.5.3 Effect of the Upstream Filter

#### *6.5.3.1 Influence of the Filter Permeability*

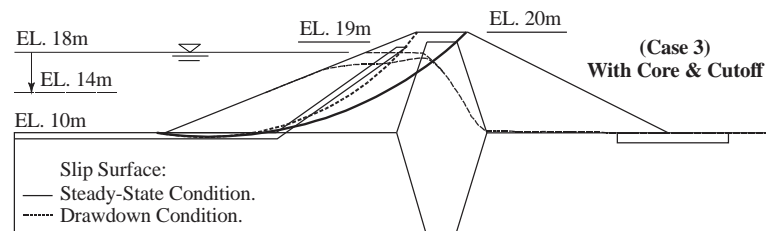
As discussed in the previous chapter, the hydraulic gradient on the upstream slope face can reach the critical condition when the dam is constructed with a core and a complete cutoff (Case 3). Installing an upstream filter was found to bring down the exit gradient to safe levels. In this section, Case 3 is studied in further detail to investigate the effect of an upstream filter on the slope stability against sliding. Two locations of the filter, a central filter and a slope filter, are installed at the upstream region to calculate the slope factor of safety against sliding before and after the drawdown event. The permeability ratio between the filter to the soil base is considered as four possible values, 25, 50, 75 and 100. The water level in the reservoir is simulated to be dropped to an elevation level of 14 m (50% of the initial reservoir level) at a rate of 4 m/day.

The results of the factor of safety in the steady-state condition at various water levels are presented in **Table 6.4**. The results showed a very slight reduction of the factor of safety in the steady-state condition when using the upstream filter. The high permeability of the filter raises the phreatic line on the upstream side, which causes an increase in the saturated area, i.e. the submerged weight. The strength of the slope against sliding failure is reduced due to the reduction of the effective stress. The permeability ratio does not have a significant effect on the factor of safety.

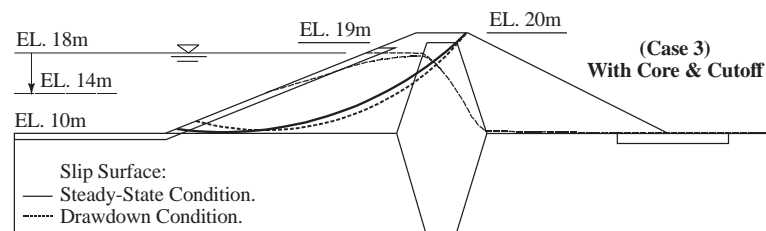
The slip surface is changed after the drawdown condition because of the change in the force diagram (**Figure 6.20**). The reason is the change in the saturated area at the upstream and the soil properties of the filter.

Table 6.4: Factor of safety in the steady-state analysis for all dam cases at different reservoir levels.

<i>Factor of Safety Against Sliding</i>								
Cases	Reservoir Level							
	At Level 18 m				At Level 14 m			
	$k_{\text{filter}}/k_{\text{soil}}$				$k_{\text{filter}}/k_{\text{soil}}$			
	25	50	75	100	25	50	75	100
Without Filter	2.336				2.039			
Central Filter	2.160	2.160	2.159	2.159	1.872	1.871	1.870	1.870
Slope Filter	2.322	2.322	2.322	2.322	2.026	2.026	2.026	2.026



(a) Central Filter - Drawdown 50% of the reservoir.



(b) Slope Filter - Drawdown 50% of the reservoir.

Figure 6.20: Critical slip surface of the upstream slope before and after the sudden drawdown condition.

Under the drawdown condition, the slope stability of the upstream is increasing with an increase in the permeability of the filter soil when adding the slope filter. **Figure 6.21** shows the results of the factor of safety for all permeability cases of the filter under the sudden drawdown condition. However, the central filter causes an additional reduction in the factor during the drawdown

process. After the drawdown is completed, the function of the central filter as a drain for the water flux begins to be observed for a higher permeability ratio. There is an increase in the stability factors. But these values are still lower than the other cases.

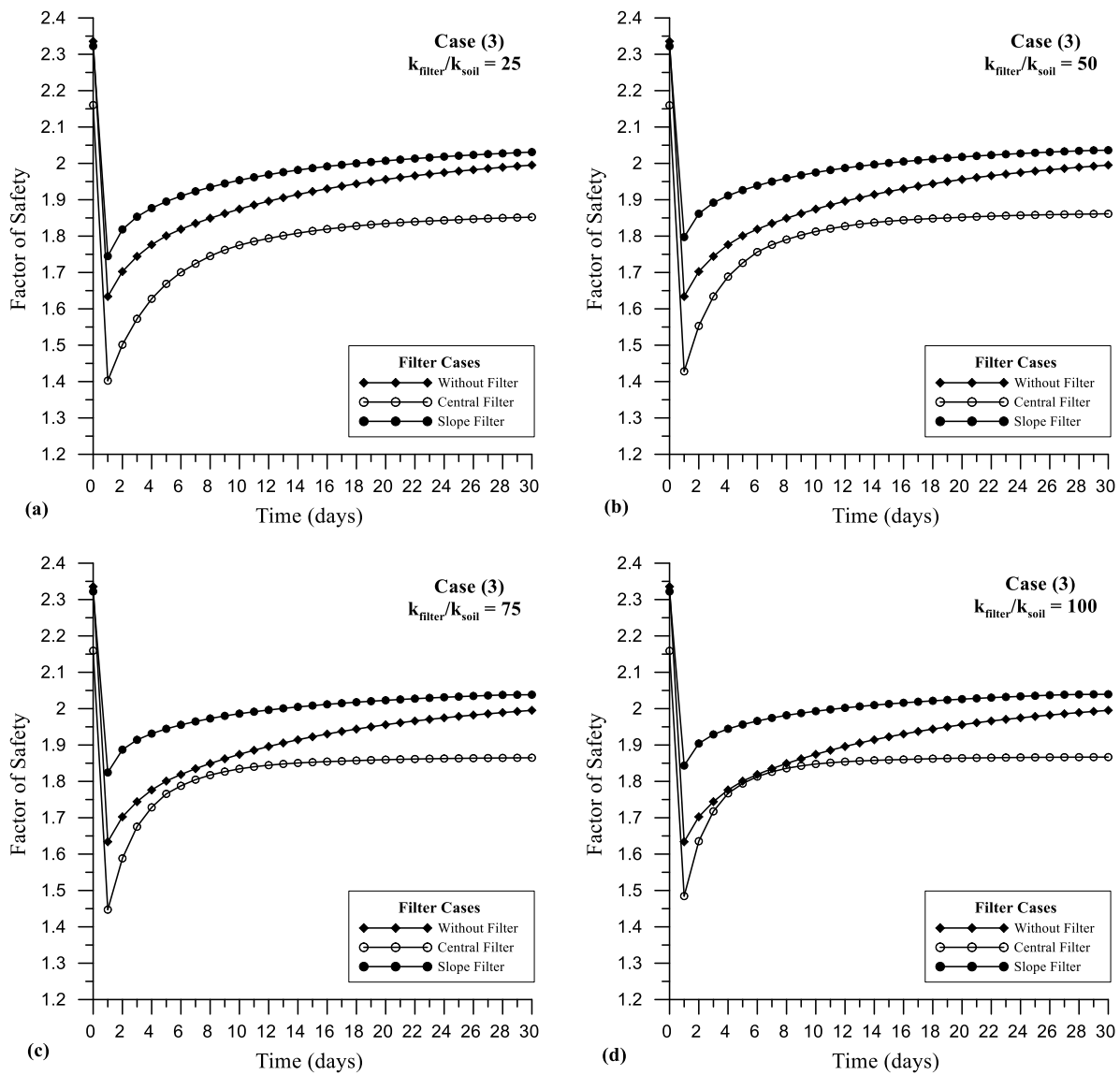


Figure 6.21: Influence of the filter permeability on the upstream slope stability under sudden drawdown condition.

In conclusion, the lowering of the upstream water level at the external boundary causes movement of the soil particles and creates potential conditions for the formation of piping. The low permeability of the core with a cutoff increases the soil deformation because of the rise of the saturated area in the upstream region. Installing a higher permeability filter increases the flux velocity inside the filter increasing the deformation around the filter. The factor of safety of the slope is also reduced because of the increased buoyancy of the soil at the upstream side of the dam. The soil properties of the *upstream* filter have a significant influence on the slope stability against sliding. An upstream slope filter increases the stability of the slope while a central filter decreases it.

## **CHAPTER SEVEN: SEEPAGE AND SLOPE STABILITY OF A REAL DAM UNDER DRAWDOWN CONDITIONS**

### 7.1 Introduction

Earth dams are man-made structures used for several purposes such as electricity production, flood control, and irrigation. Dams may be different in the size and designs depending on the function of the dam and the size of the water source. They can range from a few meters in length to many kilometers. The water level in the dam reservoirs fluctuates along the year between high levels in the winter season to lowered ones in the summer and irrigation seasons. A sudden drawdown event may take place which causes a sudden drop in the reservoir in just few hours similar to what happened at the Teton Dam. In addition, the construction of new dams on the same water source caused additional loss of water in the dam reservoir. Lastly, the rise in temperatures in the summer season especially in the Middle East causes increased evaporation of a large amount of water in the rivers and a significant reduction in the levels of these rivers in short periods.

In this chapter, the influence of lowering of the water level in the dam reservoir on the stability of the dam is studied. Of particular importance is the impact of climate change on increased demand for surface water consumption, which has led to a serious water shortage. A dam in the Middle East called the Al Adhaim Dam is studied under sudden drawdown conditions due to the various causes discussed here.

The analysis is divided into two parts - seepage analysis and strength analysis. The seepage analysis consists of investigating the seepage behavior, the exit gradient, and the influence of a proposed upstream filter before and after the drawdown event. The strength analysis consists of



estimation the movement of the soil particles using a deformation field and a calculation of the factor of safety against sliding failure of the *upstream* slope.

## 7.2 Al-Adhaim Dam

The Al-Adhaim dam is a zoned earth-fill dam with a slope core. It was constructed by the Iraqi government at a location about 100 km northeast of Baghdad, Iraq. The dam is located about 1.5 km near the intersection of two tributaries, Tuz Jay and Taq Jay, to form the Al-Adhaim river (*Al-Adhaim Earth Dam*, 1994). The surface area of water in the reservoir is 270 km at an elevation of 143 m and 122 km at elevation 130 m respectively, while the maximum capacity of the reservoir is 3750 km<sup>2</sup> at an elevation equal to 143 m. **Table 7.1** shows the surface area and volume of water in the reservoir at different elevations (Al-Majid, 2008). **Figure 7.1** represents the cross-section of the dam. The maximum level for flood design is 143 m. The base elevation of the dam is 70 m above the sea level, and the elevation at the crest of the dam is 146.5 m. The main components of the dam are comprised of a shell, core, and filters. The foundation soil of this dam consists of slope layers and a succession of overlays, marl and sandstone, of uneven thickness. The designers chose one of the marl layers of the ground soil to be an extension of the dam core and used it to assist in obstruction of the leakage of water from the upstream to the downstream. **Table 7.2** shows a summary of the materials properties used in the construction of the dam.

Table 7.1: The surface area and the water volume for Al-Adhaim reservoir. (Al-Majid, 2008)

Elevation (m)	Area (km <sup>2</sup> )	Volume (km <sup>3</sup> )	Elevation (m)	Area (km <sup>2</sup> )	Volume (km <sup>3</sup> )
100	3	70	130	122	1400
115	41	310	135	170	2150
118	52	450	140	233	3130
120	60	520	143	270	3750
125	85	980			

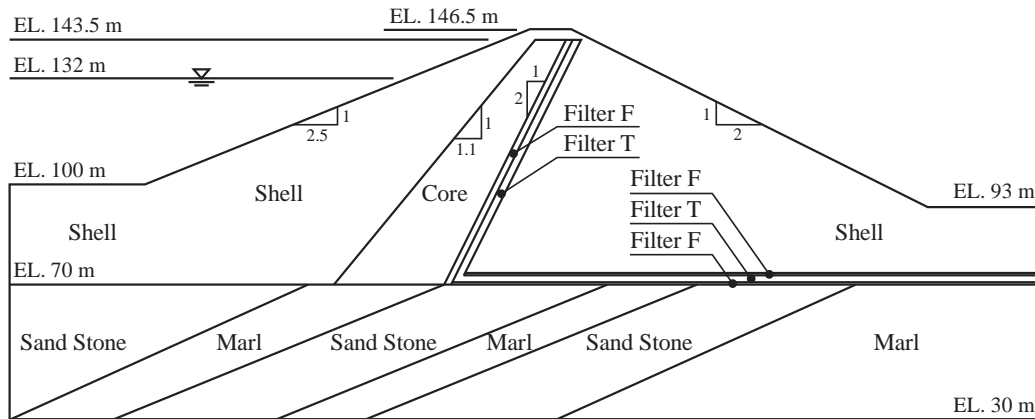


Figure 7.1: Profile section of Al-Adhaim dam (*Al-Adhaim Earth Dam*, 1994).

Table 7.2: Material properties of the earth dam used for seepage, stress, and slope stability analyses (*Al-Adhaim Earth Dam*, 1994).

	Symbols	Soil Materials					
		Shell	Core	Filter F	Filter T	Marl	S. Stone
Unit weight (kN/m <sup>3</sup> )	( $\gamma$ )	17	17	20	16	19.5	19.5
Hydraulic conductivity (m/day)	( $k$ )	1.08	$1.944 \times 10^{-5}$	1.0368	8.64	$8.64 \times 10^{-6}$	$4.752 \times 10^{-3}$
Cohesion (kPa)	( $c'$ )	0	0	0	0	600	0
Elastic Modulus (kPa)	( $E'$ )	19000	9000	19000	19000	350000	300000
Friction angle	( $\phi'$ )	37°	25°	35°	35°	10°	38

### 7.3 Numerical Models of the Dam

The Al-Adhaim dam is modeled using FEM as a real-world application in the current study. The water flowing through the earthen structure is simulated under the steady state and the transient conditions. The GeoStudio 2012 family of programs is used to run the models as it has several software tools applicable to the present study, such as SEEP/W for the seepage modeling, SIGMA/W for the stresses/deformation modeling and SLOPE/W for the slope stability. The material models used for the shell and the core soils was a saturated/unsaturated system, while the

fully saturated option was selected for the foundation and the filter soils. The boundary conditions for the seepage analysis and the finite element mesh are presented in **Figure 7.2**. The elements used to mesh the dam and other parts in the FEM models were quad and triangle shapes. The number of elements and nodes used in the main model is 6970 and 21053, respectively.

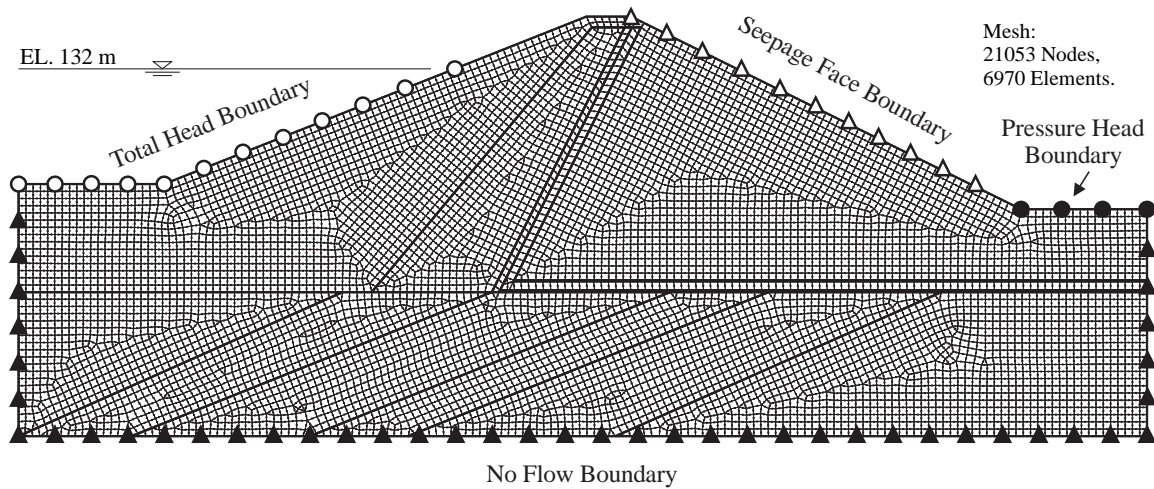


Figure 7.2: Boundary conditions for the seepage analysis and the finite element mesh.

The boundary condition for the seepage analysis in the steady state is specified as the total head on the upstream and downstream sides. The total head is 132 m on the upstream and 93 m on the downstream only at the foundation surface. The boundary condition on the downstream slope face cannot be specified because the pore water pressure depends on the location of the phreatic surface. For this reason, the boundary condition on the downstream slope surface is a potential seepage surface. For the stress analysis, the boundary condition is specified as a hydrostatic pressure for the water reservoir. The hydrostatic pressure is 132 m on the upstream side and zero on the foundation surface at the downstream side. The displacement in the x-direction is specified as a fixed boundary condition on the left and the right of the ends of the foundation, while a fixed x

and y displacement condition is specified below the dam model. For the transient analysis, the boundary condition for the seepage analysis is varying values of the head versus time, while it is varying hydrostatic pressure versus time for the stress analysis. The sudden drawdown of the upstream water is simulated by lowering the water level from 132 m to 126 m and 116 m in one day, while the slow drawdown of the upstream water is simulated at rates of 1 m/day, 0.5 m/day and 1/3 m/day. The Spencer's Method is used to calculate the slope factor of safety. This method considers both interslice shear and normal forces. The requirement for both moment and force equilibrium is fully satisfied (SLOPE/W, 2012).

#### 7.4 Seepage Analysis of Al-Adhaim Dam

Al-Adhaim dam consists of a slope core within it to reduce the magnitude of the water flux flowing through the dam in steady-state conditions. To investigate the seepage behavior during and after the reservoir level is dropped, the dam is first analyzed under steady-state conditions to locate the phreatic line inside the dam and used it for the transient condition. The dam is then tested under various drawdown conditions. **Figure 7.3a** shows the contour lines of the total head and the flow directions in the steady-state condition. As seen in the figure, the phreatic line suddenly drops inside the core, because the low permeability of the core reduces the water flux flowing through the dam. In addition, the marl layer beneath the core base improves the efficiency of the core in reducing the water flux by also preventing the flux from flowing beneath the core. The magnitude of the water flux through the dam is  $0.0061 \text{ m}^3/\text{day}/\text{m}$ . However, the core raises the phreatic line on the upstream side, which in turn increases the saturated area of the soil mass. The phreatic line at the upstream side is seen as becoming almost horizontal.

Next, under the drawdown conditions, the water flux immediately begins to flow out of the dam through both the upstream slope face and the foundation surface. **Figure 7.3b** presents the change of the total head and the flow direction after the drawdown event. The low permeability of the core and the foundation act as a wall, which significantly decreases the water flux from continuing to flow towards the downstream. So, it is seen that, most of the water flux now exits the dam through the upstream face when the water level is dropped (**Figure 7.3b**).

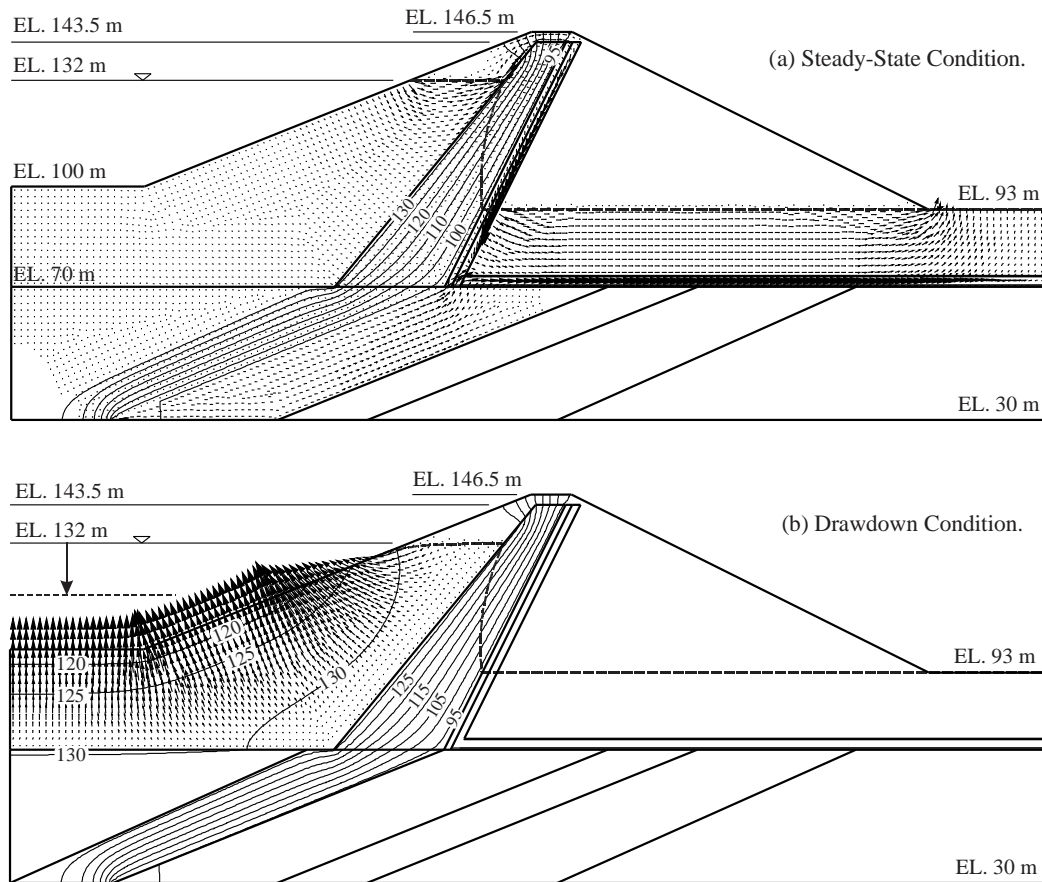


Figure 7.3: Total head contours (in m) and flow directions for Al-Adhaim dam; (a) the steady-state condition, (b) the drawdown condition.

The magnitude of the water flux rises with the drawdown process until it reaches a maximum level when the drawdown is completed. Then, it begins to decrease in magnitude until it returns to zero after about 60 days. **Figures 7.4** (a,b) show the seepage behavior on the upstream face after the two drawdown events respectively. As seen in the figures, the water flux is influenced by the rate and the depth of the drawdown. The slowing of the rate of drawdown reduces the effect of the seepage force acting on the soil particles.

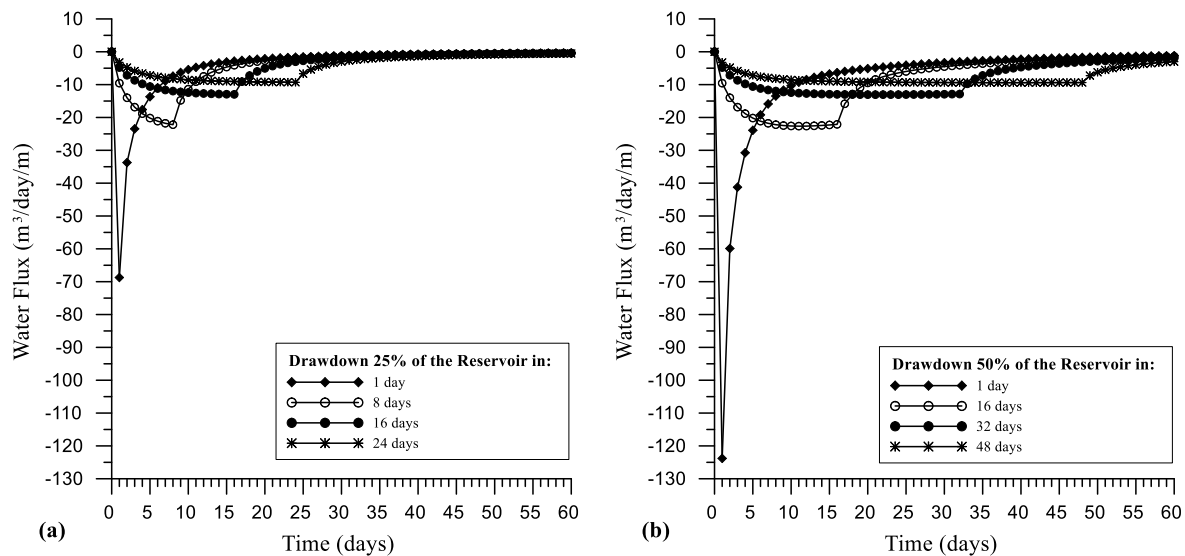


Figure 7.4: The behavior of the water flux flowing out of the upstream face under various drawdown conditions.; (a) drawdown 25% of the reservoir, (b) drawdown 50% of the reservoir.

**Table 7.3** shows a summary of the total water flux that exits the dam under various drawdown conditions for a period of 60 days. It is seen that the faster the drawdown rate, the higher the flux. The reason for this is that the change in the external boundary in a short time creates an immediate flow of the water flux toward the lower head in the reservoir. Dropping the reservoir an additional depth tends to seep a higher magnitude of the water flux out the dam through the upstream face.

The water flux flowing through the slope face is higher than that flowing through the foundation surface. This magnitude of the flux is not significantly influenced by the drawdown rates. The seepage period extends to be more than 60 days because of the low permeability of the core and the foundation.

Table 7.3: Summary of the total flux (in  $m^3/m$ ) that flows out of the earth dam for a period of 60 days under the drawdown conditions.

Total Flux		Flux through the slope		Flux through the foundation	
Drawdown (25%) of the Reservoir					
Drawdown Rate	(m <sup>3</sup> /m)	(m <sup>3</sup> /60 days/m)	(% of the total)	(m <sup>3</sup> /60 days/m)	(% of the total)
1 day	262.6132	201.102	76.58	61.5112	23.42
8 days	261.5499	200.451	76.64	61.0989	23.36
16 days	260.0383	199.336	76.66	60.7023	23.34
24 days	258.1192	197.807	76.63	60.3122	23.37
Drawdown (50%) of the Reservoir					
Drawdown Rate	(m <sup>3</sup> /m)	(m <sup>3</sup> /60 days/m)	(% of the total)	(m <sup>3</sup> /60 days/m)	(% of the total)
1 day	517.917	384.510	74.24	133.407	25.76
16 days	510.270	380.626	74.59	129.644	25.41
32 days	496.954	370.872	74.63	126.082	25.37
48 days	474.070	352.260	74.31	121.810	25.69

The calculation of the exit gradient is very important to investigate the possibility of the seepage force to cause erosion of the soil particles. As seen previously in **Figure 7.3**, the seepage is concentrated on the slope face, in the slope toe, and at the foundation surface. So, for the sake of brevity, the maximum exit gradient is studied at these three locations.

**Figures 7.5** shows the maximum values of the exit gradient recorded on the upstream face under various drawdown conditions. The maximum exit gradient occurs on the slope face at the reservoir level, followed by the slope toe, and on the foundation surface. The drawdown rate is the main factor impacting the increase of the exit gradient on the upstream face. These values of the exit

gradient decrease with the slowing of the drawdown rates because of dissipation of the excess pore pressure. The core causes a higher increase of the exit gradient on the slope face. The exit gradient *reaches the critical condition* under sudden drawdown of 25% of the reservoir, while it *exceeds the critical condition* when the reservoir is drawn down to 50%. On the foundation surface, the values of the exit gradient were lower than the other locations, but still reaches the critical value especially under drawdown 50% of the reservoir. The longer distance between the core and the foundation surface reduces the effect of the core on the exit gradient. In conclusion, it is evident that the upstream face needs to be protected against the development of seepage forces during the drawdown to reduce the likelihood of critical exit gradient and erosion. Thus, the use of a filter in the upstream region of the dam is proposed and will be discussed in the next section.

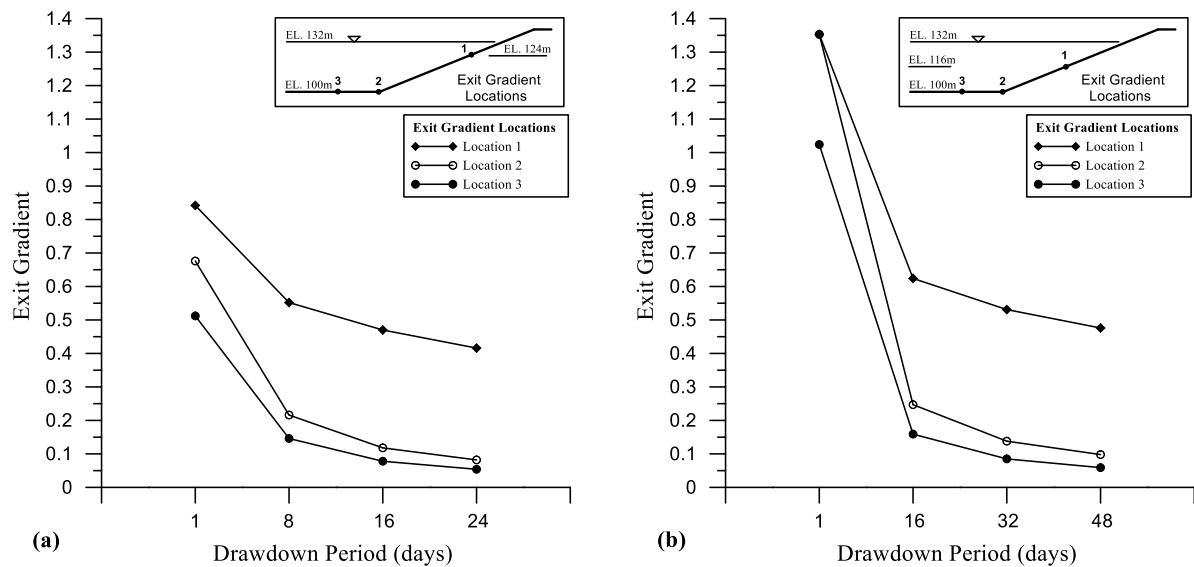


Figure 7.5: Maximum exit gradient on various locations of the upstream face under different drawdown rates; (a) drawdown 25% of the reservoir, (b) drawdown 50% of the reservoir.



### 7.5 Effect of the Upstream Filter

From the discussion in the previous section, under certain drawdown conditions, the exit gradient reaches critical conditions which may promote the migration of soil particles and cause piping. Filters are commonly used in earth dams to control the seepage flow inside the dam and to prevent the development of piping by dissipating the excess pore water pressure. Under drawdown conditions, a high change in the boundary condition occurs on the upstream slope and the dam is exposed to the risk of collapse if the upstream region is left without suitable protection. For this study, the Al-Adhaim dam is modeled with two locations of the filter at the *upstream* side to investigate a suitable location of the filter in protecting the slope under the drawdown event. The first case is one of a central location in the upstream shell with a horizontal filter extending to the foundation surface to transfer the water flux from inside the shell toward the reservoir during the drawdown process, while the second case is an upstream face slope filter. The permeability ratio of the filter soil to the shell soil is assumed to be 25. To model the most severe scenario, the water level is considered to drop 50% of the initial value in the reservoir. The drawdown rate is simulated as a sudden drawdown to test the critical condition.

The purpose is to study the effect of the filter property and location on reducing the exit gradient on the upstream slope face. **Figure 7.6** shows the results of the exit gradient for the two filter cases. The results showed that the horizontal filter effectively reduces the exit gradient on the foundation surface for both filter locations. In the central filter, the permeability of the filter is not high enough to influence the water flowing inside the dam. The water flux continues to flow out the dam through the upstream slope face instead of the filter, and the exit gradient is still higher on the slope face at critical conditions (**Figure 7.6b**).

However, the effect of the filter in reducing the exit gradient is clearly observed when using the slope filter at the upstream end. The critical exit gradient is reduced by 71.69% at level 116 m and by 95.49% on the slope toe. Thus, the slope becomes safer under sudden drawdown condition using the proposed slope filter as shown in the value of the exit gradients in **Figure 7.6c**.

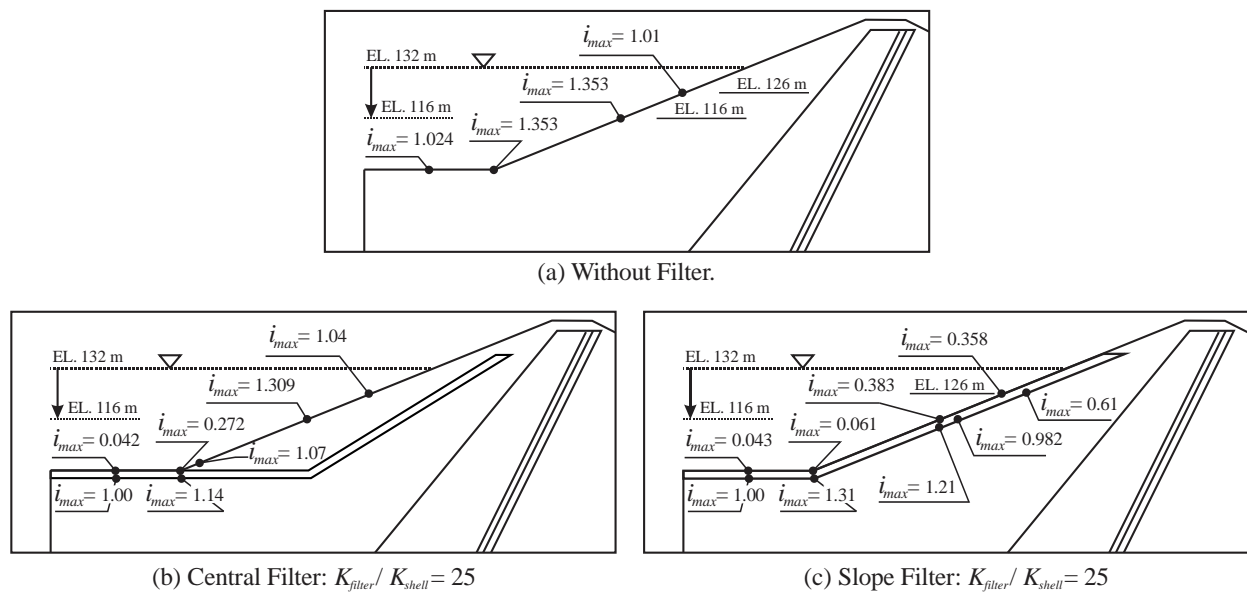


Figure 7.6: The maximum values of the exit gradient on the upstream face after dropping the water level to level 116 m, 50% of the reservoir, in one day.

Next, the permeability ratio of the filter soil to the shell soil ( $k_f/k_s$ ) is increased to 50 to investigate the influence of filter permeability on reducing the exit gradient under sudden drawdown 50% of the reservoir. **Figure 7.7** (a,b) present the results of the exit gradient on the upstream face for the cases, central filter and slope filter respectively. The results showed a reduction of the exit gradient for both filter cases compared to the no filter case. Increase the filter permeability tends to increase

the drain process of the water flux and, in turn, dissipate the excess pore pressure faster. However, even at this ratio, the performance of the central filter was not enough to reduce the exit gradient to below the critical condition (**Figure 7.7a**). The exit gradient remains at an erosion condition.

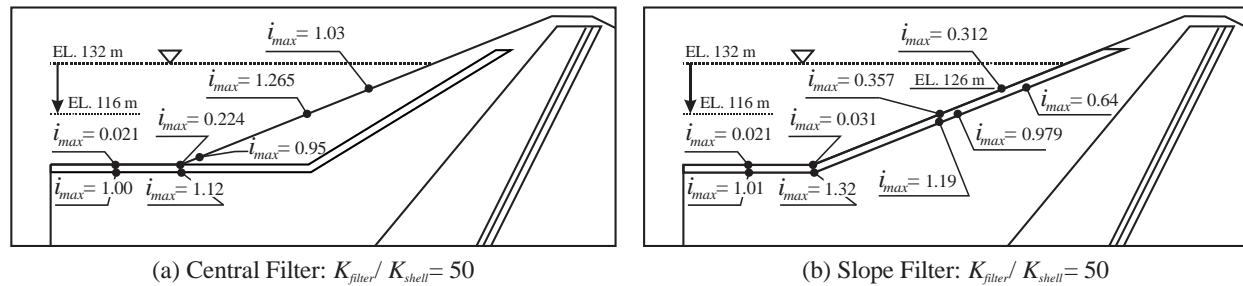


Figure 7.7: The maximum values of the exit gradient on the upstream face after dropping the water level to level 116 m, 50% of the reservoir, in one day.

In this section, the thickness of the filter is increased to 5 m for both the central and the slope filters cases. Once again, the Al-Adhaim dam under sudden drawdown condition is modeled with this new filter thickness. **Figure 7.8** shows the maximum exit gradient values under sudden drawdown of 50% of the reservoir. As shown in the figure, the results show that, in the central filter case, there is a slight reduction in the exit gradient on the slope face but an increase on the foundation surface. For the slope case, there is an increase of the exit gradient on the slope face in comparison with the thinner filter and same permeability ratio from **Figures 7.7**. The reason for the increase may be due to the phreatic line dropping further inside the filter when the filter thickness is increased because of the high permeability of the filter. This situation results in an increase in the difference of the total head between the internal wall and the external wall of both the slope filter

and the horizontal filter. Thus, it is not advisable to have a very thick upstream filter configuration to achieve the goal of reducing the exit gradient.

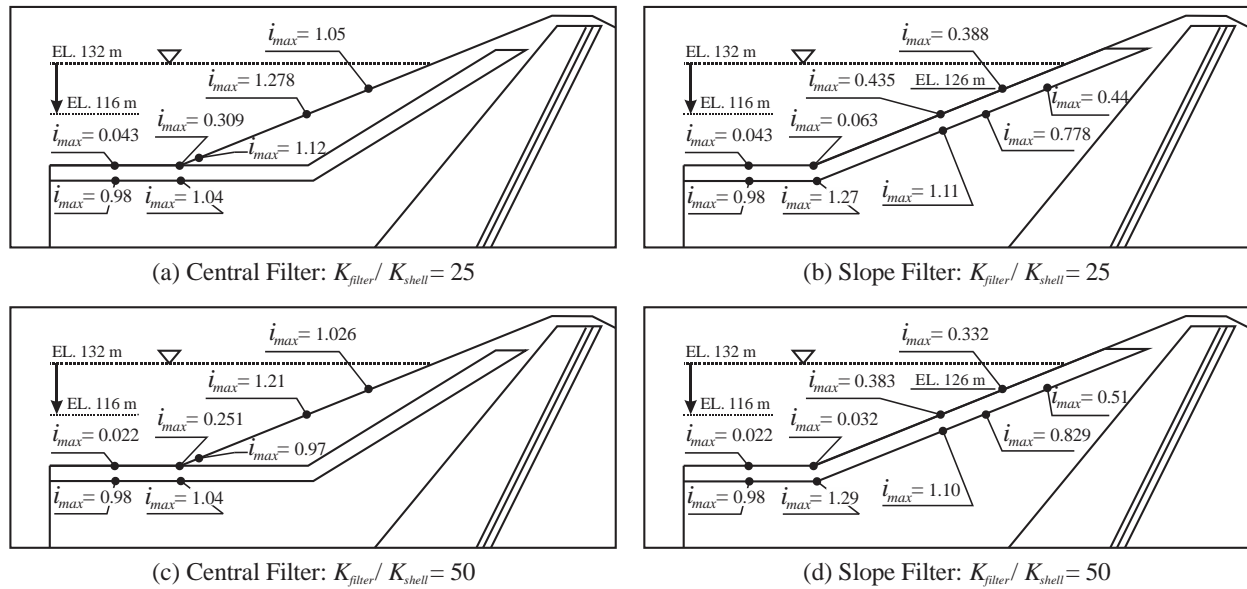


Figure 7.8: The maximum values of the exit gradient on the upstream face after dropping the water level to level 116 m, 50% of the reservoir, in one day.

## 7.6 Deformation of Al-Adhaim Dam under Drawdown Conditions

The deformation response of the Al Adhaim Dam is studied in this section. The response depends on the effective stresses acting on the soil particles because the presence of water between the soil grains provides a force that can either tend to push the particles apart or pull them closer together. The water in the soil is taking up some of the weight (body) load of the soil and thereby reducing the stress in the soil. During the drawdown condition, the hydraulic gradient inside the soil becomes higher than the reservoir, which causes the development of seepage force toward the

upstream slope. Seepage force causes an increase of the effective stresses and may also result in movement of the soil particles. The vertical deformation or settlement may affect the earth dam's stability as the water level of the reservoir is changed dramatically. Thus, it is important to evaluate the displacement of the soil particles after the drawdown event.

**Figure 7.9** shows the movement of the soil particles and the deformed shape after the reservoir is suddenly drawdown to level 116 m (50% of the reservoir). As seen in **Figure 7.9**, the seepage force causes movement of the soil particles in the direction of flow towards the reservoir. This causes a settlement at the dam crest and a swelling of the soil on the upstream face. The highest displacement value is concentrated near the water level after the drawdown, while it decreases gradually toward the foundation surface on both the upstream and the downstream sides. In comparison with the seepage behavior shown previously, in **Figure 7.4**, the magnitude of the soil movement reaches the maximum level as soon as the drawdown process is completed.

**Figure 7.10** shows the contour lines of the soil displacement in the  $x$ - and  $y$ - directions when the reservoir level is dropped to half (50%) at various drawdown rates. The negative sign indicates that the direction movement of the soil to the left side of the dam for  $x$ - displacement (**Figure 7.10a**) and downward for the  $y$ - displacement (**Figure 7.10b**). The maximum soil displacement occurs after one day of the sudden drawdown, and about 32 days are needed for the deformation to reach the maximum value. The drawdown process causes a movement of the soil particles of about 0.2 m toward the reservoir concentrated on the slope face at the new level of water (**Figure 7.10a**). This movement of the soil particles is slightly higher under the drawdown rate of 0.5 m/day. In the  $y$ -displacement, the drawdown event causes about 0.02 m vertical movement of the soil

particles at the dam crest as shown in **Figure 7.10b**. For the drawdown rate of 0.5 m/day, the settlement area becomes bigger at the upstream, while the swelling zone is reduced and concentrated on the horizontal layer of the foundation and some minor areas of the slope (**Figure 7.10b**).

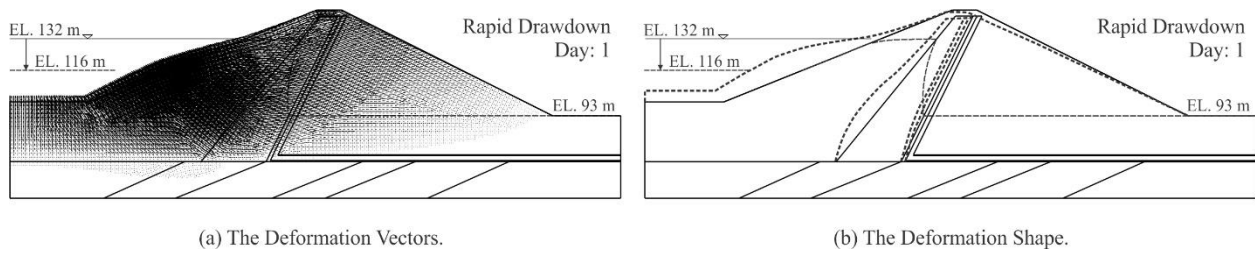


Figure 7.9: Vectors and deformation shape of the dam (at a scale of 50x) after sudden drawdown condition.

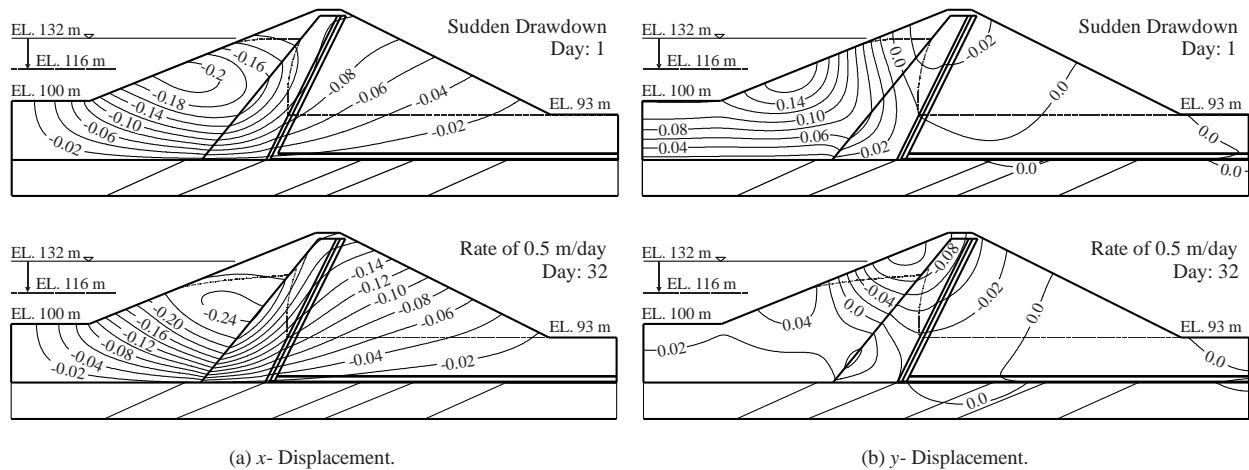


Figure 7.10: Contour lines of the maximum soil displacement (in m) in the  $x$ - and  $y$ - directions under drawdown conditions.

A high permeability filter may influence the water flow inside the dam by increasing the flow velocity inside the filter. In addition, the filter has strength properties different from the shell. To investigate the influence of the filter on the dam deformation, the response of the soil mass is calculated when the dam has a central filter and a slope filter, separately. **Figures 7.11 and 7.12** present the contour lines of the maximum movement of the dam soil particles in the  $x$ - and  $y$ -displacements respectively, as the reservoir is dropped under various drawdown rates. The results showed an increase of the particle movement around the filter for both filter locations. The maximum movement of the soil also occurred immediately when the drawdown process is completed, at the location where the maximum excess pore water pressure has developed.

In comparison to the slope filter, a central filter increases the movement of the soil particles around the filter in the  $x$ - and  $y$ - directions as shown in **Figures 7.11a and 7.12a**. Once again, the filter configuration is very important in the desired response and the slope filter performs better.

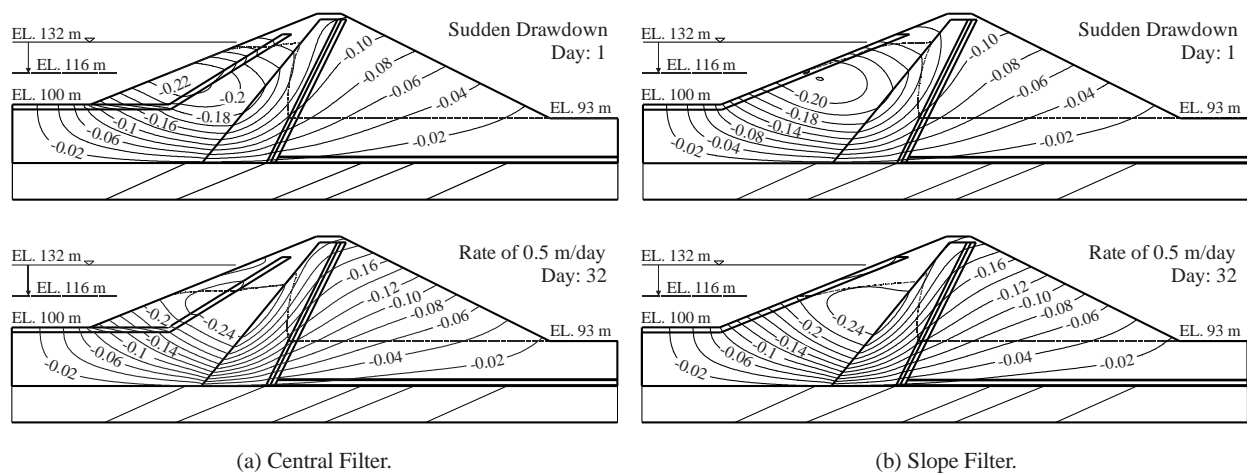


Figure 7.11: Contour lines of the maximum soil displacement (in m) in the  $x$ -direction under drawdown conditions.

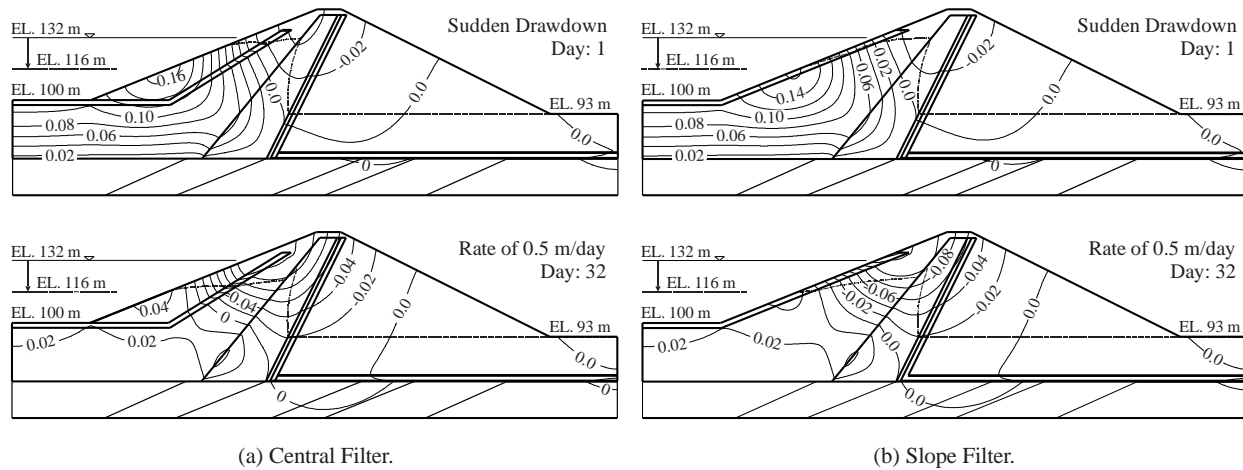


Figure 7.12: Contour lines of the maximum soil displacement (in m) in the y-direction under drawdown conditions.

## 7.7 Factor of Safety Against the Sliding under the Drawdown Conditions

### 7.7.1 Slope Stability Analysis of Al-Adhaim Dam

The results of the factor of safety against sliding failure under steady-state conditions are studied for reservoir levels of 132 m, 124 m, and 116 m. After modeling the dam and performing Spencer's method for slope stability analysis using GeoSlope, the factors of safety was found to be 1.679, 1.645, and 1.657, for the three reservoir levels, respectively.

The results display a difference in the factor of safety due to the change in the boundary condition in the reservoir and the stress condition in the upstream slope soil mass. The presence of a core above a low permeability foundation resulted in an increase of the saturated soil zone in the upstream region, which caused a reduction in effective stress. This, in turn, significantly reduces the slope factor of safety. Besides, the hydrostatic pressure coming from the water reservoir



provides additional support to the slope and resists sliding failure.

Under sudden drawdown conditions, the water inside the dam needs a longer time to escape from the dam, which causes the development of excess pore water pressure in the soil and consequently, a reduction in the shear resistance of the soil. In addition, the hydrostatic pressure on the slope is reduced resulting in the lowering of the soil resistance against sliding. **Figure 7.13** shows the critical sliding surface under a sudden drawdown of 25% of the reservoir. The results show that a shallow sliding of the soil develops on the slope when the water level is suddenly dropped to level 124 m (25% of the reservoir). These slides take place immediately after the drawdown is completed and may cause cracking on the slope face.

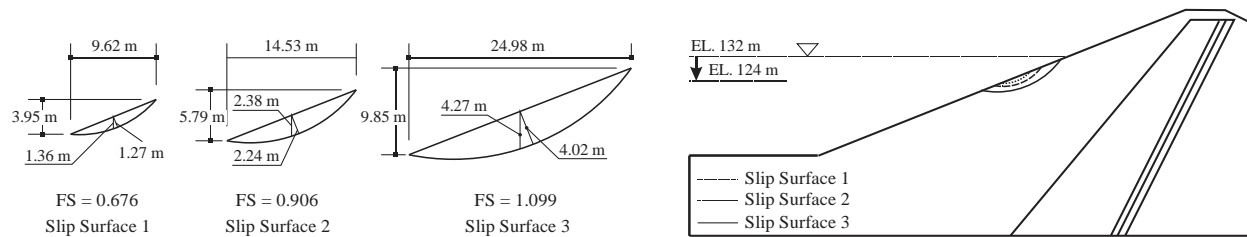


Figure 7.13: Slip surfaces that may cause cracking or sinkhole on the slope surface after the drawdown event.

The slip surface of the upstream slope in the steady-state and under sudden drawdown conditions are presented in **Figure 7.14**. The slip surface in the steady-state condition extends through the core and reaches the dam crest (**Figure 7.14a**). Under the drawdown condition, the area of slip

surface is reduced and concentrated close to the upstream slope within the water level (**Figure 7.14b**).

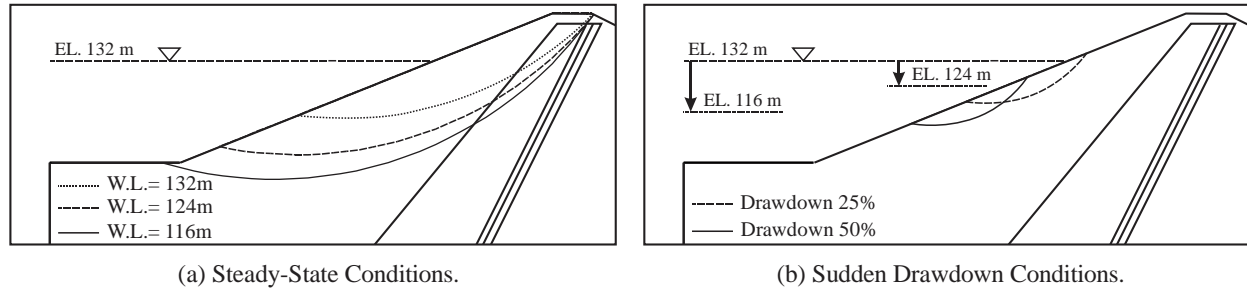


Figure 7.14: Slip surfaces of the upstream slope for the dam cases before and after the sudden drawdown event.

**Figure 7.15** presents the impact of the drawdown conditions on the slope factor of safety with time for the two transient cases. As shown in the figure, the factor of safety reaches the lowest value immediately after the drawdown is completed. Under the sudden drawdown condition, the upstream slope stability of the dam reaches a specified failure condition below 1. Assuming it can sustain this, after that stage, the factor of safety begins to increase with time due to the dissipation of the excess pore water pressure within the soil. After a period of days, the factor of safety returns to the steady-state value after dissipation of all the excess pore water pressure. However, the excess pore water pressure needs a long period of time to totally dissipate from the Al-Adhaim dam. Thus, the factor of safety does not return to the steady-state condition until almost 60 days after the completion of the drawdown event (**Figure 7.15**).

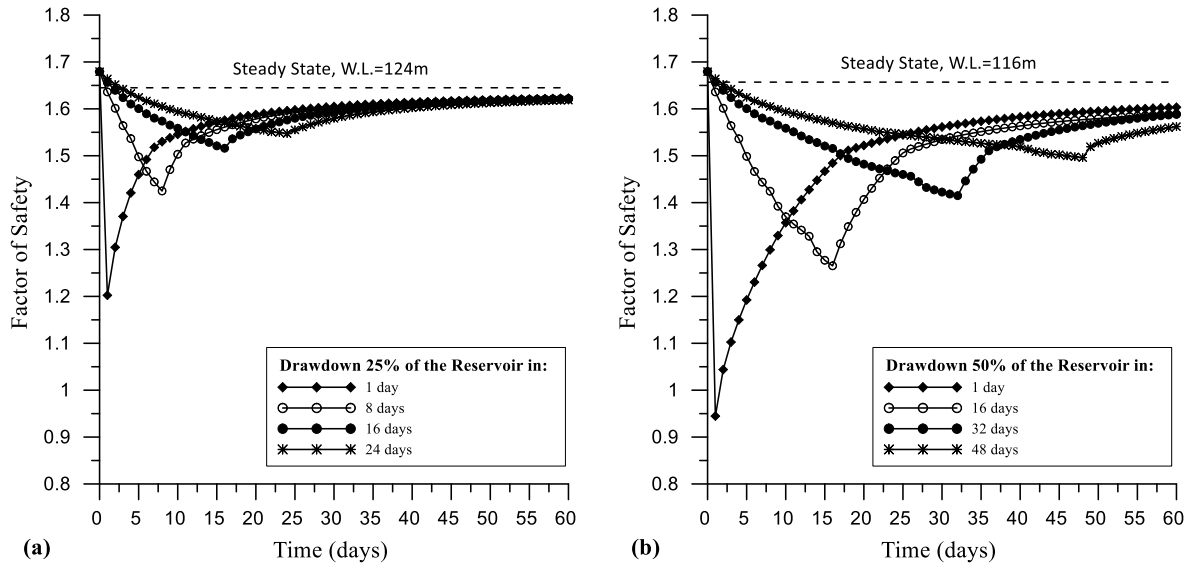


Figure 7.15: Factor of safety with time for the different dam cases under drawdown conditions; (a) drawdown 25% of the reservoir, (b) drawdown 50% of the reservoir.

### 7.7.2 Influence of the Upstream Filter

As discussed previously, the upstream filters are proposed to lower the exit gradient on the upstream face due to the drawdown. In this section, the impact of the two filter configurations on the stability of the slope is studied. The factor of safety is calculated for Al-Adhaim dam when a slope filter and a central filter are included in the upstream soil mass. The dam is tested under the most critical drawdown condition; the sudden drawdown of 50% reservoir.

The shear strength of the soil depends primarily on soil properties and groundwater conditions. The properties of the filter may influence the slope stability. **Figure 7.16** shows the slip surfaces for the filter cases in the steady state and under sudden drawdown 50% of the reservoir. As seen in the figure, there is a change of the slip surface when using the upstream filters. The slip area is reduced when using a central filter, which implies a reduction of the stability against sliding. For

the slope filter, the slip surface stays the same in the steady-state condition, while it increases under the drawdown condition when the permeability ratio ( $k_f/k_s$ ) is increased to 50 times. The higher permeability of the filter increases the draining process of water out the dam, which increases the stability.

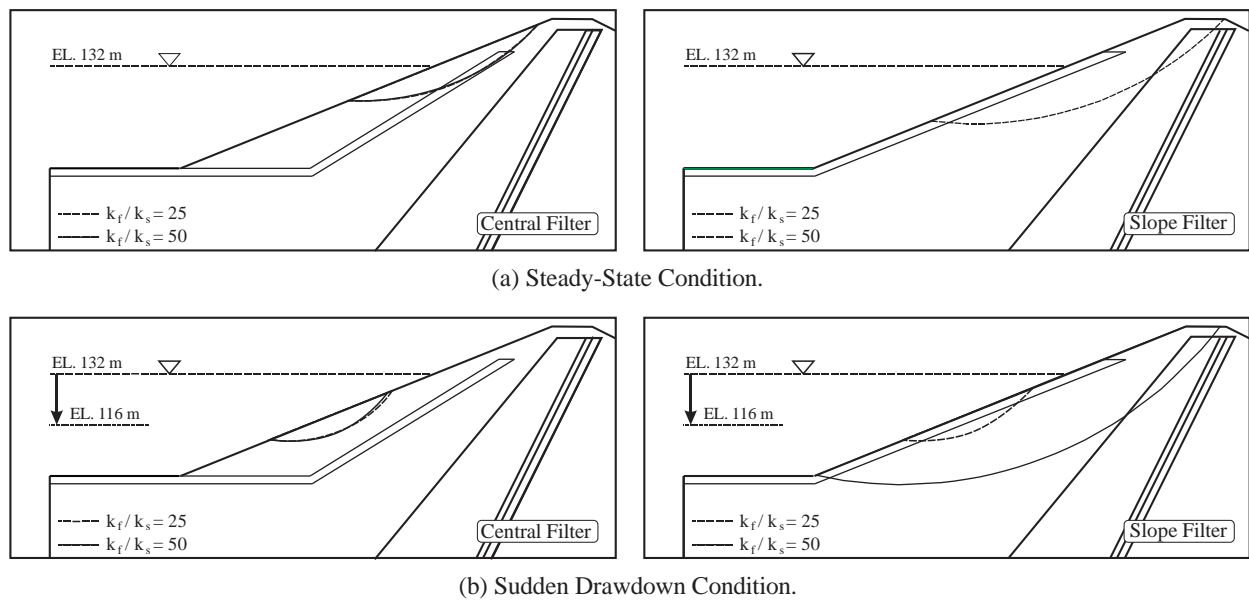


Figure 7.16: Slip surfaces of the upstream slope for the dam cases before and after the drawdown 50% of the reservoir.

**Figure 7.17** shows the factor of safety under sudden drawdown of 50% of the reservoir. The results showed a reduction of the factor of safety in the steady-state condition by 2.25% when the dam has a central filter, while there is an increase of the factor of safety by 2.3% when using the slope filter. Under sudden drawdown condition, the factor of safety for the central filter case is *reduced* by 14.79% and 15.05% at permeability ratio of  $k_f/k_s = 25$  and  $k_f/k_s = 50$ , respectively. The slope

filter *increases* the factor of safety by 28.09% for a permeability ratio of  $k_f/k_s = 25$  and 51.63%, for a permeability ratio of  $k_f/k_s = 50$ .

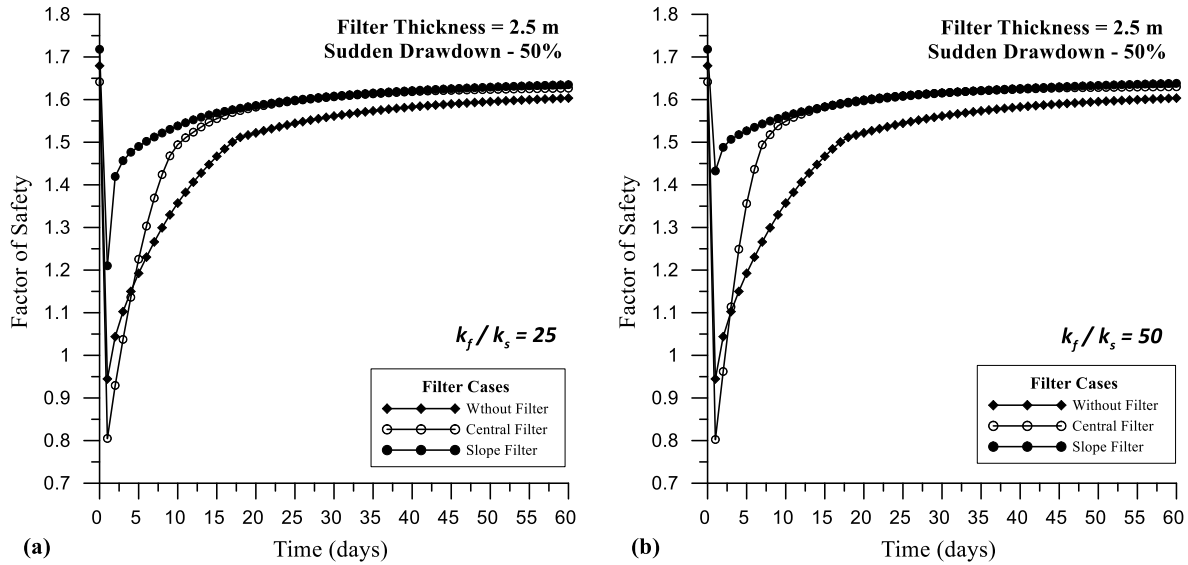


Figure 7.17: Factor of safety with time for the different dam cases under sudden drawdown condition; (a)  $k_f/k_s = 25$ . (b)  $k_f/k_s = 50$ .

**Figure 7.18** shows the factor of safety of the upstream slope against sliding when using a thicker filter of 5 m width and suddenly dropping the water level by 50% of the reservoir in one day. The results showed that the permeability of the central filter has no significant effect on the factor of safety. However, the factor of safety is improved when using the slope filter. The factor of safety increases by 41.15% when using a permeability ratio of  $k_f/k_s = 25$ , and by 50.44% using a ratio of  $k_f/k_s = 50$ . Increasing the thickness and the permeability of the slope filter accelerates the

draining process of the seepage and, in turn, increase the effective stress inside the soil. The factor of safety of the slope against sliding becomes higher because of depending on the effective stress.

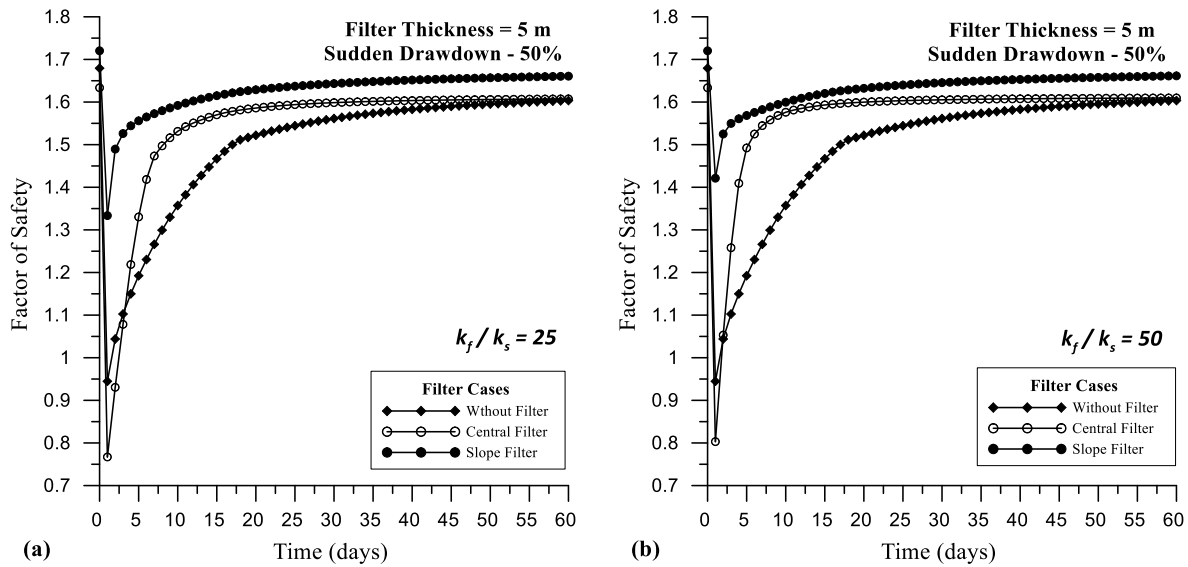


Figure 7.18: Factor of safety with time for the different dam cases under sudden drawdown condition; (a)  $k_f/k_s = 25$ . (b)  $k_f/k_s = 50$ .

In conclusion, the slope filter configuration and design is found to be the most effective in providing protection against both erosion due to critical exit gradients and improving the factor of safety of the upstream slope.

## **CHAPTER EIGHT: CONCLUSIONS AND RECOMMENDATIONS FOR FUTURE WORK**

### 8.1 Conclusions

This dissertation presents the results of a numerical study of an earth dam subjected to upstream drawdown conditions. Three different configurations of the dam cross-section are studied that include a baseline dam, a dam with a low permeability core and one with a core and complete cutoff in the foundation. In addition, this study is also applied to the investigation of a real dam in Iraq called the Al-Adhaim Dam. Based on the results of the seepage analysis, it is seen that the phreatic line and the total head gradually reduce as the flow takes place toward the downstream side because of the permeability of the soil. A downstream filter is often included for seepage control to further lower the phreatic line away from the downstream slope. The core is an important feature used to lower the phreatic line and decrease the water flux through the body of the dam. It is also seen that constructing a core on a higher permeability foundation results in the development of a concentrated flow beneath the core. The core is very effective in lowering the phreatic line and reducing the water flux when the dam is constructed with a complete low-permeability cutoff in the foundation layer under the core.

However, the results of this study also showed that the core has a strong influence on the saturated area in the upstream shell. As a consequence of its low permeability, there is a decrease in the flux velocity inside the core which subsequently raises the phreatic line in the upstream shell. This, in turn, causes a decrease in the dry unit weight of the shell soil and may accelerate the process of erosion. This saturated area is further increased with the presence of a low-permeability cutoff below the core. Under drawdown conditions, the saturated area causes an increase in the water

flux that flows out of the dam from the upstream face, and also an increase in the length of time required for the seepage to flow out. The seepage may continue for a period of more than 30 days in the case of a low-permeability cutoff with the core, which may initiate the process of piping inside the dam on the upstream side. At the same time, the exit gradient on the upstream face is also increasing due to a higher amount of the water flux. This gradient value approaches, and in some cases, reaches the critical levels for erosion. For the case with a core only, the exit gradient is not impacted. It is evident from this study that the combination of the presence of a core and cutoff, along with the process of rapid drawdown, may result in the exit gradient reaching critical values for erosion initiation and piping.

The foundation material mainly influences the seepage behavior before and after the drawdown condition. The impermeable soil of the foundation reduces the exit gradient, developed because of the reservoir dropping, on the slope face.

The upstream region can be protected against the erosion process by using a soil filter at the upstream side of the dam. The location of the filter is very important to make the filter function effectively. The results showed that the efficiency of the filter in reducing the exit gradient is extremely improvement under drawdown conditions. The proposed design called slope filter accommodates all seepage force flowing toward the reservoir after the drawdown event, which causes a higher decrease in the exit gradient on the slope face. The other configuration called the central filter showed very little influence on the reduction of the exit gradient. The water flux around the slope face continues flowing toward the reservoir instead flowing through the central



filter because of the low permeability of the filter soil in comparison to the free exit from the slope face.

The efficiency of the filter as a drain for the excess pore water pressure is further enhanced with the increase the filter permeability. The phreatic line suddenly drops inside the central filter when the filter permeability is increased. Using a transition zone around the upstream filter prevents the dam soil from the erosion under the drawdown conditions and, at the same time, increases the efficiency of the filter in reducing the effect of excess pore water pressure and decreases the exit gradient at the upstream slope face.

The results of the deformation analysis showed some movement of the soil particles with the direction of the water flowing toward the reservoir when the reservoir water level is dropped, which results in the settlement of the dam soil at the crest. In addition, the soil mass is seen as swelling on the foundation surface and some parts on the slope face because of the vertical flowing of the seepage force. The construction of an earth dam on top of a very rigid foundation layer reduces the deformation of the dam soil on the upstream and the downstream sides. The higher velocity of the water flux inside the upstream filters causes an increase in the soil movement of the earth dam under the drawdown conditions. The maximum deformation caused by the sudden drawdown condition is concentrated at the center of the upstream shell around the filter and on the slope face for the central filter. It is concentrated on the slope face for the slope filter.

Lastly, the shear strength of the slope soil is influenced primarily by the soil properties. The low permeability of the core decreases the flux velocity inside the core and subsequently increases the buoyancy force in the upstream shell. This process causes a decrease of the dry weight of the soil

(i.e. reduction in the effective stress) and a related decrease in its stability. The factor of safety against sliding failure is reduced significantly for cases with a core due to the increase in the buoyancy of the soil on the upstream side of the dam. Building an earth dam on a rigid foundation is found to increase the slope stability. During the drawdown, the result showed that the dam that is constructed with a core and a complete cutoff has lower factors of stability when compared to the other cases. By installing a slope filter on the upstream region, it is possible to increase the factor of safety against the sliding. On the flip side, a central filter is found to reduce the stability of the upstream slope and should be avoided.

## 8.2 Recommendations

There are the recommendations for future work in this area:

- Analyzing the earth dam with various values of the hydraulic conductivity to study the influence of the upstream materials on the dam stability under the drawdown conditions.
- Analyzing the earth dam under various drawdown conditions to design a suitable thickness of the upstream filters.
- Investigation the influence of the upstream slope angle on the seepage behavior and the dam stability under the drawdown conditions.
- Studying the influence of cycling (raising and dropping) of the water level on the dam stability.

## REFERENCES

- Abramson, L. W., Lee, T. S., Sharma, S., & Boyce, G. M. (2002). *Slope Stability and Stabilization Methods* (2<sup>nd</sup> Edition). Wiley.
- Al-Adhaim *Earth Dam - Final Report*. (1994). Unpublished Report, Engineering Consultancy Bureau, University of Baghdad, Iraq.
- Al-Majid, S. J. (2008). Natural Ingredients for the Great Lake Dam And Its Impact in the Development of Tourism Demand. *Iraq Academic Scientific Journals*, (71), 207–231.
- Alonso, E. E., & Pinyol, N. M. (2016). Numerical analysis of rapid drawdown: Applications in real cases. *Water Science and Engineering*, 9(3), 175–182.
- Bosela, P. A., Brady, P. A., Delatte, N. J., & Parfitt, M. K. (Eds.). (2012). *Failure Case Studies in Civil Engineering* (2<sup>nd</sup> Edition). Reston, VA: American Society of Civil Engineers.
- Budhu, M. (2011). *Soil Mechanics and Foundations* (3<sup>rd</sup> Edition). John Wiley & Sons, Inc.
- Cedergren, H. R. (Harry R. (1977). *Seepage, Drainage, and Flow Nets* (2<sup>nd</sup> Edition). John Wiley & Sons, Inc.
- Chang, C. S. (1986). Application of Boundary Element Method in Transient Flow Problems with Moving Boundaries. In *Boundary Elements VIII* (pp. 849–858). Berlin, Heidelberg: Springer Berlin Heidelberg.
- Chang, C. S. (1987). Boundary Element Method in Drawdown Seepage Analysis for Earth Dams. *Journal of Computing in Civil Engineering*, 1(2), 83–98.
- Chang, C. S. (1988). Boundary-Element Analysis for Unconfined Seepage Problems. *Journal of Geotechnical Engineering*, 114(5), 556–572.
- Chang, D. S., & Zhang, L. M. (2013). Critical Hydraulic Gradients of Internal Erosion under Complex Stress States. *Journal of Geotechnical and Geoenvironmental Engineering*, 139(9), 1454–1467.
- Das, B. M., & Sobhan, K. (2014). *Principles of Geotechnical Engineering* (8<sup>th</sup> Edition).
- Duncan, J. M., Mitchell, J. K. (James K., & Seed, H. B. (Harry B. (1990). Slope Stability during Rapid Drawdown. In *H. Bolton Seed, Vol. 2: Memorial Symposium Proceedings* (pp. 253–272). BiTech Publishers.
- Duncan, J. M., Wright, S. G., & Brandon, T. L. (2014). *Soil Strength and Slope Stability* (2<sup>nd</sup> Edition). Hoboken, New Jersey: John Wiley & Sons, Inc.
- Fannin, J. (2008). Karl Terzaghi: From Theory to Practice in Geotechnical Filter Design. *Journal of Geotechnical and Geoenvironmental Engineering*, 134(3), 267–276.

- Fattah, M. Y., Omran, H. A., & Hassan, M. A. (2015). Behavior Of An Earth Dam During Rapid Drawdown Of Water In Reservoir – Case Study. *International Journal of Advanced Research (IJAR)*, 3(10), 110–122.
- Fell, R., MacGregor, P., Stapledon, D., Bell, G., & Foster, M. (2014). *Geotechnical Engineering of Dams* (2<sup>nd</sup> Edition). CRC Press.
- Flores-Berrones, R., Ramírez-Reynaga, M., & Macari, E. J. (2011). Internal Erosion and Rehabilitation of an Earth-Rock Dam, *137*(2), 150–160.
- Fredlund, M., Lu, H., & Feng, T. (2011). Combined Seepage and Slope Stability Analysis of Rapid Drawdown Scenarios for Levee Design. In *Geo-Frontiers 2011* (pp. 1595–1604). Reston, VA: American Society of Civil Engineers.
- GEO-SLOPE, I. L. (2018). Upper San Fernando Dam. Retrieved October 16, 2018, from <https://www.geoslope.com/support/support-resources/example-files/example?id=examples:quakew:uppersanfernandodam&resourceVersion=8.15.6.13446>
- Independent Panel to Review Cause of Teton Dam Failure. (1976). *Report to the U.S. Department of the Interior and State of Idaho on Failure of Teton Dam*. Idaho Falls, ID. Retrieved from <https://www.usbr.gov/pn/snakeriver/dams/uppersnake/teton/1976failure.pdf>
- Jiang, J., Ehret, D., Xiang, W., Rohn, J., Huang, L., Yan, S., & Bi, R. (2011). Numerical Simulation of Qiaotou Landslide Deformation caused by Drawdown of the Three Gorges Reservoir, China. *Environmental Earth Sciences*, 62(2), 411–419.
- Ke, L., & Takahashi, A. (2012). Strength Reduction of Cohesionless Soil due to Internal Erosion Induced by One-Dimensional Upward Seepage Flow. *Soils and Foundations*, 52(4), 698–711.
- Khanna, R., Datta, M., & Ramana, G. V. (2014). Influence of Thickness of a Vertical Core on the Slope Stability of Earth and Rockfill Dams. *Dams and Reservoirs*, 24(4), 152–167.
- Lane, P. A., & Griffiths, D. V. (2000). Assessment of Stability of Slopes under Drawdown Conditions. *Journal of Geotechnical and Geoenvironmental Engineering (ASCE)*, 126(5), 443–450.
- Li, G. C., & Desai, C. S. (1983). Stress and Seepage Analysis of Earth Dams. *Journal of Geotechnical Engineering, ASCE*, 109(7), 946–960.
- López-Acosta, N., Sánchez, M., Auvinet, G., & Pereira, J. (2014). Assessment of Exit Hydraulic Gradients at the Toe of Levees in Water Drawdown Conditions. In *Scour and Erosion* (pp. 171–181). CRC Press.
- Luo, F., & Zhang, G. (2016). Progressive Failure Behavior of Cohesive Soil Slopes under Water Drawdown Conditions. *Environmental Earth Sciences*, 75(11), 973.

- Moharrami, A., Hassanzadeh, Y., Salmasi, F., Moradi, G., & Moharrami, G. (2014). Performance of the Horizontal Drains in Upstream Shell of Earth Dams on the Upstream Slope Stability during Rapid Drawdown Conditions. *Arabian Journal of Geosciences*, 7(5), 1957–1964.
- Reddi, L. N. (2003). *Seepage in Soils: Principles and Applications* (1<sup>st</sup> Edition). John Wiley & Sons, Inc., New Jersey.
- San Francisco Public Utilities Commission Peninsula Watershed. (2018). Retrieved from <https://sfwater.org/modules/showdocument.aspx?documentid=9615>
- SEEP/W. (2012). *Seepage Modeling with SEEP/W: An Engineering Methodology* (July 2012). GEO-SLOPE International Ltd., Calgary, Canada.
- Sherard, J. L., Dunnigan, L. P., & Talbot, J. R. (1984). Basic Properties of Sand and Gravel Filters, *110*(6), 684–700.
- Sibille, L., Marot, D., & Sail, Y. (2015). A Description of Internal Erosion by Suffusion and Induced Settlements on Cohesionless Granular Matter. *Acta Geotechnica*, 10(6), 735–748.
- SIGMA/W. (2012). *Stress-Deformation Modeling with SIGMA/W: An Engineering Methodology* (July 2012). GEO-SLOPE International Ltd., Calgary, Canada.
- Skempton, A. W., & Brogan, J. M. (1994). Experiments on Piping in Sandy Gravels. *Géotechnique*, 44(3), 449–460.
- SLOPE/W. (2012). *Stability Modeling with SLOPE/W: An Engineering Methodology* (July 2012). GEO-SLOPE International Ltd., Calgary, Canada.
- Smith, I. M. (Ian M. (2014). *Smith's Elements of Soil Mechanics* (9<sup>th</sup> Edition). Wiley-Blackwell.
- Spencer, E. (1967). A Method of Analysis of the Stability of Embankments Assuming Parallel Inter-Slice Forces. *Géotechnique*, 17(1), 11–26.
- Stark, T. D., & Duncan, J. M. (1991). Mechanisms of Strength Loss in Stiff Clays. *Journal of Geotechnical Engineering*, 117(1), 139–154.
- Stark, T. D., & Jafari, N. H. (2018). San Luis Dam Case History: Seepage and Slope Stability Analyses and Lessons Learned. In *IFCEE 2018* (pp. 317–329). Reston, VA: American Society of Civil Engineers.
- Stark, T. D., Jafari, N. H., Zhindon, J. S. L., & Baghdady, A. (2017). Unsaturated and Transient Seepage Analysis of San Luis Dam. *Journal of Geotechnical and Geoenvironmental Engineering*, 143(2), 04016093.
- Sui, W., & Zheng, G. (2017). An experimental investigation on slope stability under drawdown conditions using transparent soils. *Bulletin of Engineering Geology and the Environment*, 1–9.

- Tang, X., & Zheng, Y. (2008). The Effect on Stability of Slope under Drawdown Conditions. *Journal of Highway and Transportation Research and Development (English Edition)*, 3(1), 16–19.
- Taylor, D. W. (1948). *Fundamentals of Soil Mechanics*. New York : John Wiley & Sons, Inc.
- Terzaghi, K., Peck, R. B. (Ralph B., & Mesri, G. (1996). *Soil Mechanics in Engineering Practice* (3<sup>rd</sup> Edition). Wiley.
- Tiwari, B., Ajmera, B., Khalid, M., Donyanavard, S., & Chavez, R. (2018). Influence of Slope Density on the Stability and Deformation of Clayey Slopes. In *IFCEE 2018* (pp. 293–301). Reston, VA: American Society of Civil Engineers.
- U.S. Army Corps of Engineers. (1993). *Engineering and Design: SEEPAGE ANALYSIS AND CONTROL FOR DAMS* (EM 1110-2-). Department of the Army Corps of Engineers: Office of the Chief of Engineers.
- U.S. Army Corps of Engineers. (2003). *Slope Stability* (EM-1110-2-). Department of the Army Corps of Engineers: Office of the Chief of Engineers.
- Vandenberge, D. R. (2014). Total Stress Rapid Drawdown Analysis of the Pilarcitos Dam Failure using the Finite Element Method. *Frontiers of Structural and Civil Engineering*, 8(2), 115–123.
- VandenBerge, D. R., & Wright, S. G. (2016). Improved Undrained Strength Interpolation Scheme for Rapid Drawdown. *Journal of Geotechnical and Geoenvironmental Engineering*, 142(6), 06016002.
- Walter Bouldin Dam failure and reconstruction*. (1978). U.S. Department of Energy. <https://doi.org/10.2172/6393036>
- Wan, C. F., & Fell, R. (2008). Assessing the Potential of Internal Instability and Suffusion in Embankment Dams and Their Foundations. *Journal of Geotechnical and Geoenvironmental Engineering*, 134(3), 401–407.
- Zhang, G., & Luo, F. (2017). Simplified Stability Analysis of Strain-Softening Slopes under Drawdown Conditions. *Environmental Earth Sciences*, 76(4), 151.